Development of a Raman Spectroscopy-Based Sterility Testing Method for Silica-Based Drug Delivery Systems

University of Turku

Department of Chemistry

Materials Chemistry Research Group

Faculty of Science

Master's thesis

Katja Kallio

26.9.2025

Turku

Master's thesis

Subject: Material chemistry

Author: Katja Kallio

Title: Development of a Raman Spectroscopy-Based Sterility Testing Method for Silica-Based Drug Delivery Systems

Supervisor: Pia Damlin, Tamara Dulic

Number of pages: 79 pages

Date: 26.92025

Microbial contamination can pose a critical risk to the safety and efficacy of both sterile and non-sterile pharmaceutical products. Microorganisms can compromise product quality by causing contamination, degradation, and reduce the efficacy of the drug. While current pharmacopoeial methods offer standardized procedures for microbial testing, they are not suitable for all formulations. For example, the methods described are not suitable for drug delivery systems such as DelSiTech™ silica-based technologies. These limitations emphasize the need for alternative, rapid, and non-destructive analytical techniques.

This thesis investigates the potential of Raman spectroscopy as a microbiological quality control method for silica-based pharmaceutical products. Raman spectroscopy is a vibrational spectroscopic technique based on inelastic scattering of monochromatic light, typically from a laser, as it interacts with molecular bonds in the sample. Raman spectroscopy provides molecular fingerprints and has shown promise in detecting and identifying microorganisms, even at the single-cell level. Because each microorganism has a distinct biochemical fingerprint, which is determined by its proteins, nucleic acids, lipids, and carbohydrates, Raman spectroscopy offers a highly specific, label-free method for microbial identification.

Raman spectroscopy is label-free, non-destructive, and there is no need for extensive sample preparation. Unlike with culture-based traditional microbial identification methods, which may require days for microbial growth, with Raman measurements results can be obtained in minutes. Additionally, the technique is well suited for complex sample environments, where conventional techniques fail or interfere with analysis. These qualities make Raman spectroscopy a suitable candidate for sterility assessment even in advanced formulations.

The experimental work involves Raman analysis of silicon oxide, selected microorganisms, and one active pharmaceutical ingredient (API). Three representative microorganisms were studied: *Bacillus subtilis cf. spizizenii* (Gram-positive), *Pseudomonas chlororaphsis* (Gram-negative), and *Aspergillus versicolor* (yeast). These were analysed in different physical states: lyophilized on cellulose filters, in liquid culture and dissolved in ammonium bifluoride (NH_4HF_2), which is neutralized with silica. Serial dilutions of each microorganism were prepared to determine the detection limits.

All measurements were carefully optimized with respect to laser wavelength, laser power, exposure time, magnification, and substrate material. A variety of substrates—including quartz, stainless steel, and calcium fluoride (CaF_2) were tested to evaluate their effect on signal-to-noise ratio and background interference.

Key words: Raman spectroscopy, pharmaceuticals, microorganisms, method development

Table of Contents

Abbreviations:

API – Active pharmaceutical ingredient

AST – Antimicrobial susceptibility testing

CARS – Coherent anti-Stokes Raman spectroscopy

CCDs – Charge-coupled devices

CFU – Colony-forming units

FT-Raman – Fourier Transform Raman

LDA – Linear discriminant analysis

LPS – Lipopolysaccharides

NA – Numerical aperture

NGS – Next-generation sequencing

NIR – Near-infrared

OMV – Outer membrane vesicles

PCA – Principal component analysis

PAT – Process analytical technology

PCR – Polymerase chain reaction

PLS – Partial least squares

PLS-DA – Partial least squares discriminant analysis

RRS – Resonance Raman spectroscopy

SAL – Sterility assurance level

SERS – Surface-enhanced Raman spectroscopy

SRS – Stimulated Raman spectroscopy

SVM – Support vector machines

TAMC – Total aerobic microbial count

TERS – Tip-enhanced Raman spectroscopy

TRS – Transmission Raman spectroscopy

TVC – Total viable count

TYMC – Total combined yeast and mould count

1 Introduction

Monitoring and managing microbial contamination in pharmaceutical products is critical to ensuring both product efficacy and patient safety. Contamination in sterile or non-sterile products, poses significant risks, potentially compromising the drug's effectiveness or rendering it completely inactive. To assess these risks, sterility testing is done to confirm the absence of viable microorganisms, with sterility assurance levels (SAL) set at no greater than 10^{-6} viable microorganisms. The SAL value expresses the probability of a microorganism's survival after sterilization.

Bioburden testing complements sterility testing by quantifying the microbial load present on materials or the surfaces of the materials. Bioburden is typically expressed as total viable count (TVC). Bioburden testing includes both the total aerobic microbial count (TAMC) and the total combined yeast and mould count (TYMC). Together, sterility and bioburden testing are essential components of quality assurance and regulatory compliance in pharmaceutical manufacturing, ensuring both product integrity and safety.

Methods for microbial quality control are outlined in the different pharmacopeia. The methods for microbial quality control that are described in the pharmacopoeia include membrane filtration, and plate count. These methods rely on incubation periods of 3–5 days for bioburden testing and up to 14 days for sterility testing. Membrane filtration and plate counting are the preferred methods due to their reliability and accuracy.

The pharmacopoeia also provides detailed sample preparation protocols for standard formulations, such as water-soluble products, water-insoluble non-fatty products, fatty products, and transdermal patches. However, no standardized methods of microbial quality control for formulations, such as DelSiTech™ silica-based drug delivery systems exist. DelSiTech™ products, which incorporate active pharmaceutical ingredients (API) into biodegradable silica microparticles or microparticlehydrogel composites, face challenges in addressing microbial contamination. During the manufacturing process of the silica-based drug delivery systems, specifically during spray drying, silica microparticles have potential exposure to microbial contaminants.

The conventional sterility and bioburden testing methods are often unsuitable for silica-based drug delivery products due to the limited solubility of silica in neutral aqueous solutions and buffers used

in standard microbiological assays. While silica dissolves in fluoride-containing solutions (e.g., ammonium bifluoride or hydrofluoric acid) or strong bases (e.g., sodium hydroxide or potassium hydroxide), these conditions typically inactivate microorganisms, which complicates the microbial enumeration and testing accuracy.

There is a need for the development of a novel, adaptable microbial quality testing method that is suited for silica-based drug delivery systems. Innovative approaches must account for the physical and chemical properties of silica while ensuring compatibility with microbial viability assays, thereby enabling accurate and reliable sterility and bioburden testing for these advanced pharmaceutical products.

The aim of the thesis work was to develop a microbial quality testing method for DelSiTech silica based drug delivery products. The instrument that was chosen for the method development was Raman spectroscopy as it has previously shown potential in detecting micro-organisms even in low concentrations. Raman spectroscopy could replace the conventional methods sterility testing that are described in the pharmacopoeia. The methods currently described in the pharmacopoeia are not suitable for silica-based products and additionally require significant time and resources.

Raman spectroscopy is considered a sensitive and specific method that requires minimal sample preparation, allows for rapid analysis of multiple samples, and performs rapid classification of microorganisms. Raman-based technologies offer a promising alternative for assessing the microbial quality of pharmaceutical products. Raman spectroscopy has been successfully used in clinical practices for identifying microbes on a single-cell level, even in complex samples.

2 Raman spectroscopy

The Raman effect was first theoretically predicted by Smekal in 1923, and it was experimentally confirmed by C.V Raman and K.S. Krishnan in 1928. [1] They observed the inelastic scattering of light, a phenomenon where a small fraction of the scattered light changes its wavelength when it interacts with molecules. [2] The Raman effect is based on interaction of light with the molecular vibrations in a sample. When monochromatic light that is typically from a laser is directed at a sample, most of the light is scattered elastically. This elastically scattered light is known as Rayleigh scattering and the wavelength of the light remains unchanged. Small fraction of the light is scattered inelastically however, resulting on a shift in the light's wavelength. This inelastic scattering is known as the Raman scattering.[2] Raman spectroscopy provides information on the vibrational modes of the molecules in the sample and creates a unique "fingerprint" for each molecule. [1]

Nowadays Raman spectroscopy is a powerful vibrational spectroscopic technique that can be used to obtain information on the structures of molecules on a variety of materials.[1] Raman is suitable for organic and inorganic materials and has found many applications in many fields of research. The applications have expanded because of advancements such as surface-enhanced Raman spectroscopy (SERS) and tip-enhanced Raman spectroscopy (TERS). [3] The fields of study, where Raman spectroscopy has been used in include material characterization, geology, forensic science and pharmaceuticals.[4]

One of the rising applications of Raman spectroscopy is using it to identify and characterize different microbes on a single-cell level. This is due to the fact that bacterial infections have become a significant public health concern due to the rapid spread of antibiotic-resistant bacteria.[5] As Raman spectroscopy provides a unique "fingerprint" for each molecule, it can also do the same for different bacterial strains, so a strain of bacteria can be identified in minutes using Raman spectroscopy. [6] One of the main advantages that Raman spectroscopy has in studying bacterial samples, is the non-destructive nature of the technique, meaning that the same sample can be studied multiple times. Another great advantage is the ability to detect bacterial infections even at low concentrations. [7]

2.1 Basic principles of Raman spectroscopy

Vibrational spectroscopy techniques include infrared and Raman techniques. They are techniques that study intramolecular vibrations of molecular bonds, when they are irradiated with light. [8] Raman spectroscopy especially is a solid and versatile tool in analysing several materials in a non-destructive nature.[3] Since the development of the first commercial Raman spectrometer in 1953, advances in lasers and detectors and the discovery of new phenomena have expanded the use of this technique in several research fields.[4] Raman spectroscopy has provided more detailed knowledge of materials, with a special focus on carbonaceous materials, for example graphite.[3]

Raman spectroscopy is a non-invasive technique that does not require the use of labels. During Raman spectroscopy measurements, molecular bonds are excited to cause vibrations with visible or near-infrared light to produce a spectrum of vibrational bonds in seconds.[9] Raman spectroscopy provides an unique fingerprint to each substance which allows for precise analysis of chemical composition and molecular structure.[2] Raman spectroscopy is widely applied in various fields, such as biomedicine, forensics science and materials science. The technique is highly applicable due to

its many advantages over other techniques, such as the ability to provide detailed molecular information, minimal sample preparation, and non-destructive nature.[4]

Technological advances in the instrumentation of Raman spectrometers have increased the possible applications for Raman spectroscopy. The technological advancements include Rayleigh filters and high-throughput optics, for example.[10] Other enhancements Raman spectroscopy has acquired are new Raman techniques such as surface-enhanced Raman spectroscopy and coherent anti-Stokes Raman spectroscopy (CARS).[2] The continuous advancements in Raman technology are expanding its applications, making it an indispensable technique in scientific research and industrial processes.

As mentioned before, Raman spectroscopy is a non-destructive technique, which means that it is suitable even for precious and sensitive materials. The non-destructive nature also means that the measurements do not damage the sample, so measurements can be easily repeated on the same sample. Raman spectroscopy is also suitable for both, organic, and inorganic materials.[4] Raman spectroscopy also has one major advantage over infrared spectroscopy, which is that Raman signals are not affected by the presence of water in the sample. So, Raman spectroscopy can be applied where infrared analyses are not reliable because of the presence of water.[3] Another advantage of Raman spectroscopy is that minimal sample preparation is requires which allows for rapid analysis of multiple samples.[11]

Even though the technique comes with many advantages, it does have its drawbacks. One of the major drawbacks is fluorescence. Fluorescence can interfere with Raman signals, especially when studying biological samples. But the issue of fluorescence can be fought for example, by using a specific laser wavelength.[10] Another disadvantage is that it is impossible for samples to decompose under high excitation intensities as the temperature is fairly high. So, the technique is not completely non-destructive in nature.[11] Raman spectroscopy also produces large, complex data sets that can be hard to interpret. This issue can be fought with multivariate analysis approaches, which help extract meaningful information.[10]

Raman spectroscopy also suffers from a difficulty in developing a quantitative robust and trustworthy method of data analysis.[3] Raman scattering is also a weak phenomenon that can easily be overshadowed by for, example fluorescence. There have been improvements regarding the weakness of the signal from Raman scattering. For example, CCD detectors are used to improve the signal, but the problem still exists.[4] Another problem with Raman signals is that the presence of highly active Raman species, such as carbon particles can mask the presence of other species.[3] The equipment is also quite expensive, so it is not used regularly in analysis.[11]

2.1.1 Raman effect

Matter can interact with electromagnetic radiation through either absorption, transmittance and/or scattering phenomena. The process of absorption requires that the incident photon's energy matches with energy gap between the two electronic energy levels. Scattering processes instead do not require the presence of matching energy levels. The scattering mechanism occurs when a photon interacts with a crystal lattice or a molecule. The interaction induces a distortion of the electron cloud and changes the species polarization involving virtual states. The virtual state is short lived, and the electron is left in the real electronic level of the system as it decays, and the photon then departs from the system. [3] If the energy of the scattered photon matches the incident photon the scattering is elastic and is also known as Rayleigh scattering. If the energy does not match it is inelastic scattering.[1]

Inelastic scattering can be defined as the loss or gain of the photon energy, which has equal energy to the energy difference between the initial and final electronic levels. Stokes scattering is when the outgoing photon has a lower energy than the incoming one. Anti-Stokes scattering is the opposite, so when the outgoing photon has a higher energy than the incoming one. The Raman shift is defined as the energy difference between the incoming photon and the outgoing one.[3] This shift provides a molecular fingerprint that is unique to each molecule, making Raman spectroscopy a powerful tool especially for molecular identification and characterization. [4] So, the Raman effect occurs when light interacts with molecular vibrations, rotations, or other low-frequency modes in a material, and it leads to inelastic scattering of photons. The phenomenon was theoretically predicted by Adolf Smekal in 1923 and experimentally confirmed by Chandrashekhara Venkata Raman and K. S. Krishnan in 1928.[1]

The Raman effect is utilized in Raman spectrometers, where monochromatic light, usually from a laser, is directed at a sample so that the light can interact with the molecules in a sample. The irradiation of a molecule with a monochromatic light will always lead to both elastic and inelastic scattering.[2] Most of the photons are scattered elastically, meaning that they have the same wavelength as the incident light. A small section is scattered inelastically, which results in a change in energy that corresponds to the vibrational energy levels of the molecules. This is the Raman effect, and it can also be divided into Stokes and anti-Stokes scattering. The different energies of the different types of scattering can be seen in the Jablonski energy diagram in Figure 1. The intensity of Raman scattering is dependent on the polarizability of the molecule's electron cloud. Vibrational modes that can cause a change in polarizability are Raman-active and will produce a Raman signal.[4]

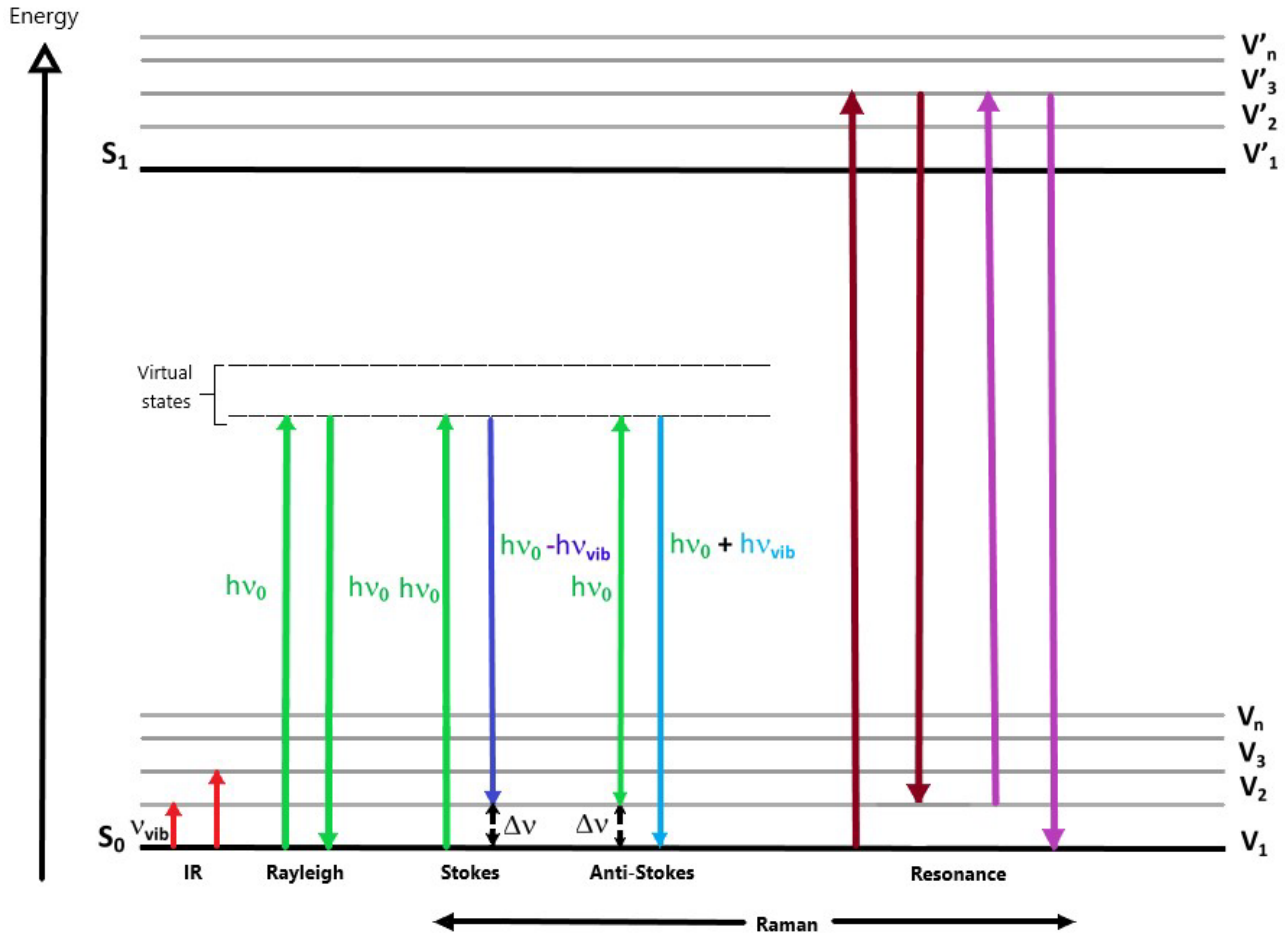

Figure 1. Jablonski energy diagram that shows the transitions of infrared absorption, Rayleigh, Raman Stokes, anti-Stokes and resonance Raman scattering. Interpreted from [8]

Raman scattering is a very weak phenomenon compared to Rayleigh scattering, as only one in 10^8 scattered photons will undergo Raman scattering. As the phenomenon is so weak, all Raman spectrometers are equipped with components to remove the Rayleigh scattering. Usually, the component is a notch filter.[3] Some materials are not Raman-active and as a result produce a weak Raman signal. Water is one of these materials that provide a weak Raman signal, which allows for the analysis of aqueous solutions without significant interference. [4]

2.1.2 Instrumentation

The instrumentation used in Raman spectroscopy consists of several key components that include a light source, sample light delivery and collection system, and a detection system. [4] Despite the weak nature of the Raman signal, modern advancements in the instrumentation have made Raman spectroscopy applicable even in complex samples.[12] For example, advancements such as surface

enhanced Raman spectroscopy (SERS) and resonance Raman spectroscopy (RRS) have significantly increased the sensitivity and application possibilities of Raman spectroscopy.[13]

The light source used in Raman spectroscopy is typically a laser. Commonly used lasers include diode lasers, which are compact and efficient and are also able to provide a stable output that is necessary for reliable Raman measurements.[12] Lasers are used because they provide monochromatic light that is needed for excitation. [13] There are several different laser types that one can choose from, and the choice of laser can be crucial in achieving reliable results when measuring due to the weak Raman signal.[12] Raman spectroscopy utilizes various laser sources, including argon ion lasers, which operate at wavelengths of 488 nm and 514.5 nm and krypton ion lasers which operate at wavelengths 530.9 nm and 671.1 nm. There are also helium-neon lasers, diode lasers, and near infrared laser which operate at higher wavelengths. The laser is selected for each sample based on its ability to reduce fluorescence, minimize sample damage, and provide the necessary excitation energy for Raman scattering.[4]

Next key component in the Raman system is the component responsible for the delivery and collection of light. In Raman systems the light is delivered to and collected from the sample using fibre optic probes. These probes are typically designed to minimize interference from Raman-active materials within the probe itself, such as silica. This design is to ensure a robust and repeatable measurement.[12] Another possible way to deliver and collect light is an articulated arm. The same system is often used for delivering the excitation light to the sample and collecting the scattered light. This simplifies the optical setup and ensures the efficient use of light. [4]

The detection system in a Raman spectrometer typically consists of two components a spectrograph and a detector. [4] A spectrograph disperses the collected light into its component wavelengths.[13] Filters can be used to isolate the Raman signal from the intense Rayleigh scattered light. Notch filters, holographic filters, and edge filters can be used to achieve the isolation.[4] The system can also include a monochromator, which can be used to ensure that only Raman-scattered light is detected, and Rayleigh-scattered light is filtered out.[1] A monochromator is typically used in dispersive Raman instruments. [13]

Charge-coupled devices (CCDs) are silicon-based detectors that are one of the most used in spectroscopic applications. CCDs consist of a one- or two-dimensional grid of tiny resolution elements, known as pixels, embedded on a silicon chip. Each pixel contains multiple metal-oxide semiconductor electrodes, referred to as gates. Silicon-based detectors are ineffective for detecting infrared wavelengths beyond 1100 nm because the photons in the material lack the necessary energy to generate electron-hole pairs in silicon that are required for the detector to perform. Instead,

germanium (Ge) detectors are used. Nowadays the Ge detectors have been improved, and instead indium gallium arsenide (InGaAs) used as they offer enhanced performance over Ge-based devices.[14] Multichannel CCD detectors are utilized for laser wavelengths below 1 μm, whereas single-element, low-bandgap semiconductors like Germanium (Ge) or Indium-Gallium-Arsenide (InGaAs) detectors are employed for laser wavelengths exceeding 1 μm.[13]

A simplified schematic diagram of a Raman instrumentation can be seen in Figure 2.

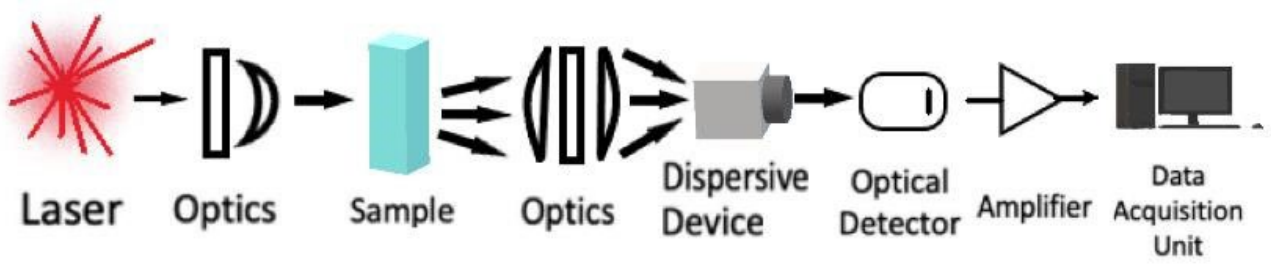

Figure 2. Schematic diagram of a simplified Raman instrumentation. Interpreted from[15].

For accurate Raman measurement, the proper calibration of the spectrometer is essential. It is crucial for the reproducibility of Raman measurements. The calibration process consists of spectral calibration in which, a known standard is used, for example Si, and intensity calibration, which is used to correct for the wavelength-dependent response of the system components.[12] In spectral calibration pixel numbers are converted to wavenumbers and intensity calibration is done to account for the variations in detector response. Regular calibration using standard light sources ensures consistency and reliability of the data.[4] Different data processing techniques can be used to remove background fluorescence, smooth noise, and extract meaningful spectral information.[12]

Raman instrumentation has gone through many advancements, for example the development of portable systems and evolution of data analysis methods.[12] The portable Raman device allows for on-site and field measurement. They are very compact devices that can have the sensitivity and accuracy of traditional laboratory-based spectrometers, but they are also more convenient for various applications. [13] The developed data analysis methods can for example, help with baseline correction with techniques like polynomial fitting, noise reduction using common approaches such as Savitzky-Golay smoothing, and peak detection algorithms can be used to identify locations and intensities of Raman peaks.[12]

There are also several types of Raman instrumentation that can be used to enhance the capabilities and applications of Raman spectroscopy. The types of Raman instruments are: Dispersive Raman

spectrometers, Fourier Transform Raman spectrometers (FT-Raman), surface enhanced Raman spectroscopy (SERS), confocal Raman microscopy, coherent anti-Stokes Raman spectroscopy (CARS), tip-enhanced Raman spectroscopy (TERS), resonance Raman spectroscopy (RRS), stimulated Raman spectroscopy (SRS), spatially offset Raman spectroscopy (SORS), and others.[1,12]

Raman spectrometers are either dispersive or non-dispersive.[13] Dispersive Raman spectroscopy is commonly used in standard Raman spectrometers. The technique uses a diffraction grating or prism to disperse the scattered light.[1] Dispersive Raman spectroscopy is suited for a wide range of applications because of the high resolution and sensitivity it can provide.[4] Fourier transform Raman (FT-Raman) spectrometers utilize a Michaelson interferometer for light dispersion and they are often paired with near-infrared (NIR) lasers to minimize fluorescence interference. FT-Raman instruments are non-dispersive.[13] FT-Raman is commonly used for samples that fluoresce under visible light excitation as the NIR laser is used to minimize the fluorescence interference.[4]

Surface-enhanced Raman spectroscopy (SERS) enhances Raman signals by using roughened metal surfaces such as, silver or gold, which increase the electromagnetic fields near the surface, which leads to an increase in the Raman scattering.[1] The roughened metal surfaces are metallic nanostructures, for example gold nanoparticles. The main advantage of the technique is that it significantly increases sensitivity so that samples even with low concentrations can be detected. It also allows for single-molecule detection.[4] Another technique that utilizes metals is tip-enhanced Raman spectroscopy (TERS). TERS combines a scanning probe microscopy with Raman spectroscopy.[1] The metallic tip enhances the Raman signal, which allows for nanoscale chemical imaging of surfaces. As the metal tip is brought close to the sample, the localized electric field at the tip enhances the Raman signal.[4]

Coherent anti-Stokes Raman spectroscopy (CARS) is a nonlinear Raman technique that uses multiple lasers to generate a strong anti-Stokes signal.[1] The technique provides high sensitivity and spatial resolution, making the technique ideal for studying biological samples and dynamic processes in real-time.[4] Resonance Raman spectroscopy (RRS) involves the tuning of laser frequency to match an electronic transition of the molecule, which amplifies the Raman signal.[13] RRS technique is useful in studying chromophores and provides enhanced sensitivity for specific molecular vibrations.[4]

Stimulated Raman spectroscopy (SRS) uses two synchronized laser pulses to stimulate Raman scattering. It is a fast and sensitive technique that provides high-speed imaging capabilities. These properties make it suitable for in vivo studies and real-time monitoring of biological processes.[4] Confocal Raman spectroscopy combines Raman spectroscopy with confocal microscopy, which

allows for high spatial resolution. The confocal microscopy makes it possible to focus the laser beam on a small spot on the sample and collects the backscattered light through a pinhole. This helps in obtaining detailed 3D images of the sample.[1]

Spatially offset Raman spectroscopy (SORS) instead collects the scattered Raman light from regions below the surface of a sample by offsetting the collection optics from the laser illumination spot. This technique is valuable in analysing layered structures, such as pharmaceutical tablets and biological tissues. Each type of Raman instrumentation has its unique advantages and is chosen based on the specific requirements of the application, such as sensitivity, spatial resolution, speed, and the nature of the sample being studied.[4]

Portable Raman devices have gained popularity in many fields of research, including forensic science, pharmaceutical, geosciences, art analysis, and planetary exploration. The gained popularity is due to the non-destructive nature of the devices and their ability to analyse a wide range of materials.[16] The advancements on optoelectronics have made it possible to make the spectrometers smaller and have reduced the costs. The non-contact method of obtaining material fingerprints allows for field chemical analysis. [17]

A typical portable Raman spectrometer setup includes a narrowband laser, a CCD-based spectrometer, and an electronic control unit with a user interface. The current standard in portable devices uses a 785 nm diode laser due to its efficient reduction of fluorescence interference, compact size, long lifetime, and availability of spectral databases. However, limitations such as CCD noise and weak Raman signals leave room for improvement.[17] Portable Raman spectrometers with 1064 nm excitation lasers have the potential to expand the types of samples that can be analysed compared to those using 785 nm lasers. This includes the capability to study complex biological samples and detect substances of forensic interest without the issue of fluorescence background emission.[16]

2.1.3 Applications

Raman spectroscopy has found applications in many fields of research. The field of study, where Raman spectroscopy is the most widely applies is material science. Raman spectroscopy can be extensively used to study the properties and behaviours of materials. It can be used to characterize different types of materials, including semiconductors, polymers, and nanomaterials. [2] It can also be used in identifying crystallographic defects, the phase transitions of materials, and different allotropes of carbon, such as graphene and carbon nanotubes. [4]

Another important field of research, where Raman spectroscopy has gained popularity is biological and medical applications. Raman spectroscopy is used to study biological tissues and cells and it can be used in identifying proteins, nucleic acids, and lipids.[2] Raman spectroscopy coupled with multivariate analysis, has been used to classify different types of cancer tissues, providing complementary information to traditional techniques.[10] It has also been used in stem cell research, where it can help with identifying and characterizing stem cells based on their biochemical markers.[18]

In medical applications Raman spectroscopy can be used to detect diseases and monitor biochemical changes in tissues.[2] It can also be used to track drug distribution within cells and to study biochemical responses to treatments. The technique's ability to provide detailed biochemical information at the cellular level suggests it could complement or even replace some current diagnostic methods.[18] One of the main applications of Raman spectroscopy in the medical field is the rapid identification of pathogens in clinical samples, such as blood and urine. The technique is particularly useful in detecting urinary tract infections and other microbial infections.[19]

Raman spectroscopy has also found its way into the field of environmental monitoring. Raman spectroscopy is used in monitoring environmental pollutants and studying their interactions with natural systems. It helps in detecting microplastics in water, analysing soil contaminants, and monitoring air quality.[4] Raman spectroscopy can be used to identify hazardous chemicals and monitor environmental changes. It also plays a role in assessing water quality by detecting trace amounts of contaminants.[2] The portability of Raman spectroscopic devices enables in situ analysis of environmental samples, which is crucial for ecological and environmental monitoring.[20]

On top of environmental monitoring, Raman spectroscopy can also be used to monitor food safety. Raman spectroscopy can be used to detect foodborne pathogens, ensuring the safety of food products by identifying contaminants like salmonella, E. coli, and Listeria.[19] It can also help in analysing the nutritional content and composition of food products. So, Raman spectroscopy is a means of quality control and helps ensure the food is safe for consumers.[2]

Forensic chemistry is defined as a part of chemistry that deals with forensic investigation in the field of specialized chemistry that is required to meet the judicial requirements.[4] Raman spectroscopy has gained popularity in the field of forensic chemistry recently as it is a non-destructive study method, which allows for samples to be studied multiple times.[2] The technique is used to analyse samples such as drugs, fingerprints, explosives, and inks. Another field, where preservation of the sample is important are the fields of art and archaeology. Raman spectroscopy is used in these fields to analyse pigments, binders, and degradation products in artworks and historical artifacts.[4]

Raman spectroscopy has many applications in pharmaceutical industry. It is used in different stages of the manufacturing process such as quality control, and formulation analysis.[2] With Raman spectroscopy active pharmaceutical ingredients (APIs) can be identified and to ensure that the components have uniformly distributed in the pharmaceutical products.[4] It also helps in studying drug interactions and pharmacokinetics by providing detailed chemical composition analysis.[10] In quality control Raman spectroscopy is used in ensuring the consistency and quality of pharmaceutical products by providing bulk chemical analysis and detecting contaminants or variations in formulations.[21] The whole production process can be monitored ensuring the consistency and purity of pharmaceutical products.[2]

3 Raman based technologies in identifying microorganisms

The traditional methods to identify microorganisms rely heavily on cultivation-based techniques. In cultivation-based techniques microorganisms are grown in controlled environments, such as petri dishes or liquid media. After the microorganisms have been grown, they can be isolated, and specific strains can be studied. These traditional methods have a few setbacks.[20] One of the major setback is that the tests can take 2-3 days to yield results.[22] Other methods have been tested to ensure fast and reliable bacterial identification, such as mass spectroscopy, fluorescence immunoassay, flow cytometry and polymerase chain reaction.[23] Molecular biological techniques such as polymerase chain reaction (PCR), while faster, are expensive and require highly trained personnel.

Molecular diagnostics are rarely the only method used to identify microorganisms. So, there is a need for a technique that can be used to rapidly identify microorganisms.[24,19]

Fast and reliable identification of microorganisms is a key component in many fields of study, including environment, food quality, and medical diagnosis. In the food industry, quick identification of pathogens can prevent spoilage, and ensure product hygiene, which provides companies with significant savings and can increase product self-life. All the different Raman spectroscopy techniques are gaining popularity in these fields as a means to identify microorganisms.[25]

The advantages of Raman spectroscopy compared to currently applied techniques in identifying microorganisms are its rapid nature, it is an efficient technique, and it is minimally invasive. The technique works by detecting molecular vibrations that provide a unique spectral fingerprint of

bacteria. Raman spectroscopy is also label-free and requires minimal sample preparation. However, it has challenges like weak Raman signals, and interference from fluorescence.[7]

Confocal Raman microspectroscopy has been used to identify microorganisms directly from microcolonies after 6 hours of culture. The method is suitable for the analysis of small sample volumes, which makes it suitable for rapid microbial identification.[24] Current applications often require bacterial culture to increase the biomass and signal strength, but surface-enhanced Raman spectroscopy can amplify the signals, making it possible to detect low-concentration samples without any culture.[7]

In addition to requiring time for cultivation of microorganisms, another major setback of the traditional methods to identify microorganisms is that some microorganisms are not easily cultivable under laboratory conditions. This can lead to only a small fraction of microorganisms in a sample to be cultivated, and it is especially common in environmental microorganisms.[20] Environmental samples are also often very complex, as they can be a mixture of different microorganisms. With Raman spectroscopy, pathogens can be detected even from complex matrixes including, soil, food, and body fluids with Raman spectroscopy.[25]

Raman spectroscopy stands out due to its non-invasive nature, rapid analysis, and comprehensive data output. It can also be applied to a wide range of organisms, such as bacteria, fungi, and even viruses. The method is also consistent regardless of the sample type, whether dealing with young, old, or inactivated bacteria. It is adaptable to different sample types through options like varying excitation wavelengths or enhancing Raman signals for better detection sensitivity.[25] Raman spectroscopy can identify even single bacterial cells with high accuracy.[23]

Microbial samples are typically analysed in liquid form. However, the strong infrared absorption of water can interfere with the spectral analysis of other components within the microorganism, making infrared spectroscopy unsuitable for liquid samples. In contrast, Raman spectroscopy is well-suited for studying aqueous materials because water exhibits a weak Raman signal due to the asymmetry of its molecular bonds.[20]

Raman spectroscopy provides spectral fingerprints of microorganisms, which allows for high specificity in identifying different species and strains based on minute biochemical differences. In the Raman spectra, the complete molecular makeup of the microorganisms can be seen, comprising of many different vibrational modes of reliable taxonomic markers, such as DNA/RNA, proteins, lipids, and carbohydrates.[25]

While Raman spectroscopy has shown great promise for rapid and non-invasive microorganism identification, several challenges need to be addresses for it to become a routine clinical tool. These include improving signal quality, developing better computational tools, and creating standardized databases of, for example various bacterial species.[7] A robust database of Raman spectra and proper validation are essential for accurate identifications of microorganisms. Raman spectroscopy could also be integrated with other detection methods to achieve broader applications. [19]

Advanced statistical methods can also be applied to enhance the identification process by handling large datasets and identifying phenotypic differences.[19] Machine learning and statistical methods are essential for analysing the complex data generated by Raman spectroscopy.[7] Advanced statistical analysis methods, such as principal component analysis (PCA) and support vector machines (SVM), are often employed to enhance the precision of detection and identification.[25] Further research and development is needed to bridge the gap between laboratory research and clinical applications.[7]

3.1 Raman spectroscopy in bacterial infections

Bacterial infections pose a significant public health challenge. Rapid identification and characterization of pathogens is crucial for effective treatment and safety of patients.[7] The rapid identification of pathogens would also lead to reduced healthcare costs and would help in mitigating the rise of antimicrobial resistance.[26] Antimicrobial resistance is a growing threat towards global health. Antimicrobial resistance can lead to treatment failures and fatalities. There is a growing need for antimicrobial susceptibility testing (AST) as the current methods are slow and labor-intensive.[5]

Traditional methods of microbial identification are effective but as mentioned their downfall is that they require a significant amount of labour and are time consuming. The time-consuming nature of the traditional methods leads to delays in obtaining laboratory results which can then lead to inappropriate antibiotic prescriptions and increased antimicrobial resistance. [27] Traditional methods for bacterial identification include culture techniques, biochemical tests, and serological tests. Molecular methods like PCR and next-generation sequencing (NGS) have improved the speed and accuracy of bacterial diagnostics but can be costly.[7]

Raman spectroscopy has emerged as a promising fast, non-culture-based technique for identifying microorganisms at a single-cell level, making it a valuable tool for point-of-care diagnostics.[26] Raman spectroscopy could be integrated into point-of-care devices, which could provide bedside diagnostics and enable immediate therapeutic decisions.[27] Raman spectroscopy offers reduced

culturing time, minimal sample handling and faster results compared to traditional methods, and with proper standardization and optimization, the technique can significantly enhance diagnostic microbiology. The timely results provided with Raman spectroscopy could aid in effective antimicrobial therapy and reduce the reliance on broad-spectrum antibiotics.[24]

Different Raman technologies can be used in identifying microorganisms. For example, microRaman spectroscopy is effective in studying both bulk and single-cell analysis. Combining microRaman spectroscopy and support vector machine the average recognition rate was as high as 89.2% at the strain level, and 93.6% at the species level. The micro-Raman system used in the study was a standard dispersive Raman microscope equipped with an optical microscope, which enables single-cell analysis for microbial identification.[28] Surface enhanced Raman spectroscopy is used as a method for antimicrobial susceptibility testing (AST) in clinical microbiology. SERS is especially useful when the sample volumes are small. SERS has potential in real-time pathogen identification, which can be detrimental to effective infection disease management, especially in severe conditions, such as sepsis. Compared with the traditional methods, SERS can provide identifications in hours rather than days.[27]

Multi-excitation Raman spectroscopy (ME-RS) in combination with whole-genome sequencing (WGS) and SVM analysis achieves high classification accuracies. With this method, the species level identification was 99.93% and gram-negative vs. gram-positive differentiation was 100%. In the method ME-RS provides quick preliminary results, while WGS offers comprehensive genomic insights. Another Raman technique used in microbial identification is coherent anti-Stokes Raman scattering (CARS). It offers high sensitivity and specificity, making it suitable for identifying pathogens directly from clinical samples.[5] SERS is also capable of identifying pathogens directly from complex biological samples, such as cerebrospinal fluid, blood, urine, stool, and wound smears.[27]

Despite its potential in microbial identification, Raman spectroscopy faces several challenges in clinical laboratories. The main issue is the lack of standardization. There are no well-annotated and standardized databases of microbial Raman fingerprints.[26] The integration of artificial intelligence with Raman spectroscopy could improve the data analysis and identification accuracy. [5] Raman spectroscopy combined with deep learning could significantly enhance the efficiency of bacterial diagnostics and aid in the appropriate prescriptions of antibiotics.[29] Another issue is the high instrumentation cost; the initial investment is high. [26]

The third major issue is variability in spectral data due to differences in instruments and sample preparation methods.[26] Other issues are the need for improves understanding of Raman spectra, and

the reproducibility of spectral data.[5] Data processing algorithms are crucial for improving the interpretability of spectral data.[30] For example, vector correction methods can be used to effectively subtract medium signals, which results in reproducible bacterial spectra. [24] Data processing techniques such as principal components analysis (PCA) can be combined with Raman spectroscopy to increase the accuracy of detection.[31]

Future research and development in this field could lead to the widespread of Raman- based technologies in clinical microbiology laboratories.[27] For Raman- based techniques to reach their full potential in clinical laboratories, there are some issues that need to be addressed. The most pressing issue is the creation of standardized and annotated Raman spectral libraries for various pathogens.[26] Other improvements include the integration of Raman techniques with other diagnostic technologies, such as fluorescence and microfluidics to broaden their clinical applications.[5] The instrumentation could also go through updates, such as automatization and miniaturization.[26] There is a need for continued research and development to overcome existing challenges and fully realize the benefits of these advanced diagnostic tools in identifying pathogens.[5]

3.2 Gram-positive and Gram-negative bacteria

Bacteria can be divided into two groups gram-negative and gram-positive bacteria. The division to gram-negative and gram-positive relies on the response of bacteria to Gram staining. Christian Gram developed the staining regimen in 1884 for light microscopy. Gram staining is used to differentiate these two types of bacteria based on the chemical composition and structural format of their cell walls. In gram staining the samples are treated with crystal violet to determine if the sample is gram-positive or gram-negative bacteria, and because of the thicker cell wall structure the crystal violet stains the gram-positive sample, making it remain purple when wiped with the decolorizing alcohol step.[32]

3.2.1 Gram-positive bacteria

The cell walls of gram-positive bacteria consist mainly of a thick peptidoglycan layer, which can be up to 100 nm thick. The layer is composed of repeating units of disaccharides N-acetylglucosamine (NAG), and N-acetylmuramic acid (NAM) that are cross-linked by short peptide chains. Other important components of the gram-positive cell walls are teichoic acids (TAs) and lipoteichoic acids (LTAs).[33] The thick peptidoglycan layer provides mechanical strength and contributes to the

retention of the Gram stain. Gram-positive cells lack an outer membrane, and they are simpler in structure compared to gram-negative bacteria. The teichoic acids contribute to cell wall maintenance and ion regulation.[32] The cell wall structure of a gram-positive bacteria can be seen in Figure 3.

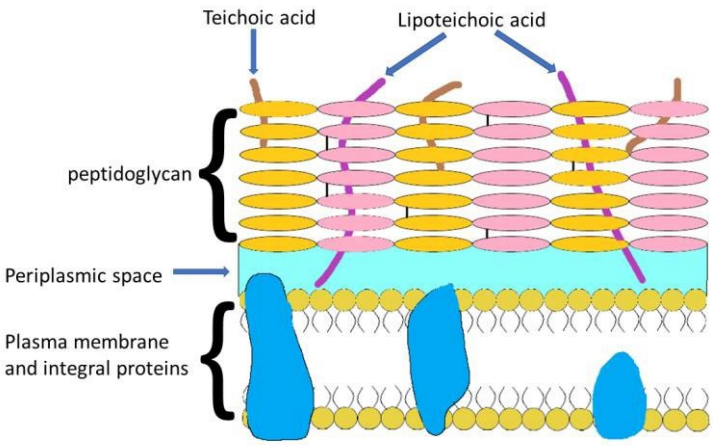

Figure 3. Simplified configuration of the cell wall structure of gram-positive bacteria. Interpreted from [34]

Some gram-positive bacteria, such as Streptococcus and Bacillus species have an additional capsule made of polysaccharides or polypeptides. This capsule enhances their virulence by protecting the bacteria from host immune defences.[33] The inflammatory response triggered by gram-positive bacteria is typically less severe compared to gram-negative bacteria.[35] The lipoteichoic acids give gram-positive bacteria an anionic surface, which makes them more susceptible to antibiotics that target the cell wall.[36] The exposed peptidoglycan layer is exposed directly to environment due to the lack of an outer membrane, which makes it also more susceptible to antibiotics that target peptidoglycan synthesis.[33]

Gram-positive bacteria undergo a turnover of their peptidoglycan during growth, with older layers being hydrolysed by enzymes. New peptidoglycans are synthesized to maintain a cell shape and integrity. Membrane vesicles are historically thought to be unique to gram-negative bacteria, but studies have shown that gram-positive bacteria also produce membrane vesicles. The membrane vesicles are typically derived from the cytoplasmic membrane. They play a role in transporting enzymes, virulence factors, and even antibiotic resistance proteins.[33]

3.2.2 Gram-negative bacteria

Gram-negative bacteria have a more complex cell envelope consisting of an outer membrane, a thin peptidoglycan layer, and an inner plasma membrane. The outer membrane is unique to gram negative bacteria, comprising of lipopolysaccharides (LPS), proteins and phospholipids. The outer membrane serves as a barrier to harmful substances but allows for nutrients to pass through porins.[32] The peptidoglycan layer is only 2-7 nm thick, which is a lot thinner compared to the gram positive cell's peptidoglycan layer. The outer membrane of LPS provides a strong barrier against many antibiotics and hydrophobic antimicrobial agents and contributes to the bacteria's pathogenicity. The thin peptidoglycan layer is located between the outer membrane and inner plasma membrane, making it more difficult to penetrate.[36]

The outer membrane LPSs plays a crucial role in triggering a strong immune response, often leading to a more severe systemic inflammatory response. Gram-negative bacteria are associated with a higher release of proinflammatory cytokines compared to gram-positive bacteria, and this is due to the presence of LPS of the outer membrane which gram-positive bacteria lack.[35] Between the outer membrane and plasma membrane lies the periplasmic space, which is filled with a gel-like matrix. It contains various enzymes, binding proteins, and transporters that are crucial for cell survival.[32] The periplasmic space houses enzymes that contribute to nutrient processing, antibiotic resistance, and cell wall maintenance.[33] There are also components that are involved in synthesizing and maintaining the peptidoglycan layer.[32] A simplified cell wall structure of Gram-negative bacteria can be seen in Figure 4.

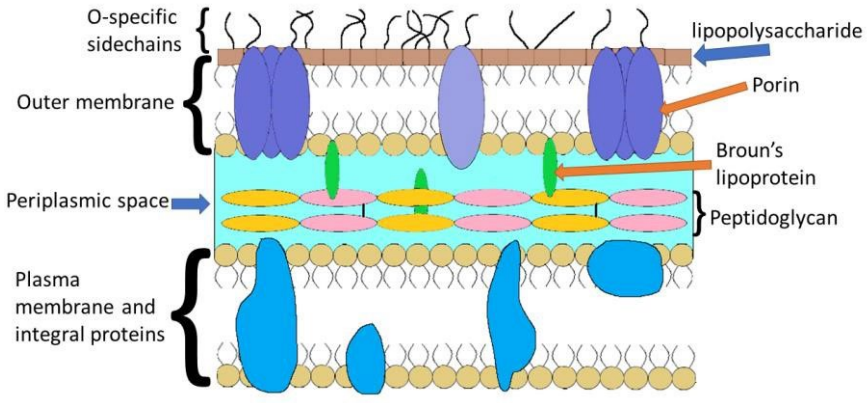

Figure 4. Simplified configuration of the cell wall structure of gram-negative bacteria. Interpreted from[34].

Due to the thin peptidoglycan layer and the presence of an outer membrane, Gram-negative bacteria lose the primary Gram stain (crystal violet) during Gram staining.[32] Gram-positive bacteria retain the crystal violet dye and appear purple, while gram-negative bacteria lose the dye and take up the

counterstain (safranin), appearing red due to their differences in cell wall structure. Gram-negative bacteria also release outer membrane vesicles (OMVs), which serve as vehicles for transporting toxins, enzymes, and other molecules that contribute to infection and survival.[33] OMVs are small spherical structures containing outer membrane components and periplasmic materials. They are also used in nutrient acquisition, and communication with other bacteria.[32]

The key differences between the gram-positive and negative bacteria include the significant difference in the thickness of the peptidoglycan layer, gram-positive bacteria have a much thicker layer. The second key difference is the outer membrane, which only the gram-negative bacteria have. [33] Gram-negative bacteria have a more complex cell wall structure, including the outer membrane and membrane vesicles. Only gram-negative bacteria have a well-defined periplasmic space, which contains numerous enzymes and proteins essential for cell metabolism.[32]

Even though both of the bacteria types produce the membrane vesicles, the mechanisms and challenges behind the production differ due to the structural differences in their cell walls.[33] In conclusion, due to the more complex cell wall structure, gram-negative bacteria are more versatile in various environments, while gram-positive bacteria are more robust despite their simpler structure due to their thick peptidoglycan layer.[32]

*3.2.*3 Raman spectroscopy of bacteria

Raman spectroscopy provides information into both the chemical composition and biomolecular structure of the organism during bacterial sample analysis. [37] With Raman spectroscopy it is possible to distinguish even between different growth phases of single bacterial species.[23] Unlike other commonly used techniques to identify bacteria, Raman spectroscopy records a comprehensive molecular profile of the sample that is being studied. It detects a wide range of vibrational modes linked to taxonomic markers such as DNA/RNA, proteins, lipids, and carbohydrates, as well as non-species-specific components like carotenoids.[25]

Raman spectroscopy is capable of detecting all molecular vibrations within an individual microbial cell. Each single-cell Raman spectrum contains over a 1000 distinct Raman bands. The bands provide critical information about macromolecules such as proteins, nucleic acids, lipids, and carbohydrates.[20] Microbial Raman spectra reflect both genotypic and phenotypic features, which is why the spectra are often referred to as spectral fingerprints. Different microorganisms exhibit unique Raman spectral signatures, as variations in proteome composition, cell wall structure, and other biochemical characteristics create subtle but distinctive spectral differences.[25]

The width of Raman bands is influenced by both structural and crystalline properties of the analysed compound. The majority of Raman bands associated with biomolecules are found in the fingerprint region.[20] For example, characteristic Raman signals include the C-H stretching vibration at approximately 2930 cm^{-1} and the C-H deformation vibration at approximately 1440 cm^{-1}. Proteins on bacterial samples exhibit the amide I vibration at 1665 cm^{-1}.[37] Raman spectra serve as effective microbial fingerprints, particularly when assessed as a whole spectrum rather than individual peaks.[20]

Raman spectroscopy can differentiate, classify, and identify bacteria, fungi, and yeast at both species and subspecies level.[25] When distinguishing Gram-positive bacteria from Gram-negative bacteria, studies have shown notable differences in Raman peaks at 540 cm^{-1} and 1380 cm^{-1}. These spectral variations are primarily attributed to glycosidic bonds in N-acetylglucosamine and N-acetylmuramic acid, which are key components of peptidoglycan in bacterial cell walls.[37] Certain biological macromolecules exhibit specialized Raman bands that can be used as useful biomarkers for identifying microorganisms and analysing intracellular content. For example, poly-βhydroxybutyrate (PHB), a common bacterial storage polymer, is characterized by a strong Raman band at 1735 cm^{-1} due to its C=O stretching vibrations. [20]

Specific strains of bacteria can be identified even from a group of closely related strains with high confidence using Raman spectroscopy.[23] Additionally Raman spectroscopy has been applied in live bacterial studies, which enables the minimization of metabolic variety across different growth phases. This has improved the understanding of cellular dynamics.[37] The technique can also be used to analyse various morphotypes, such as vegetative cells and endospores. [25]

Due to the complexity of Raman spectra and the often subtle spectral differences between the microorganisms that are being studied, advanced mathematical algorithms are required to extract relevant data.[25] The data is often pre-processed using computational methods.[23] Common computational methods in Raman-based microbial analysis are: principal component analysis (PCA), linear discriminant analysis (LDA), partial least squares (PLS) regression, and support vector machines (SVM). These techniques help extract meaningful patterns from Raman spectra.[25] The pre-processed Raman data undergoes chemometric analysis and the results are then compared with the spectra in databases if there is a suitable database. Previously unknown samples that are not originally included in the database cannot be identified.[19]

3.3 Filamentous fungi

Microorganisms are essential for many processes, for example in the food industry. For example, yeasts are required for bread and beer, and lactic acid bacteria are needed for milk products.[25] Filamentous fungi are dynamic organisms capable of moving, synthesizing, and degrading cytoplasm within their structures in response to environmental conditions, nutrient availability, and resource distribution. Filamentous fungi also have several important functions in different ecosystems. Filamentous fungi for example, take part in decomposition of organic matters and release minerals to the environment. They are also important in the movement of nutrients within the fungal hyphae unit. They also take part in releasing chemicals that affect soil chemistry and biology. [38]

The structure of a filamentous fungi consists of two primary components: a rigid hyphal network that provides structural support, and cytoplasm, which moves within the network and adapts to changing conditions. The primary structure component is a hypha, a tubular filament that forms a network known as the mycelium. [38] Filamentous fungi grow by extending these tubular cells, known as hyphae. The hyphae play a crucial role in secreting enzymes and invading host cells.[39] The cell walls of the hyphae are a crucial structure as they provide both integrity and viability to the cell. The cell walls have several biological roles, such as regulating permeability, maintaining osmotic balance, and protecting against mechanical stress.[40]

The fungal cell wall consists of multiple layers. The outer layers vary depending on the fungal species, developmental stage, and environmental conditions. Glucans are the primary structural polysaccharides in the fungal cell wall, and they account for 50-60% of its dry weight.[40] Chitin is another major component of the fungal cell wall, and it gives the hyphae their structural strength. [38] In filamentous fungi chitin makes up around 10-20% of the dry weight of the cell wall. In yeasts chitin comprises only 1-2% of the dry weight. Another major component of the fungal cell wall is glycoproteins. They account for 20-30% for the dry weight in filamentous fungi. Glycoproteins help in maintaining cellular shape and protecting the cell from external substances.[40]

The hyphae structure of the filamentous fungi can grow in multiple directions. This growth style forms a dense network that allows them to explore and exploit their environment for nutrients. The hyphae of filamentous fungi can either be filled with cytoplasm or be devoid of it (evacuated). Cytoplasm-filled hyphae are considered the "living" portions of the fungal network, where metabolic activities such as nutrient absorption, growth, and reproduction occur. The evacuated hyphae are typically older sections of the mycelium that have been abandoned as the fungi shift their resources to more favourable growth regions. [38]

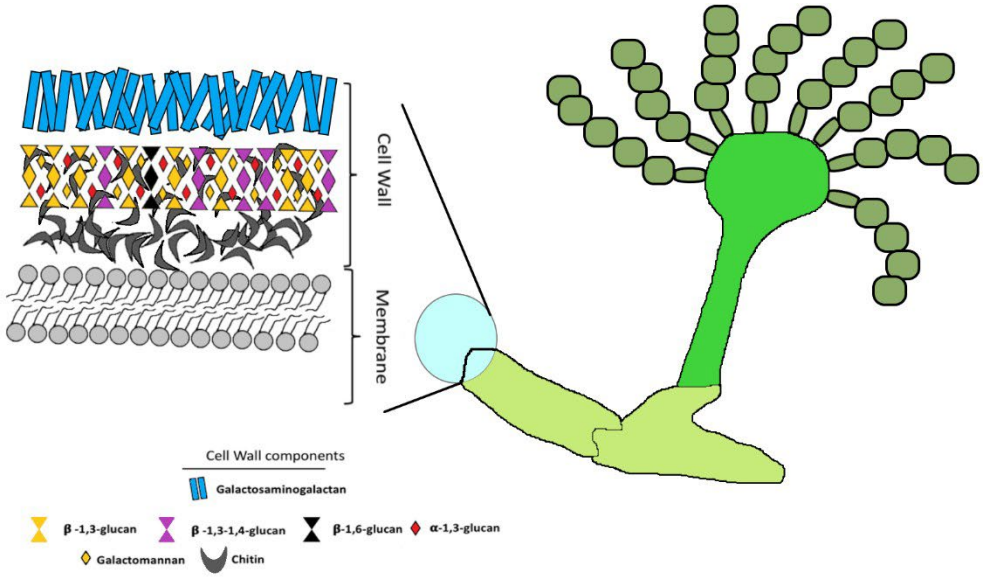

Figure 5. Simplified configuration of the cell wall structure of *Aspergillus fumigatus* cell wall. Interpreted from [40].

These before mentioned structures are also typical for filamentous fungi from the genus *Aspergillus*. [41] The Aspergillus cell wall is composed of two layers. Its main structural components are polysaccharides, and glycosyl hydrolases. [40] The *Aspergillus* genus have been traditionally classified based on morphological characteristics, but molecular studies have shown that many taxonomic groupings need refinement.[42] Species in the *Versicolores* section of the *Aspergillus* genus are characterized by specific conidiophore and conidial structures, but microscopic similarities make species identification difficult.[42]

The outer cell wall layer varies based on fungal morphology, such as between hyphae and conidia. [40] Species in the *Versicolores* section have unique structural features such as biseriate conidial heads and conidiophores with subgloose to pyriform vesicles. The conidia or spores are usually rough walled and greenish in colour. Despite these being common features, the species can be hard to distinguish based on morphology alone because their microscopic structures appear very similar across different species.[42]

When filamentous fungi were first studied, the studying focused mainly on direct observations, without consideration for internal structures or cytoplasmic content. By the mid-1970s, researchers began using biochemical markers, such as ergosterol, and chitin derivatives to assess fungal presence. However, these single-measurement methods could not provide information about the physical structure of fungi. Later on, molecular approaches such as bulk nucleic acid extraction and cloning have been used, but they fail to connect taxonomic and phylogenetic data to specific fungal

structures.[38] Typically, molecular techniques have been used to identify fungi, as traditional morphological methods are insufficient. [42]

The *Aspergillus* genus is widely distributed and includes species with industrial and biotechnical significance. Accurate species identification is essential to understand their distribution and clinical relevance. Microscopic similarities make species identification in the *Aspergillus* genus difficult. Over the years, molecular analysis has helped clarify this section's taxonomy, and currently, 20 species are recognized, with A. versicolor and A. sydowii being the most studied.[42] Advancements now allow for molecular analysis of individual fungal structures, such as hyphae, spores, and fruiting bodies. This capability makes it possible to link specific fungal structures to taxonomic and phylogenetic information, offering a more comprehensive understanding of fungal growth and function within microbial ecology.[38]

Fluorescence imaging techniques have also been used to investigate filamentous fungi. Traditional fluorescence imaging has provided insight into fungal growth, but the technique has limitations in offering chemical specificity and non-invasive analysis. Raman spectroscopy offers a non-invasive alternative to the traditional imaging methods. Raman spectroscopy allows for non-destructive imaging with high chemical specificity. Raman spectroscopy can provide spatially resolved information on intracellular components, such as polysaccharides, proteins, lipids, and cytochromes. It provides a detailed understanding of fungal structures and processes. Using Raman techniques in researching filamentous fungi is still in its early stages.[39]

Raman spectroscopy has provided insights into the internal compositions of filamentous fungi. The full potential of Raman spectroscopy in visualizing fungal subcellular structures remains underutilized. Multivariate data analysis techniques such as multivariate curve resolution–alternating least squares (MCR-ALS) have been used to analyse Raman imaging data. This approach has successfully mapped the spatial distribution of major biomolecules in fungal cells. For example, in *Aspergillus nidulans*, Raman imaging combined with MCR-ALS has allowed for the detailed visualization of intracellular components such as polysaccharides, lipids, and cytochromes. Additionally, it has provided molecular fingerprints of fungal cell wall components and revealed the oxidation states of cytochromes.[39]

Time-lapse Raman imaging with deuterium-labelled glucose has been used to analyse metabolic activity within growing hyphae. The method allows visualization of glucose accumulation at hyphal tips and the incorporation of glucose-derived components into proteins. Time-lapse Raman imaging

provides a powerful platform for studying the metabolic dynamics of filamentous fungi in real time. Another application where Raman spectroscopy can be used in studying filamentous fungi is in fungal identification and biological characterization. For the identification to be accurate, the background fluorescence must be minimized, as it can introduce noise and misleading spectral artifacts. Shifted Excitation Raman Difference Spectroscopy (SERDS) has been developed to address this issue. This method, combined with hydrophobin mutants, confirmed that Raman signals in *A. nidulans* originate from dye molecules within the cell wall.[39]

4 Raman spectroscopy in the pharmaceutical industry

Raman spectroscopy has a significant role in the pharmaceutical industry. It is a versatile, non-invasive, and efficient analytical technique, that has the capability to provide detailed molecular information. These qualities make Raman spectroscopy an ideal technique in pharmaceutical applications.[11] Raman spectroscopy is used in various stages of drug development, from early-phase research to quality control of final products. [43] The technique is particularly useful for characterizing drug formulations, identifying contaminants, and analysing the solid-state properties of drug molecules.[11]

Compared with other commonly used techniques, such as infrared spectroscopy, Raman spectroscopy has several advantages, for example minimal sample preparation, non-invasive testing through packaging, and the ability to study small particles, and all this can be performed in a rapid, non-destructive manner. [44] Another advantage over infrared spectroscopy is the ability to analyse aqueous solutions due to minimal interference from water. [11] Techniques such as confocal Raman microscopy and surface-enhanced Raman spectroscopy (SERS) are also studied in pharmaceutical applications for their enhanced capabilities in probing depths within samples and their increased sensitivity.[44] Raman spectroscopy provides complementary data to infrared spectroscopy, and in many applications, they are both used.[11]

In the pharmaceutical industry, there are various stages of drug development, in which Raman spectroscopy can be applied in. It can be used in the early stages of the process, such as the identification of raw materials.[44] Raman spectroscopy can also be used in preformulation studies, which include solid-form screening, phase transformation analysis, and degradation studies. It helps in identifying the optimal solid form of a drug, understanding phase changes, and monitoring potential degradation in various environments. [43] Drug development is a complex process that requires a significant amount of time, and the process has a high failure rate, especially in the

formulation stage. There is a growing demand for drug products with better efficacy, and patient compliance.[45]

Detailed information on the composition and distributions of components within pharmaceutical products can be provided by Raman spectroscopy. Raman spectroscopy could be combined with artificial intelligence to enhance the efficiency of drug formulation development. For example, artificial intelligence could be used to analyse the complex data generated by Raman spectroscopy to predict the behaviour of formulations and guide the design of new drug producuts.[45] Overall Raman spectroscopy can help in finding the optimal solid form of a drug, understand the phase changes, and monitor potential degradation in various environments during the drug development process.[43] The integration of Raman spectroscopy is proposed as a method to bridge the gap between formulation development and clinical trials.[45]

Bulk products can be studied in a non-invasive method by using Raman spectroscopy. The technique can be used for monitoring drug hydration states, hydration formation, blending processes, and polymorph turnover kinetics.[11] Raman spectroscopy has potential as a process analytical technology (PAT), that can enhance the robustness and efficiency of pharmaceutical manufacturing processes. [46] Raman spectroscopy can be used as a PAT tool for monitoring pharmaceutical manufacturing processes such as crystallization, granulation, and coating.[43] It can also be used as a tool for real-time monitoring and control during pharmaceutical manufacturing. In-line monitoring capabilities are essential for ensuring product quality and process consistency.[46]

Raman spectroscopy can be used throughout the production lifecycle. The techniques applications have expanded significantly due to the technological advancements. These expansions include real time release testing, continuous manufacturing, and statistical process control in pharmaceutical environments.[47] Real-time in-line testing reduces the need for labour-intensive offline analyses, which improves the overall efficiency of the manufacturing process.[46] The efficiency from real time testing is achieved through the immediate detection of any deviations in the formulation process that affect the quality of the final product.[44] Raman spectroscopy improves process efficiency, and enables better control of critical process parameters, which leads to higher quality and more reliable pharmaceutical products.[47]

One of the main applications of Raman spectroscopy is the analysis of pharmaceutical formulations. It is very suitable for the application because of its non-destructive nature, high specificity, and the ability to analyse compounds in various states.[44] The technique is effective in studying the polymorphism of drugs, where crystalline forms of a substance can have distinct therapeutic

properties.[11] Transmission Raman spectroscopy (TRS) can overcome challenges that traditional techniques such as HPLC and X-ray diffraction for quantifying polymorphs face. TRS is effective in quantifying polymorphic content in pharmaceutical formulations, which is an important factor in drug quality and stability. [21]

Raman spectroscopy can also be used in quantification of active pharmaceutical ingredients (API). TRS can be used to analyse pharmaceutical formulations with high precision, even in the presence of interfering signals from capsule shells. TRS allows deeper penetration into samples, which reduces sub-sampling issues and enables for better bulk analysis.[21] Raman spectroscopy is also used to assess the homogeneity of pharmaceutical formulations. By mapping the distribution of different components within a sample, it helps ensure that the drug is evenly distributed throughout the formulation, which is essential for consistent drug performance.[44]

Raman spectroscopy can also be applied to characterizing microstructures in drug delivery systems. Raman chemical imaging has been applied to assess the size distribution within composite tablets. It is being used to study API distribution homogeneity in composite formulated tablets. For

developing innovative drug products, this kind of information that Raman chemical imaging can provide, is extremely important, especially with increasingly complex and highly engineered structures. Raman spectroscopy can also be valuable in characterizing protein and peptide drug delivery systems. A Raman-based method has been developed for monitoring the secondary structure of proteins during frozen and thawed storage.[43]

Another important application of Raman spectroscopy in the field of pharmaceutical industry is quality control. Major part of the quality control of pharmaceutical products is the ability to perform in-line and at-line analysis with Raman spectroscopy. It allows for continuous monitoring of pharmaceutical processes without the need to remove samples from the production line, thereby reducing the risk of contamination and improving process efficiency.[44] Raman spectroscopy can also be used in quality control to assess the solid-state forms of drugs, content uniformity, and detecting counterfeit products. The technique's non-destructive nature and ability to analyse products in their final packaging make it an effective tool for ensuring product integrity.[43] The non-destructive nature of the technique is essential for quality control processes as there is usually a need to preserve the original sample.[44]

Despite the many benefits of Raman spectroscopy in the field on pharmaceutical analysis, the technique does come with a few drawbacks. One of the main issues is the potential interference from fluorescence. Another issue is the high cost of the equipment. There is also potential for

thermal decomposition of samples under high excitation intensities.[11] The drawbacks are outweighed by the benefits, making Raman spectroscopy a valuable technique in pharmaceutical analysis. Raman spectroscopy is a potent technique that complements other methods.[44]

While Raman spectroscopy is a powerful technique, it should be used together with other analytical methods as a part of a multidisciplinary approach to pharmaceutical analysis. It should especially be combined with infrared spectroscopy and advanced imaging techniques.[11] The instrumentation also requires improvements, such as further development of portable devices and the instrumentation being more user-friendly. If these improvements are achieved Raman spectroscopy has potential in fields such as personalized medicine and continuous pharmaceutical manufacturing.[43] Raman spectroscopy has become a highly valuable tool in pharmaceutical analysis due to its several advantages compared to other techniques and it has potential for even more.[44]

4.1 Quality control of pharmaceutical products

Pharmaceutical products can be divided into two groups sterile and non-sterile. It is crucial to study the possible microbial contaminations of both sterile, and non-sterile pharmaceutical products. Microbial contaminants can for example, reduce the efficiency of the drug, make the drug inactive or even cause drug-induced infections. The different Pharmacopoeias have set purity criteria for non-sterile drugs that must be met to ensure the drugs are efficient and safe to use.[48] A bioburden assessment is required for non-sterile products. Bioburden can be defined as the microbial content of a material or its surface. [49] For sterile products, the sterility assurance level (SAL) must be determined. SAL is the probability of viable microorganisms present on a product. SAL is determined after proper sterilization process.[50]

Ensuring the sterility of drug products before their commercial release is a fundamental aspect of pharmaceutical quality control. Standard sterility testing procedures are expensive and limited by their reliance on microbial growth conditions. Traditional sterility testing methods are also time consuming which is their greatest disadvantage.[51] Traditional methods used for bioburden testing, that are outlined in the US and European pharmacopeia, rely on plate-based enumeration of colony forming units (CFU). These methods require 3–5 days for microbial quantification. This delay in gaining result makes traditional methods not suitable for real-time bioburden monitoring.[52]

Bioburden is commonly evaluated using the total viable count (TVC) method. The TVC method involves plating a portion of the sample onto agar or mixing it with agar before incubation. After

incubation microbial growth is assessed. TVC methods for detecting microbial presence include membrane filtration, pour plate, and spread plate techniques. Membrane filtration is a technique, where a sample or rinse is passed through a microbially retentive filter. It is the preferred method as it allows testing for larger sample volumes. The other methods are typically used when filtration is not feasible.[49]

Quality assessment testing is performed both on raw materials and finished products. The testing involves microbial enumeration tests for total aerobic microbial counts (TAMC) and total yeast and mold counts (TYMC).[48] The colony-forming unit (CFU) remains a widely used metric for microbial enumeration, as bioprocessing companies traditionally set alert and action limits based on CFU per mL of sample.[53] Traditional microbiological testing methods, as outlined in the US and European Pharmacopeia, are based on agar plate culture techniques that have been used for over a century. Conventional plate counts for bioburden monitoring typically require an incubation period of 3–5 days for microbial enumeration.[52]

The European Pharmacopoeia is a vital tool for quality assessment as it outlines microbiological specifications, testing criteria, and methods for examining non-sterile pharmaceutical products. Compliance with these requirements ensures both raw materials and finished products meet the required microbiological purity levels.[48] Maintaining sterility in pharmaceutical production requires strict control of cleanliness, personnel intervention, and manufacturing conditions. The manufacturing process of pharmaceutical products requires aseptic processing. In aseptic processing pharmaceutical products are manufactured in a controlled environment, where air supply, materials, equipment, and personnel interactions are managed to maintain microbial and particulate contamination at acceptable levels.[50]

Sterile drug products require absolute freedom from microorganisms. Non-sterile drug products instead only must comply with specific microbiological purity standards outlined in the pharmacopoeia.[48] Sterilization is the process, where all viable microorganisms are eliminated from a product. Sterility assurance level (SAL) is the probability of microbial presence in a sterilized product, and it is typically expressed as 10^{-n}. After terminal sterilization, which is a process that is applied to a product in its final packaging, SAL should be $\leq 10^{-6}$.[50]

The pharmaceutical industry requires a faster and more cost-effective alternatives in detecting bacterial contamination in pharmaceutical products.[51] Ensuring real-time release of pharmaceutical products, including small molecules and biologics, requires continuous in-process monitoring to maintain product quality. Culture-based methods can take 1-21 days for bioburden and sterility

testing, which makes the traditional methods impractical for real-time release testing.[54] In traditional sterility testing methods there is also risk for false positives caused by laboratory handling errors.[51] While the conventional methods for bacterial identification are well-established and dependable, many bacteria are believed to be unculturable, making them inaccessible through this method.[19]

In biopharmaceutical manufacturing, maintaining microbiological control throughout the entire process is essential. Quality control strategies rely on routine bioburden testing, both as an in process control (IPC) during drug substance manufacturing, and for final drug product release.[52] Conventional microbial detection methods provide limited benefits in increased control bioprocessing due to the long turnaround time required for results, which often exceeds the full cycle of a manufacturing process. Rapid microbial detection has been under discussion for a long time, but it has yet to be widely implemented in commercial biopharmaceutical manufacturing.[53] Although microbial contamination is rare, it can have severe financial implications. For instance, large-scale bioreactors used in biologics production can operate at 15 000 litres, with media costs averaging $8 per litre. A single contamination event can result in financial losses exceeding $120,000 due to product loss and downtime.[54] Delays in obtaining bioburden contamination data, sometimes days after production, make traditional testing methods inefficient for real-time process monitoring and contamination control.[53] Even low levels of harmful microorganisms can compromise product safety and reduce or eliminate the drug's therapeutic effectiveness. Contamination can also cause drug-induced infections in patients.[48]

Nucleic acid-based techniques such as polymerase chain reaction (PCR) and next-generation sequencing (NGS) have reduced the detection time to a few hours. Although they provide faster detection times, the techniques still require sample preparation which makes them invasive and not suitable for continuous monitoring.[54] Currently the more effective approach is leveraging current microbial detection capabilities in a two-tiered approach. In the two-tiered approach an initial, less sensitive rapid test is conducted to monitor processes. A secondary more detailed test is performed if necessary. This secondary test provides confirmation and quantification of bioburden presence and identifies the specific microorganisms involved. Assuming daily sample collection, detection does not occur until 72 hours after testing begins. By that point contaminated material may have already reached the final production stage.[53]

A novel approach to the issue of traditional sterility testing methods being slow and labour-intensive is using Raman spectroscopy as a sterility testing and bioburden assessing method. Raman spectroscopy shows promise in the field, especially combined with different data processing

techniques, such as partial least squares discriminant analysis (PLS-DA).[51] Another novel method is combining Raman spectroscopy together with deep learning to detect and classify microbial contaminants. Raman spectroscopy is non-invasive in nature and requires minimal sample preparation which makes it suitable for real-time analysis. Raman spectroscopy with deep learning can accurately identify and classify contaminants based on subtle differences in their molecular composition.[54]

A dataset of Raman spectra for 12 different microorganisms, which are common contaminants in pharmaceutical productions has been developed. The dataset consists of 12 microbial species, including Gram-positive bacteria, Gram-negative bacteria, and fungi.[54] Raman spectroscopy can distinguish between bacterial contaminants and other organic materials in the pharmaceutical drug products, and the accuracy of the technique is as high as 99%. Additionally, the method does not require opening or contamination of the primary packaging of the studied sample which is a major advantage [48]

Raman spectroscopy provides results in minutes, so it is even faster than the nucleic acid-based techniques. This quality also makes Raman spectroscopy suitable for real-time process monitoring.[54] Raman Spectroscopy has been effectively used to detect bacterial components such as lipids, proteins, amino acids, and nucleic acids and can differentiate bacterial strains in water-based solutions and solid pharmaceutical formulations. However, achieving detection limits comparable to standard methods while maintaining high accuracy remains a challenge. Their limit of detection is often too high for sterility acceptance criteria.[51]

Raman spectroscopy has problems with detecting low numbers of bacteria due to weak Raman signals. The problem has been answered using for example, PLS-DA for data analysis, which allows for detection of concentrations of as low as 10 colony-forming units (CFU) per millilitre.[48] Despite the spectral similarities between contaminated and uncontaminated drug products, PLS-DA effectively differentiates samples with bacterial contaminants. Validation using bacterial spore spiked samples resulted in a 99% detection accuracy, demonstrating the potential for Raman spectroscopy combined with PLS-DA being a cost-effective, high-precision sterility testing in pharmaceutical quality control.[51]

A challenge in using Raman spectroscopy paired with PLS-DA is the complex data processing and statistical analysis required for accurate bacterial identification.[51] A major obstacle is also integrating new technologies into existing process control strategies and quality management

systems. [53] Raman spectroscopy also struggles with interference from fluorescent compounds, and other excipients that contribute to the background noise.[51]

Although culturing and nucleic acid- based techniques such as PCR are widely used and reliable for detection of microorganisms, further advancements in detection technologies are needed. Improvements in this field could benefit various applications. Among the alternatives to culturing and PCR, Raman spectroscopy shows promise as a valuable tool in detecting microorganisms.[19] Pairing Raman spectroscopy with other techniques such as deep learning shows even more promise for ensuring the sterility and quality of pharmaceutical products, with the potential to significantly enhance the efficiency of real-time quality control processes.[54]

4.2 Bioburden

Bioburden can be defined as the population of viable microorganisms present in a sample or system. It is a crucial parameter that requires constant monitoring.[52] Bioburden testing is an essential part of process control, as it helps detect contamination early, preventing it from affecting the product's quality. Traditional bioburden testing is a time-consuming process. The most common test is culturing microorganisms on plates, which typically takes 3-5 days to yield results.[53] The traditional testing method is reliable, but it also poses a risk for further contamination due to manual sample handling.[52]

Bioburden testing methods need to be suitable for detecting any microbial contamination. The testing method must be accurately assessed during the sterilization process to ensure product safety and the method to test bioburden must be validated.[55] The method validation includes a documented confirmation process that ensures that facilities, equipment, procedures, and quality control measures lead to expected results.[50] For non-sterile drugs, some level of bioburden is expected, but the bioburden level must be acceptable and needs to be monitored. For sterile drugs bioburden must be controlled until the final sterilization step, which is terminal sterilization.[49] Terminal sterilization is a process where the product is sterilized in its final container or packaging. A sterile product is free from all viable microorganisms.[50]

The traditional bioburden testing methods are not very well suited for continuous manufacturing processes, as the manufacturing cycle can be much shorter than the time required for traditional microbial testing.[53] Key steps in validating a bioburden test include the suitability of the test, which includes ensuring that no inhibitory substances in the product prevent microbial growth in the test.

The effectiveness of the method in recovering the microorganisms from the sample needs to be verified. The enumeration process must be accurate, and the recovered microorganisms must be identified and classified correctly.[55]

As the traditional methods to test bioburden require time and pose a risk for further contamination, Raman spectroscopy offers an alternative method. It is much faster than the traditional methods and can be used as an automated bioburden detection method, that can be used for continuous real-time process monitoring. Raman spectroscopy eliminates the need for manual sampling and speeds up contamination detection significantly.[52] Other faster microbial technologies that offer quicker detection are electrical conductivity measurements, and image processing, which can significantly shorten detection times, and enable timely interventions to ensure product quality.[53]

Results from traditional bioburden tests are expressed as colony-forming unit (CFU) per unit of volume. For example, CFU/mL. [49] Bacterial identifications can also be done with equipment such as mass spectrometry (MS) and especially MALDI-TOF MS. The technique has high throughput and accuracy, but it is not accurate with closely related species differentiation.[7] Monitoring and controlling bioburden is also necessary for non-sterile pharmaceutical products. Bioburden testing for both sterile and non-sterile pharmaceutical products involve estimating the number of bacteria and fungi present in the sample, typically using total viable count (TVC) methods. TVC methods include for example, membrane filtration and pour plate method. [49]

5 Materials and methods

The method creation proceeded in a trial-and-error type of study. Many samples were studied using different methods and parameters and as the project advanced, some methods and samples were discarded as unnecessary or not suitable for the required result. The final product, which is the primary focus of this study, comprises silica microparticles containing active pharmaceutical ingredients, ammonium bifluoride, and various microorganisms.

The methodology involved optimizing signal detection for each individual component of the final product, as well as for various combinations of these components. Ultimately, all individual components were compared to assess their distinct contributions. Measurements for each individual component would be performed both in dry and in solution phase, if possible. For example, the microorganisms would be studied in dry form (lyophilized culture on cellulose filter), in liquid culture, and in solution of ammonium bifluoride.

Various substrate materials were initially tested to determine their suitability for sample analysis. In parallel, different laser types were evaluated to identify the most effective configuration for each sample. For each component intended for inclusion in the final composition, spectral data were acquired under a range of conditions to ensure high-quality signal detection.

Each component was analysed individually to assess its unique spectral features. Particular attention was given to identifying peaks that could be attributed specifically to microorganisms, distinguishing them from signals produced by other materials. To further characterize the microbial signal, serial dilutions were prepared to determine the limit of detection. The most concentrated microbial sample was retained as a potential reference spectrum.

Experimental parameters including laser power, integration time, and number of accumulations were systematically varied for each sample. Initial measurements were conducted using lower settings, which were incrementally increased based on sample stability and signal quality. This approach allowed for the identification of optimal conditions for spectral acquisition across all sample types.

5.1 Instrumentation and measuring parameters

The instrumentation used in the project was the inVia™ confocal Raman microscope by Renishaw. It is a high-performance, research-grade Raman spectroscopy instrument. The instrumentation is equipped with multiple lasers covering a broad range from UV to IR wavelengths. It also has confocal capabilities which allow for precise spatial resolution by minimizing the sampling volume. The inVia™ confocal Raman microscope also uses high quality objective lenses with varying magnifications and working distances. The advantages of the instrumentation include non-destructive and non-invasive sample analysis, and the system is also easy to use, while it is still highly advanced. The instrument can also be used to analyse materials through transparent containers.

With the inVia™ confocal Raman microscope several parameters for doing measurements can be altered to affect the quality of the results. The different parameters that can be altered are choice of laser, laser power, choice of microscope objective, laser exposure time, and adding accumulations. The equipment offers also several other measuring parameters that can be altered. For example, with the grating selection, slit width, and detector settings, the resolution and sensitivity of the Raman measurements can be adjusted to optimize data quality for specific samples.

The choice of laser can greatly affect the results in Raman spectroscopy. It has a huge impact on for example, Raman scattering, fluorescence interference, sample heating, and spectral resolution. Lasers are chosen depending on the application, sample type and desired spectral range. The lasers that were tested during this project were the 532 nm, 633 nm, and 785 nm lasers.

UV lasers (wavelength 200-400 nm) provide strong Raman scattering but face high risk of fluorescence. UV lasers also require specialized optics due to high energy, but they can enable resonance Raman enhancement for certain molecules. Visible lasers (wavelength 400-700 nm) offer a good balance between Raman intensity and fluorescence. This makes visible lasers suitable for a variety of materials. The biggest limitation with these lasers is that for certain samples, for example organic compounds, they have moderate fluorescence. Commonly used wavelengths are 488 nm, 514 nm, and 532 nm.

Near-infrared lasers (wavelength 700-1000 nm) minimize fluorescence interference but suffer with reduced Raman scattering. Commonly used wavelengths are 785 nm, 830 nm, and 1064 nm. They also require more sensitive detectors, for example an InGaAs detector for 1064 nm laser. The sample needs to be taken in consideration, when choosing a laser. Does the sample require minimization of fluorescence or the maximization of Raman intensity.

Another parameter that can be adjusted is the choice of objective. The choice of objective has a huge impact in the quality of measurements and the sensitivity. The choice in objective is also related to the collection efficiency of the Raman signal and sample illumination. The objectives used in this project are the 20x, 50x, and a 50x long-working distance magnification objectives. Other magnifications that are available include for example, the 5x and 100x magnification objectives. Low magnification objectives (5x-20x) offer a larger field of view and longer working distance.

The advantage of lower magnification objectives is that with them it is possible to quickly map out large sample areas. They are also suited for rough surfaces. Medium magnification (50x) offers a good balance between spatial resolution and field of view. This makes it suitable for most general Raman applications. High magnification (100x) provides high spatial resolution but is faced with shorter working distances, which makes it most suitable for thin samples. A higher magnification provides detailed information of small areas.

On top of different magnifications, the objectives also have different numerical apertures (NA). NA determines the light-gathering ability and spatial resolution of the objective. If the NA is higher, it provides a larger light collection angle, which increases the intensity of the Raman signal. A higher

NA means better signal collection, but the drawback is the shorter depth of field. When there is a need to study larger areas, a lower NA is required. A lower NA is more suitable to study samples with lower intensity signals, liquids, and thick samples.

Another parameter that can be altered that the objectives have is the focal length. A shorter working distance is used for high-resolution imaging. It also offers higher magnification and better spatial resolution. A short focal length for flat, thin samples. Long working distance objectives are better suited for analysing thicker and more bulky samples. The objectives can also have different materials and coatings. There are for example, standard glass objectives and quartz objectives.

When the most suitable laser has been found for the sample, another parameter that can be changed is the laser power. With the equipment used in this project, the laser can be altered from 0.1% to 100%. Laser power must also be optimized individually to each sample. With the change in laser power there is a balance between signal intensity and the risk of sample damage. With higher laser power there is also the risk of overexposure, which can saturate the detector and distort the data. The advantage of higher laser power is the increase in the intensity of the Raman signal. It enhances the signal-to-noise ratio, which makes peaks clearer.

When performing Raman measurements, it is a common practice to start with a lower laser power. If the intensity of the Raman signal is not sufficient, the laser power will be gradually increased. Monitoring the sample for signs of thermal damage, peak shifts, or fluorescence interference is needed during the measuring process when the laser power is increased. For example, organic materials and biological samples face problems with thermal damage more often, so a lower laser power is recommended.

Another parameter that can be changed during Raman measurements is the laser exposure time. The laser exposure time determines how long the spectrometer collects light from the sample. The standard laser exposure is 10 seconds. Laser exposure time has a huge impact on the quality of the Raman spectrum. A longer laser exposure time increases the amount of light collected which leads to stronger Raman signals. It leads to enhanced signal-to-noise ratio (SNR), which makes weak Raman peaks more distinguishable. A longer laser exposure time is useful for low-concentration samples and weak Raman scatterers. The drawback is that increasing the laser exposure time can lead to saturation of the detector, if the Raman signal is too strong. A longer laser exposure time can also lead to more fluorescence.

Prolonged laser exposure can also cause thermal degradation of the sample, especially if the sample is sensitive material. Another disadvantage of longer laser exposure time is that the overall

measuring time increases. Shorter laser exposure time provides faster data acquisition. Shorter laser exposure time is suitable for strong Raman-active materials that already produce high-intensity spectra. A shorter laser exposure time means a weaker signal, which can lead to reduced peak resolution. Peaks might become less distinguishable from the background. Shorter exposure time is useful for rapid screening or mapping applications.

When setting up Raman measurements, it is recommended to start with shorter exposure times. The exposure time can be gradually increased if the signal is too weak or noisy. The results need to be monitored constantly to notice signs of thermal degradation, for example. There needs to be a balance between adequate peak intensity and oversaturation and fluorescence of the spectra. If peaks are too weak the laser exposure time needs to be increased, as long as sample damage is not a risk. If the sample is sensitive a lower laser exposure time is required.

Accumulations can be added to measurements. Increasing the number of scans is another way of enhancing the quality of the Raman spectrum. Adding accumulations means repeating measurements multiple times. Fewer accumulations are suggested for samples that have strong Raman signal. For these samples a recommended number of scans would be 1-5. Using accumulations has on effect on signal quality, noise reduction, and overall reliability of the measurements. Accumulations improve peak clarity and baseline stability. But using accumulations adds to the overall time. For example, if the original measuring time was 10 seconds, adding 5 accumulations increases the measuring time to 50 seconds.

Accumulations are useful for detecting weak Raman signals. Increasing the number of scans reduces variability caused by laser fluctuations or detector noise. Fragile samples may require a fewer number of scans, as increasing the number of accumulations rises the risk of sample damage. Continuous laser exposure can heat the sample which may cause increasement of fluorescence. Fewer accumulations are also better suited for quick sample screening or high-throughput measurements.

In conclusion, the best practice in choosing all the measurement parameters is to find a balance between SNR improvement and practical constraints. For samples that struggle with low Raman intensity, increasing the number of scans, laser power, and laser exposure time is necessary, but with delicate samples there must be a balance between adequate Raman sensitivity and thermal degradation. The choice of objective must also be made based on for example, the shape of the surface of the material. When choosing the correct measuring parameters there is always a balance between adequate Raman signal strength and fluorescence.

5.2 Sample preparation

All the sample preparation was done at DelSiTech using their equipment and products. The details for sample preparation will be covered in more detail in later chapters. Ammonium bifluoride (NH_4HF_2) was present in several of the samples analysed in this work. Due to its corrosive and hazardous nature, all handling of the compound was carried out exclusively by trained professionals at DelSiTech. The samples provided for this study were always neutralized with silica before I handled them. Ammonium bifluoride needs to be handled with care, as it is corrosive and can release hydrogen fluoride, which is hazardous to human health. Proper protective equipment

and ventilation are necessary when working with it. All the Milli-Q water used during the project was also obtained from the equipment at DelSiTech.

All other sample preparation was done by me, with help form a professional at DelSiTech. The liquid samples were transported between DelSiTech and University of Turku in Falcon tubes or Eppendorf tubes depending on the sample size unless otherwise mentioned. If the sample contained microorganisms, the sample was stored in a refrigerator, when not being measured, to avoid microorganism growth.

The samples were prepared at DelSiTech but the setup for measurements was done at the University of Turku. For every measurement, the substrates were cleaned using ethanol and soft paper before and after measuring. When measuring samples containing the different microorganisms, the Raman microscope stage was also cleaned using ethanol to avoid contamination.

5.2.1 Substrate materials

First material to be studied were the different substrate materials. The samples studied would be studied later would need a surface, where they could be disposed on. So, the different substrate materials, where the samples would be disposed on needed to be studied. The spectra from the different samples could then be compared with the spectra from the substrate material used.

The first substrate material that was studied was quartz glass. The first goal was to find the most suitable laser for this material. Quartz glass is a commonly used substrate material in Raman spectroscopy. It is commonly used due to its excellent optical, chemical, and physical properties.

Quartz glass has a very low Raman scattering background and it does not interfere significantly with the sample's Raman signal. Quartz glass is also suitable for various sample types, as it can be used to study solids, liquids using a quartz cuvette and thin films and coatings. A quartz glass slip, and a quartz cuvette were used during measurements.

The other substrate material that was started with was cellulose paper. Cellulose paper was studied as a substrate material as it was known that the first actual sample would be the different microorganisms lyophilized on cellulose paper. From a sheet of cellulose paper, an appropriately sized piece was cut out for measurements.

The measurement setup for studying the different substrate materials was simple. The quartz glass slip and later the quartz cuvette were cleaned with ethanol before measurements. Then the quartz glass slip/quartz cuvette/cellulose paper was simply placed on the microscope stage under the microscope objectives. The aim was to first determine the most suitable laser for each of the substrate materials and then different other measuring parameters were tested to find the best possible spectra for each substrate material.

The project started out with these substrate materials quartz glass slip, quartz cuvette, and cellulose paper. Later, other substrate materials were introduced. First additional substrate material was aluminium. Aluminium has minimal background interference and provides a clean baseline, which are great advantages in Raman spectroscopy. The measurement setup was similar to those mentioned before, the substrate was simply placed on the microscope stage under the microscope objectives. As the best possible laser was determined for the earlier substrate materials and it had proved to be suitable for samples, the aluminium substrate was studied with the same laser changing the other parameters to achieve the best possible spectrum for the material.

Mirror-polished stainless steel was the next substrate material that was used for measurements. It was chosen as a substrate material as it is an excellent substrate material for Raman spectroscopy for several reasons. Mirror-polished stainless-steel substrates enhance signal intensity. The highly reflective surface of mirror-polished steel allows the laser to reflect back through the sample, which increases the interaction between the laser and the sample. Stainless steel also has minimal Raman active modes, so it contributes little to the background noise. Stainless steel is also a cheap material and highly durable, which makes it ideal for routine laboratory use.

Last substrate material used in the project was calcium fluoride (CaF_2). CaF_2 has a relatively weak Raman background, but it has a characteristic peak at 321 cm^{-1}. It is a standard choice as a substrate material for Raman spectroscopy, especially in biomedical research. CaF_2 has good optical

transparency, as it transmits visible and near-infrared (NIR) light with minimal losses. This allows researchers to use the same sample for both FTIR and Raman analysis. The material's biggest drawback is that it is brittle and easily breakable, and it is expensive compared with other substrate materials. It is also more difficult to clean in between uses compared with the other substrate materials.

5.2.2 Microorganisms lyophilized on cellulose paper

The first actual sample were the different microorganisms lyophilized on cellulose paper. Lyophilization is a freeze-drying process used to preserve perishable materials and making the material more convenient for transport. During lyophilization water is removed from the sample by first freezing it, then reducing the pressure and adding heat to allow for the frozen water in the sample to sublimate. The microorganism samples were *Bacillus subtilis cf. spizizenii* (HAMBI 692), *Pseudomonas chlororaphsis* (HAMBI 15), and *Aspergillus versicolor* HAMBI 3340. The samples of these microorganisms lyophilized on cellulose paper were obtained from DelSiTech and each sample was delivered inside a glass ampoule.

First, the glass ampoules needed to be opened. To start the glass ampoules were cleaned with ethanol and soft paper. To ensure safety, safety goggles and gloves were put on. Next, using a sharp tool, a scored line was done around the surface of the ampoule to indicate where it should break. Then the ampoule was wrapped in soft paper to prevent glass shards from flying around during the opening process. After the ampoule was wrapped in paper, pressure was applied gently away from body until the ampoule was cracked open. After the ampoule was cracked open the glass shards were carefully removed and the microorganism sample was removed using tweezers, avoiding the ampoule's neck. The broken glass ampoule was disposed of accordingly. The process was repeated for all three microorganism samples.

The measurement setup for the lyophilized microorganism samples was simple. After the sample had been obtained from the ampoule it was placed on the microscope stage under the microscope objectives. The lyophilized samples varied in thickness, so the choice of suitable microscope objective was important, as there was a risk for the objective to touch the sample during measurements as the thickness of the sample varied so much. Different measuring parameters were tested out to find the best possible spectra for each sample. After the measurements were done, the microscope stage was wiped with ethanol to ensure cleanness.

5.2.3 Placebo silica microparticles

Next sample to be studied were dry placebo silica microparticle beads provided by DelSiTech. The silica beads were studied as the final sample composition, where all the components are put together contain these beads. The beads were studied using the quartz glass as a substrate. The beads were pressed down so that they would form a flatter surface that is more suitable for Raman measurements, using another piece of quartz glass. The measurements were also done on another substrate, an aluminium substrate. On this substrate the sample was again pressed flatter with a piece of quartz glass. The silica sample was also studied on an aluminium surface as quartz glass may be problematic when studying silica, as there is overlap in quartz glass's peaks with silica's primary Raman peak. The overlap can make it difficult to distinguish between the substrate and the sample.

After the dry silica beads were pressed down using the piece of quartz glass on the quartz glass slip/ aluminium substrate, the substrate was placed on the microscope stage for measurements. Different parameters were tested out to find the best possible Raman spectra for the sample on both substrates. Both substrate materials were cleaned by wiping the materials with ethanol using soft paper.

5.2.4 Silica solution

The next sample was a silica solution. The sample consisted of the same placebo silica microparticle beads that were previously studied dry, but this time they were dissolved in ammonium bifluoride (NH_4HF_2). The silica beads have low solubility in most solvents but in the presence of free fluoride ions, for example the free fluoride ions of ammonium bifluoride, the silica beads are soluble. The sample was a liquid, and it was prepared by a specialist at DelSiTech inside a quartz cuvette (High precision cell, Hellman Analytics, path length 10 mm, Art. No. 117-200-10-40). The quartz cuvette could not be opened during measurements to ensure sterility of the sample and also due to the toxicity of ammonium bifluoride.

The measurement setup with the quartz cuvette was simple, the quartz cuvette was simply placed on the microscope stage and measurements were performed through the quartz glass of the cuvette. Different measuring parameters were tested to get the best possible spectrum for the sample. With the quartz cuvette, the most significant choice of parameter was the choice of objective, as it was

necessary to measure the liquid inside the cuvette, and not just the surface material. After the measurements were done, the quartz cuvette was returned unopened to DelSiTech, where the contents were disposed of accordingly.

5.2.5 Organic solutions and microorganisms

Next, more liquid samples were studied inside the quartz cuvette. The next sample was malt extract broth, in which the *Aspergillus versicolor* sample, is grown in. The liquid malt extract broth (P-Code 102562422) was prepared by measuring 2.00 g of malt extract broth, that is suitable for microbiology and adding 100 mL of Milli-Q water. The solution was then placed into an autoclave for sterilization. The malt extract broth was studied inside the quartz cuvette. Different measuring parameters were tested to get the best possible spectrum for the sample. With the quartz cuvette, the most significant choice of parameter was the choice of objective, as it was necessary to measure the liquid inside the cuvette, and not just the surface material.

After the measurements were done with the malt extract broth, it was disposed of, and straight after the cuvette was filled with *Aspergillus Versicolor* biomass that was grown for three days at room temperature in the malt extract broth. The biomass sample was provided by DelSiTech. After the *Aspergillus Versicolor* biomass sample was studied to get the best possible spectrum for the sample using different measuring parameters, a droplet of the biomass sample was disposed on the quartz glass slip. On the quartz glass slip again, measurements were done to gather the best possible spectrum for the sample, using different measuring parameters. The *Aspergillus Versicolor* biomass sample was disposed on the quartz glass slip using a Pasteur pipette.

The next liquid sample was nutrient broth, in which both the gram-positive (*Bacillus subtilis cf. spizizenii*) and the gram-negative (*Pseudomonas chlororaphsis*) bacteria are grown in. The nutrient broth (P-Code 1003483173) was prepared by measuring 800 mg of nutrient broth for bacteria and adding 100 mL of Milli-Q water. The nutrient broth was then also sterilized in the autoclave. As with the malt extract broth, the nutrient broth was first studied in the quart cuvette. But with this sample, it was also studied as a droplet on the quartz cuvette slip. The different measuring parameters were changed to get the best possible spectra for the sample, both in the quartz cuvette, and on the quartz glass slip.

After the sample had been studied, the sample was disposed of, the quartz cuvette was first filled with gram-positive biomass sample. The gram-positive biomass sample was prepared by a specialist at DelSiTech. The sample was first studied inside the quartz cuvette to get the best possible

spectrum for the sample. The sample was then disposed on a quartz glass slip with a Pasteur pipette. Measurements were again done to gather the best possible spectrum, using different measuring parameters. Then the quartz glass cuvette and quartz glass slip were thoroughly cleaned using ethanol in preparation for the next sample. The next sample was gram-negative biomass sample. The sample was provided by DelSiTech, and as with the gram-positive biomass sample, it was first studied inside the quartz glass cuvette, and then on the quartz glass slip. The sample was studied with different parameters to gather the best possible spectra on both, the quartz glass slip, and in the quartz cuvette. They were again cleaned with ethanol after use.

5.2.6 First API in organic solutions

The next two samples contained the first API in both organic solutions, malt extract broth and nutrient broth. The desired concentration for the sample was 265 µL/mL. And the volume of the sample would be 1 mL. First, 262.34 mg of the first API was measured and then 1 mL of previously prepared malt extract broth was added. The next sample was prepared by measuring 259.80 mg of the first API and adding 1mL of the previously prepared nutrient broth.

In both samples there was a problem with the liquid separating into two phases. From both samples, measurements were done as a droplet on the quartz glass slip from the upper phase of the sample. The droplet was disposed on the quartz glass slip with a Pasteur pipette. Different parameters were tested out to gather the best possible spectra for both samples.

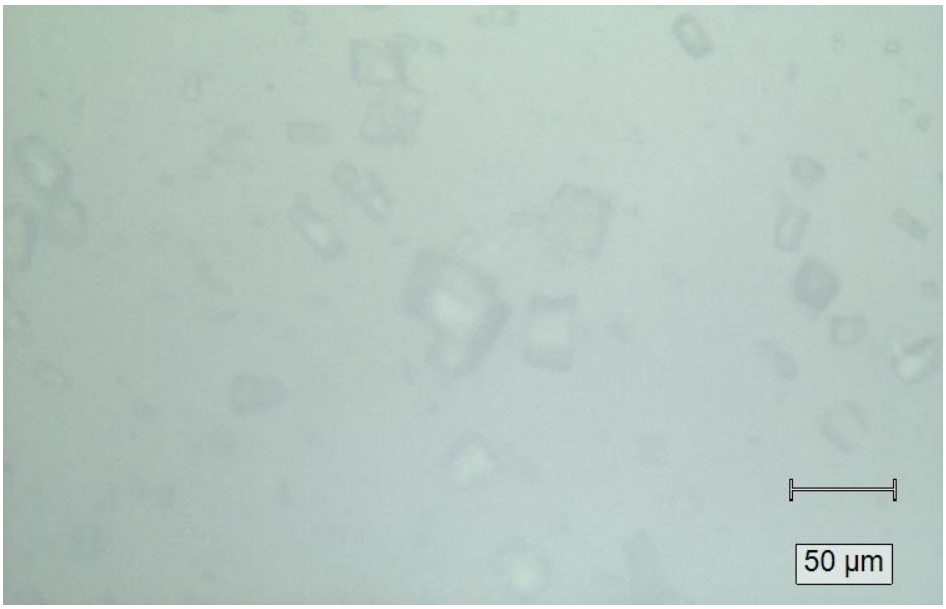

Figure 6. The first API in malt extract broth under the 20x microscope objective. The solution has solid particles that can be easily observed. Measurements were done from both the liquid phase and the solid particles. But as the solid particles are in a liquid, they are prone to moving, so the particles could move during the measuring process.

The samples were then put into a centrifuge to mix the two phases. After that process was complete, measurements were again done on a quartz glass slip, where the samples were disposed on with a Pasteur pipette. With the microscope, the different compositions of the sample could be observed. There were distinct solid formations and a liquid phase. Different parameters were again tested out to gather the best possible spectra for both samples. After the measurements were done, the quartz glass slip was cleaned with ethanol and the unused sample was delivered back to DelSiTech for proper disposal.

5.2.7 Placebo microparticles and API microparticles

1. 10.27 mg of placebo microparticles was weighed. Next 100 mL of Milli-Q water was added.
2. 10.93 mg of API microparticles was weighed. Next 100 mL of Milli-Q water was added.

Both samples were in sample containers, and next the sample containers were put into a water bath (temperature 27˚C, 60 strikes per minute movement) for a few hours to enhance the solubility of the compounds.

Measurements for both samples were done on a quartz glass slip and also on the aluminium substrate. The samples were disposed on the substrates with a Pasteur pipette. Different measuring parameters were again tested out to gather the best possible spectra for both samples. Both substrates were cleaned with ethanol when measurements were done for each sample.

5.2.8 API/Placebo microparticles + microorganisms + nutrient broth/malt extract broth

Again, malt extract broth was prepared for the *Aspergillus Versicolor* sample. The desired measurements were 2 g of malt extract broth in 100 mL of water. 2.00 g of the malt extract broth was weighed, and 100 mL Milli-Q was added.

Next, agar for the *Aspergillus Versicolor* sample was prepared. The desired measurements were 5 g of the agar in 100 mL of water. Two batches of the agar were prepared. For the first batch, 5.01 g of Agar (P-Code 102582972) was weighed, and 100 mL of Milli-Q water was added. For the second batch 5.01 g of agar was weighed and 100 mL of Milli-Q water was again added.

Two batches of the nutrient broth for the bacteria were prepared. The desired measurements were 800 mg in 100 mL of water. For the first batch 0.80 g of nutrient broth (P-Code 1003483173) was weighed and 100 mL of Milli-Q water was added. For the second batch 0.81 g of nutrient broth (P-Code 1003483173) was weighed and 100 mL of Milli-Q water was added.

All 5 solutions were in sample containers that had lids. The solutions were sterilized in an autoclave inside the containers. After the sterilization the containers were moved into a cleanroom. Inside the cleanroom both sterilized Agar solutions were poured out onto 6 petri dishes with even distribution. The petridishes were left to cool down until the next day. The other three solutions were left in their containers to the cleanroom to wait for sample preparation.

The first sample that was prepared was the *Aspergillus Versicolor* sample as the agar was prepared for it first. Serial dilutions were made from the stock solution. The serial dilutions were also plated onto Petri dishes, that were prepared the previous day, for cultivation. The serial dilution process was done in the cleanroom using a stock solution of *Aspergillus Versicolor*. The process began with first filling 7 Falcon tubes with 9 mL of the malt extract broth that was prepared and sterilized the previous day. Next from the stock solution of *Aspergillus Versicolor* 1 mL was taken with a pipette and added to the first Falcon tube that had 9 mL of malt extract broth. The solution then containing 1 mL of the stock solution and 9 mL of malt extract broth was next shaken well. This was the 10^{-1} dilution of the stock solution. To make the 10^{-2} serial dilution, 1 mL of the 10^{-1} solution was taken with a pipette and added to the next Falcon tube containing malt extract broth. The 10^{-2} serial dilution that was prepared was shaken well in preparation of making the 10^{-3} serial dilution. Again, 1 mL of the 10^{-2} serial dilution was added to a Falcon tube containing 9 mL of malt extract broth. The process was repeated until a 10^{-7} serial dilution was achieved.

Only the 10^{-2} - 10^{-7} serial dilutions were plated onto Petri dishes for cultivation. The Petri dishes were prepared by taking 100 µL of each serial dilution and placing the liquid onto the Petri dish using a pipette. Each liquid sample was evenly spread on the agar plate using a yellow plastic L-shaped spreader. The tool was disposed of after use on every sample.

The process of preparing the serial dilution and plating the serial dilution onto the Petridishes is shown more clearly on Figure 7.

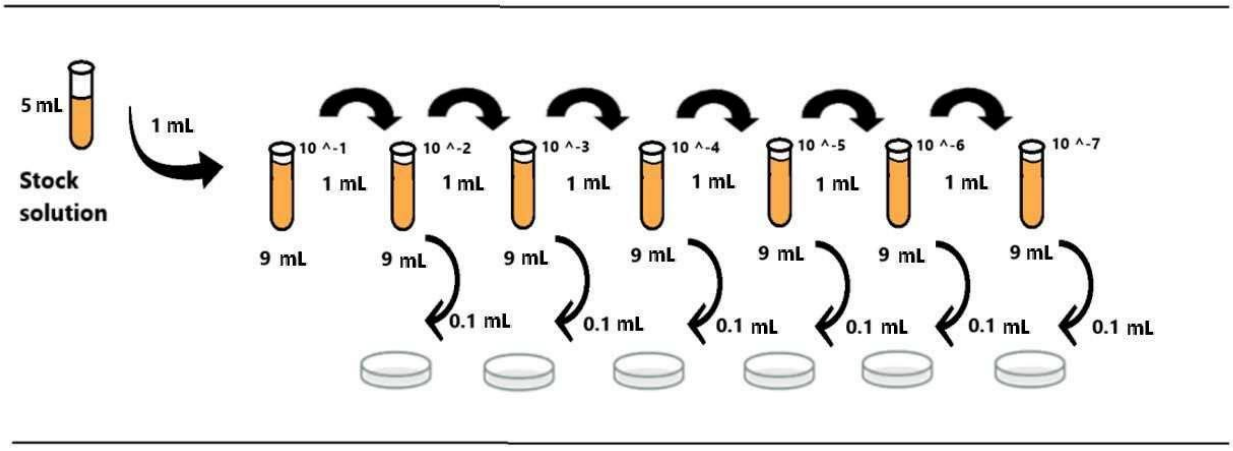

Figure 7. The serial dilution process.

The next samples to be studied were prepared from the 10^{-1} serial dilution mixed with the previously prepared placebo microparticles and API microparticles samples.

1. 0.2 mL of the 10^{-1} serial dilution was measured using a pipette and added to 1.8 mL of the placebo microparticles that was also measured with a pipette. The total volume of the sample was 2 mL.
2. 0.2 mL of the 10^{-1} serial dilution was measured using a pipette and added to 1.8 mL of the API microparticles that was also measured with a pipette. The total volume of the sample was 2 mL.

Measurements for both samples were done on a quartz glass slip and also on the aluminium substrate. The samples were disposed on the substrates with a Pasteur pipette. Different measuring parameters were again tested out to gather the best possible spectra for both samples. Both substrates were cleaned with ethanol when measurements were done for each sample. The unused sample was brought back to DelSiTech for proper disposal.

The Petri dishes were left to incubate at room temperature until the next day to allow colony growth. From the Petri dish that had the 10^{-7} serial dilution, CFU was determined. After incubation, visible colonies were counted manually.

$$\frac{CFU}{mL} = \frac{Number\ of\ colonies\ x\ dilution\ number}{Volume\ plated\ (mL)}$$

The number of colonies for the 10^{-7} *Aspergillus Versicolor* sample was 11.

$$\frac{11\ CFU}{0.1\ mL} = 110\ CFU/mL$$

So, the concentration in stock is:

$$110\ x\ 10^7\left(\frac{CFU}{mL}\right) = 1.1x10^9(\frac{CFU}{mL})$$

Next, agar was prepared for both of the bacteria samples. The desired measurements were 3.1 g per 100 mL of water. 300 mL was needed in total so, 3.1 g was measured 3 times. For the first batch, 3.17 g of the agar was weighed, and 100 mL of Milli-Q water was added. For the second batch 3.10 g of the agar was weighed and 100 mL of Milli-Q water was added. Last, for the third batch 3.12 g of the agar was weighed and 100 mL of Milli-Q water was added. The three batches were then placed into an autoclave for sterilization. When the sterilization was finished, the three batches were brought into the cleanroom. The agar was then poured out onto 12 petri dishes that were left to cool down until the next day.

Serial dilutions were made from the stock solution. The serial dilutions were also plated onto the Petri dishes with agar, that were prepared the previous day, for cultivation. The serial dilution process was done in the cleanroom using a stock solution of *Bacillus subtilis cf. spizizenii*. The process began with first filling 7 Falcon tubes with 9 mL of the nutrient broth that had been prepared previously with the malt extract broth and agar for the *Aspergillus Versicolor* sample. Next from the stock solution of *Bacillus subtilis cf. spizizenii* 1 mL was taken with a pipette and added to the first Falcon tube that had 9 mL of nutrient broth. The solution then containing 1 mL of the stock solution and 9 mL of nutrient broth was next shaken well. This was the 10^{-1} dilution of the stock solution. To make the 10^{-2} serial dilution, 1 mL of the 10^{-1} solution was taken with a pipette and added to the next Falcon tube containing nutrient broth. The 10^{-2} serial dilution that was prepared was shaken well in preparation of making the 10^{-3} serial dilution. Again, 1 mL of the 10^{-2} serial dilution was added to a Falcon tube containing 9 mL of nutrient broth. The process was repeated until a 10^{-7} serial dilution was achieved.

The exact same process was repeated for the *Pseudomonas chlororaphsis* sample.

Only the 10^{-2} - 10^{-7} serial dilutions of both samples were plated onto Petri dishes for cultivation. The Petri dishes were prepared by taking 100 µL of each serial dilution and placing the liquid onto the Petri dish using a pipette. Each liquid sample was evenly spread on the agar plate using a yellow plastic L-shaped spreader. The tool was disposed of after use on every sample.

The next samples to be studied were prepared from the 10^{-1} serial dilutions mixed with the previously prepared placebo microparticles and API microparticles samples.

1. 0.2 mL of the 10^{-1} *Bacillus subtilis cf. spizizenii* serial dilution was measured using a pipette and added to 1.8 mL of the placebo microparticles that was also measured with a pipette. The total volume of the sample was 2 mL.
2. 0.2 mL of the 10^{-1} *Bacillus subtilis cf. spizizenii* serial dilution was measured using a pipette and added to 1.8 mL of the API microparticles that was also measured with a pipette. The total volume of the sample was 2 mL.
3. 0.2 mL of the 10^{-1} *Pseudomonas chlororaphsis* serial dilution was measured using a pipette and added to 1.8 mL of the placebo microparticles that was also measured with a pipette. The total volume of the sample was 2 mL.
4. 0.2 mL of the 10^{-1} *Pseudomonas chlororaphsis* serial dilution was measured using a pipette and added to 1.8 mL of the API microparticles that was also measured with a pipette. The total volume of the sample was 2 mL.

Measurements for all the samples were done on a quartz glass slip and also on the aluminium substrate. The samples were disposed on the substrates with a Pasteur pipette. Different measuring parameters were again tested out to gather the best possible spectra for both samples. Both substrates were cleaned with ethanol when measurements were done for each sample. The unused sample was brought back to DelSiTech for proper disposal.

The Petri dishes were left to incubate until the next day to allow colony growth. From the Petri dish that had the 10^{-1} serial dilution, CFU was determined. After incubation, visible bacterial colonies were counted manually.

The number of colonies for the 10^{-7} *Bacillus subtilis cf. spizizenii* sample was 11.

$$\frac{11\ CFU}{0.1\ mL} = 110\ CFU/mL$$

So, the concentration in stock is:

$$110\ x\ 10^7\left(\frac{CFU}{mL}\right) = 1.1x10^9(\frac{CFU}{mL})$$

The number of colonies for the 10^{-7} *Pseudomonas chlororaphsis* sample was 62.

$$\frac{62\ CFU}{0.1\ mL} = 620\ CFU/mL$$

So, the concentration in stock is:

$$620x\ 10^7\left(\frac{CFU}{mL}\right) = 6.2x10^9(\frac{CFU}{mL})$$

5.2.9 API/Placebo microparticles + microorganisms + Milli-Q water

Again, agar for the *Aspergillus Versicolor* sample was prepared. The desired measurements were 5 g of the agar in 100 mL of water. Two batches of the agar were prepared. For the first batch, 5.01 g of Agar (P-Code 102582972) was weighed, and 100 mL of Milli-Q water was added. For the second batch 5.05 g of agar was weighed and 100 mL of Milli-Q water was again added. This time instead of malt extract broth, only 100 mL of Milli-Q water was put into a sample container.

All solutions were in sample containers that had lids. The solutions were sterilized in an autoclave inside the containers. After the sterilization the containers were moved into a cleanroom. Inside the cleanroom both sterilized Agar solutions were poured out onto 6 petri dishes with even distribution. The petridishes were left to cool down until the next day. The Milli-Q water was left in its container to the cleanroom to wait for sample preparation.

Serial dilutions were made from the *Aspergillus Versicolor* stock solution. The serial dilutions were also plated onto Petri dishes, that were prepared the previous day, for cultivation. The serial dilution process was done in the cleanroom using a stock solution of *Aspergillus Versicolor*. The process began with first filling 7 Falcon tubes with 9 mL of the Milli-Q water that was sterilized the previous day. Next from the stock solution of *Aspergillus Versicolor* 1 mL was taken with a pipette and added to the first Falcon tube that had 9 mL of Milli-Q water. The solution then containing 1 mL of the stock solution and 9 mL of Milli-Q water was next shaken well. This was the 10^{-1} dilution of the stock solution. To make the 10^{-2} serial dilution, 1 mL of the 10^{-1} solution was taken with a pipette and added to the next Falcon tube containing Milli-Q water. The 10^{-2} serial dilution that was prepared was shaken well in preparation of making the 10^{-3} serial dilution. Again, 1 mL of the 10^{-2}

serial dilution was added to a Falcon tube containing 9 mL of Milli-Q water. The process was repeated until a 10^{-7} serial dilution was achieved.

Only the 10^{-2} - 10^{-7} serial dilutions were plated onto Petri dishes for cultivation. The Petri dishes were prepared by taking 100 µL of each serial dilution and placing the liquid onto the Petri dish using a pipette. Each liquid sample was evenly spread on the agar plate using a yellow plastic L-shaped spreader. The tool was disposed of after use on every sample.

The next samples to be studied were prepared from the 10^{-3} serial dilution mixed with the previously prepared placebo microparticles and API microparticles samples.

1. 0.2 mL of the 10^{-3} serial dilution was measured using a pipette and added to 1.8 mL of the placebo microparticles that was also measured with a pipette. The total volume of the sample was 2 mL.
2. 0.2 mL of the 10^{-3} serial dilution was measured using a pipette and added to 1.8 mL of the API microparticles that was also measured with a pipette. The total volume of the sample was 2 mL.

Measurements for both samples were done on a quartz glass slip and also on the aluminium substrate. The samples were disposed on the substrates with a Pasteur pipette. Different measuring parameters were again tested out to gather the best possible spectra for both samples. Both substrates were cleaned with ethanol when measurements were done for each sample. The unused sample was brought back to DelSiTech for proper disposal.

The Petri dishes were left to incubate at room temperature until the next day to allow colony growth. From the Petri dish that had the 10^{-7} serial dilution, CFU was determined. After incubation, visible colonies were counted manually.

$$\frac{CFU}{mL} = \frac{Number\ of\ colonies\ x\ dilution\ number}{Volume\ plated\ (mL)}$$

The number of colonies for the 10^{-7} *Aspergillus Versicolor* sample was 27.

$$\frac{27\ CFU}{0.1\ mL} = 270\ CFU/mL$$

So, the concentration in stock is:

$$270\ x\ 10^{7}\left(\frac{CFU}{mL}\right) = 2.7x10^{9}(\frac{CFU}{mL})$$

Again, agar for the *Bacillus subtilis cf. spizizenii* sample was prepared. The desired measurements were 3 g of the agar in 100 mL of water. Two batches of the agar were prepared. For the first batch, 3.10 g of agar was weighed, and 100 mL of Milli-Q water was added. For the second batch 3.14 g of agar was weighed and 100 mL of Milli-Q water was again added. Again, instead of nutrient broth, 100 mL of Milli-Q water was put into a sample container.

All solutions were in sample containers that had lids. The solutions were sterilized in an autoclave inside the containers. After the sterilization the containers were moved into a cleanroom. Inside the cleanroom both sterilized Agar solutions were poured out onto 6 petri dishes with even distribution. The petridishes were left to cool down until the next day. The Milli-Q water was left in its container to the cleanroom to wait for sample preparation.

Serial dilutions were made from the *Bacillus subtilis cf. spizizenii* stock solution. The serial dilutions were also plated onto Petri dishes, that were prepared the previous day, for cultivation. The serial dilution process was done in the cleanroom using a stock solution of *Bacillus subtilis cf. spizizenii*. The process began with first filling 7 Falcon tubes with 9 mL of the Milli-Q water that was sterilized the previous day. Next from the stock solution of *Bacillus subtilis cf. spizizenii* 1 mL was taken with a pipette and added to the first Falcon tube that had 9 mL of Milli-Q water. The solution then containing 1 mL of the stock solution and 9 mL of Milli-Q water was next shaken well. This was the 10^{-1} dilution of the stock solution. To make the 10^{-2} serial dilution, 1 mL of the 10^{-1} solution was taken with a pipette and added to the next Falcon tube containing Milli-Q water. The 10^{-2} serial dilution that was prepared was shaken well in preparation of making the 10^{-3} serial dilution. Again, 1 mL of the 10^{-2} serial dilution was added to a Falcon tube containing 9 mL of Milli-Q water. The process was repeated until a 10^{-7} serial dilution was achieved.

Only the 10^{-2} - 10^{-7} serial dilutions were plated onto Petri dishes for cultivation. The Petri dishes were prepared by taking 100 µL of each serial dilution and placing the liquid onto the Petri dish using a pipette. Each liquid sample was evenly spread on the agar plate using a yellow plastic L-shaped spreader. The tool was disposed of after use on every sample.

Measurements for both samples were done on a quartz glass slip and also on the aluminium substrate. The samples were disposed on the substrates with a Pasteur pipette. Different measuring parameters were again tested out to gather the best possible spectra for both samples. Both substrates were cleaned with ethanol when measurements were done for each sample. The unused sample was brought back to DelSiTech for proper disposal.

The Petri dishes were left to incubate at room temperature until the next day to allow colony growth. From the Petri dish that had the 10^{-7} serial dilution, CFU was determined. After incubation, visible colonies were counted manually.

$$\frac{CFU}{mL} = \frac{Number\ of\ colonies\ x\ dilution\ number}{Volume\ plated\ (mL)}$$

The number of colonies for the 10^{-7} *Aspergillus Versicolor* sample was 27.

$$\frac{14\ CFU}{0.1\ mL} = 140\ CFU/mL$$

So, the concentration in stock is:

$$140\ x\ 10^{7}\left(\frac{CFU}{mL}\right) = 1.4x10^{9}(\frac{CFU}{mL})$$

This time only the *Bacillus subtilis cf. spizizenii* and *Aspergillus Versicolor* samples were prepared.

5.2.10 Serial dilutions of the microorganisms + NH_4HF_2

Again, agar for the *Aspergillus Versicolor* sample was prepared. The desired measurements were 5 g of the agar in 100 mL of water. Two batches of the agar were prepared. For the first batch, 5.03 g of Agar (P-Code 102582972) was weighed, and 100 mL of Milli-Q water was added. For the second batch 5.03 g of agar was weighed and 100 mL of Milli-Q water was again added. This time instead of malt extract broth, or Milli-Q water, 50 mL of ammonium bifluoride NH_4HF_2 neutralized with silica was used. The neutralization process was done by a specialist at DelSiTech.

All solutions were in sample containers that had lids. The solutions were sterilized in an autoclave inside the containers. After the sterilization the containers were moved into a cleanroom. Inside the cleanroom both sterilized Agar solutions were poured out onto 6 petri dishes with even distribution.

The petridishes were left to cool down until the next day. The sterilized ammonium bifluoride was left in its container to the cleanroom to wait for sample preparation.

5 mL of neutralized NH_4HF_2 was put into 8 Falcon tubes using a pipette in preparation of making serial dilutions of the *Aspergillus Versicolor.* This time the stock solution was prepared by using the previously grown *Aspergillus Versicolor* samples that were on a Petri dish. The stock solution of *Aspergillus Versicolor* was prepared by scraping the growth from the Petri dish using an inoculation loop and putting the gathered growth into one of the 8 prepared Falcon tubes. The final stock solution was supersaturated with the *Aspergillus Versicolor* growth, and it was shaken well to evenly distribute the growth.

Serial dilutions were made using this stock solution of *Aspergillus Versicolor* and ammonium bifluoride. The serial dilutions were also plated onto Petri dishes, that were prepared the previous day, for cultivation. In the cleanroom there was 1 Falcon tube filled with the prepared stock solution and 7 Falcon tubes filled with 5 mL of neutralized ammonium bifluoride. From the prepared stock solution of *Aspergillus Versicolor* 1 mL was taken with a pipette and added to the first Falcon tube that had 5 mL of neutralized ammonium bifluoride. The solution then containing 1 mL of the stock solution and 5 mL of neutralized ammonium bifluoride was next shaken well. This was the 10^{-1} dilution of the stock solution. To make the 10^{-2} serial dilution, 1 mL of the 10^{-1} solution was taken with a pipette and added to the next Falcon tube containing neutralized ammonium bifluoride. The 10^{-2} serial dilution that was prepared was shaken well in preparation of making the 10^{-3} serial dilution. Again, 1 mL of the 10^{-2} serial dilution was added to a Falcon tube containing 5 mL of neutralized ammonium bifluoride. The process was repeated until a 10^{-7} serial dilution was achieved.

Only the 10^{-2} - 10^{-7} serial dilutions were plated onto Petri dishes for cultivation. The Petri dishes were prepared by taking 100 µL of each serial dilution and placing the liquid onto the Petri dish using a pipette. Each liquid sample was evenly spread on the agar plate using a yellow plastic L-shaped spreader. The tool was disposed of after use on every sample.

The Petri dishes were left to incubate at room temperature until the next day to allow colony growth.

During the sample preparation process, when the 8 Falcon tubes were filled with 5 mL of ammonium bifluoride, there was an error in the sample preparation process. The ammonium bifluoride was inactivated using silica. The silica was in solid particles in the solution, that gathered to the bottom of the container. When pipetting the 5 mL to each Falcon tube, the pipetting was done from the bottom of the container, so the samples had to be discarded as they were oversaturated with silica.

New samples had to be prepared, this time with smaller sample sizes. The growth on the Petri dishes was normal even with the presence of excess silica, so the new smaller sample sizes of the same sample were not plated again. This time to avoid making the same mistake, the pipetting was not done from the bottom of the container of inactive ammonium bifluoride. The inactivated ammonium bifluoride was also shaken well to more evenly distribute the silica particles.

1.5 mL of neutralized NH_4HF_2 was put into 7 Eppendorf tubes using a pipette in preparation of making serial dilutions of the *Aspergillus Versicolor.* The 7 Eppendorf's containing the inactivated ammonium bifluoride were centrifuged for 10 minutes at maximum rounds per minute. Another stock solution was prepared by using the previously grown *Aspergillus Versicolor* samples that were on a Petri dish. The stock solution of *Aspergillus Versicolor* was prepared by scraping the growth from the Petri dish using an inoculation loop and putting the gathered growth into a Falcon tube containing 5 mL of inactivated ammonium bifluoride. The final stock solution was supersaturated with the *Aspergillus Versicolor* growth, and it was shaken well to evenly distribute the growth.

Serial dilutions were made using this stock solution of *Aspergillus Versicolor* and ammonium bifluoride. The serial dilutions were also plated onto Petri dishes, that were prepared the previous day, for cultivation. In the cleanroom there was 1 Falcon tube filled with the prepared stock solution and 7 Eppendorf tubes filled with 1.5 mL of neutralized ammonium bifluoride. From the prepared stock solution of *Aspergillus Versicolor 150* µL was taken with a pipette and added to the first Falcon tube that had 1.5 mL of neutralized ammonium bifluoride. The solution then containing 150 µL of the stock solution and 1.5 mL of neutralized ammonium bifluoride was next shaken well. This was the 10^{-1} dilution of the stock solution. To make the 10^{-2} serial dilution, 150 µL of the 10^{-1} solution was taken with a pipette and added to the next Eppendorf tube containing neutralized ammonium bifluoride. The 10^{-2} serial dilution that was prepared was shaken well in preparation of making the 10^{-3} serial dilution. Again, 150 µL of the 10^{-2} serial dilution was added to an Eppendorf tube containing 1.5 mL of neutralized ammonium bifluoride. The process was repeated until a 10^{-7} serial dilution was achieved.

Measurements were done for each serial dilution and from the stock solution. They were done were done on a quartz glass slip and on the aluminium substrate. The samples were disposed on the substrates with a Pasteur pipette. Different measuring parameters were again tested out to gather the best possible spectra for both samples. Both substrates were cleaned with ethanol after measurements for each sample. The unused sample was brought back to DelSiTech for proper disposal.

Again, agar for the *Bacillus subtilis cf. spizizenii* sample was prepared. The desired measurements were 3 g of the agar in 100 mL of water. Two batches of the agar were prepared. For the first batch, 3.14 g of agar was weighed, and 100 mL of Milli-Q water was added. For the second batch 3.16 g of agar was weighed and 100 mL of Milli-Q water was again added. The prepared solutions were put into an autoclave for sterilization. The prepared agar was evenly distributed to six Petri dishes in the cleanroom, and they were left to cool until the next day.

It was decided that smaller sample sizes would be done again to avoid the issue of the solid silica particles gathering to the bottom of the container as had happened before. 2 mL of neutralized NH_4HF_2 was put into 10 Eppendorf tubes using a pipette in preparation of making serial dilutions of the *Bacillus subtilis cf. spizizenii.* The 10 Eppendorf's containing the inactivated ammonium bifluoride were centrifuged for 10 minutes at maximum rounds per minute. From 7 of the Eppendorf tubes, 1.5 mL of the inactivated ammonium bifluoride was transferred into a 1.5 mL Falcon tube. The remaining 3 Eppendorf's were combined into a larger volume Falcon tube in preparation of making the stock solution. The combining was done by taking 1.5 mL from each tube with a pipette. So, the volume of the stock solution was 4.5 mL. The stock solution was prepared by using the previously grown *Bacillus subtilis cf. spizizenii* samples that were on the Petri dishes. The stock solution of *Bacillus subtilis cf. spizizenii* was prepared by scraping the growth from the Petri dish using an inoculation loop and putting the gathered growth into the Falcon tube containing the combined 3 Eppendorf's of inactivated ammonium bifluoride. The stock solution was supersaturated with the *Bacillus subtilis cf. spizizenii* growth, and it was shaken well to evenly distribute the growth.

Serial dilutions were made using this stock solution of *Bacillus subtilis cf. spizizenii* and ammonium bifluoride. The serial dilutions were also plated onto Petri dishes, that were prepared the previous day, for cultivation. In the cleanroom there was one Falcon tube filled with the prepared stock solution and 7 Eppendorf tubes filled with 1.5 mL of neutralized ammonium bifluoride. From the prepared stock solution of *Bacillus subtilis cf. spizizenii* 150 µL was taken with a pipette and added to the first Falcon tube that had 1.5 mL of neutralized ammonium bifluoride. The solution then containing 150 µL of the stock solution and 1.5 mL of neutralized ammonium bifluoride was next shaken well. This was the 10^{-1} dilution of the stock solution. To make the 10^{-2} serial dilution, *150* µL of the 10^{-1} solution was taken with a pipette and added to the next Eppendorf tube containing neutralized ammonium bifluoride. The 10^{-2} serial dilution that was prepared was shaken well in preparation of making the 10^{-3} serial dilution. Again, 150 µL of the 10^{-2} serial dilution was added to

an Eppendorf tube containing 1.5 mL of neutralized ammonium bifluoride. The process was repeated until a 10^{-7} serial dilution was achieved.

Only the 10^{-2} - 10^{-7} serial dilutions were plated onto Petri dishes for cultivation. The Petri dishes were prepared by taking 100 µL of each serial dilution and placing the liquid onto the Petri dish using a pipette. Each liquid sample was evenly spread on the agar plate using a yellow plastic L-shaped spreader. The tool was disposed of after use on every sample.

Measurements were done for each serial dilution, from the stock solution, and also a blank of the inactivated ammonium bifluoride was recorded also. They were done were done on a quartz glass slip and on the aluminium substrate. The samples were disposed on the substrates with a Pasteur pipette. Different measuring parameters were again tested out to gather the best possible spectra for both samples. Both substrates were cleaned with ethanol after measurements for each sample. The unused sample was brought back to DelSiTech for proper disposal.

The exact same process was repeated for the *Pseudomonas chlororaphsis* sample, that was done for the *Bacillus subtilis cf. spizizenii* sample.

6 Results

In the results section only the most significant results and the best possible spectra for each sample will be presented. All results were thoroughly reviewed to find the spectra that had the highest Raman intensity. This was done separately for each sample. The project had a trial-and-error approach, so a lot of different parameters were used and tested out for each sample. The results will be presented in chronological order.

Raman spectra can have substantial differences in intensity for example, due to sample concentration, laser power, or other measuring parameter settings. For instance, the Raman intensity values (y-axis) in the Raman spectra varied by tens of thousands of counts between measurements, even for the same sample, depending on the measurement parameters. This large variation in Raman intensity can complicate the comparison of spectra. A solution to this issue is normalization, which scales the intensity values to a range between 0 and 1. This enables direct comparison of spectral features across different samples while preserving the relative differences in peak intensities and positions.

6.1 Substrate materials

The first goal was to find the best laser for the substrate materials. The first two substrate materials that were used were cellulose paper on which the different microorganism sample would be lyophilized on. The other first substrate material to be used for samples was quartz glass.

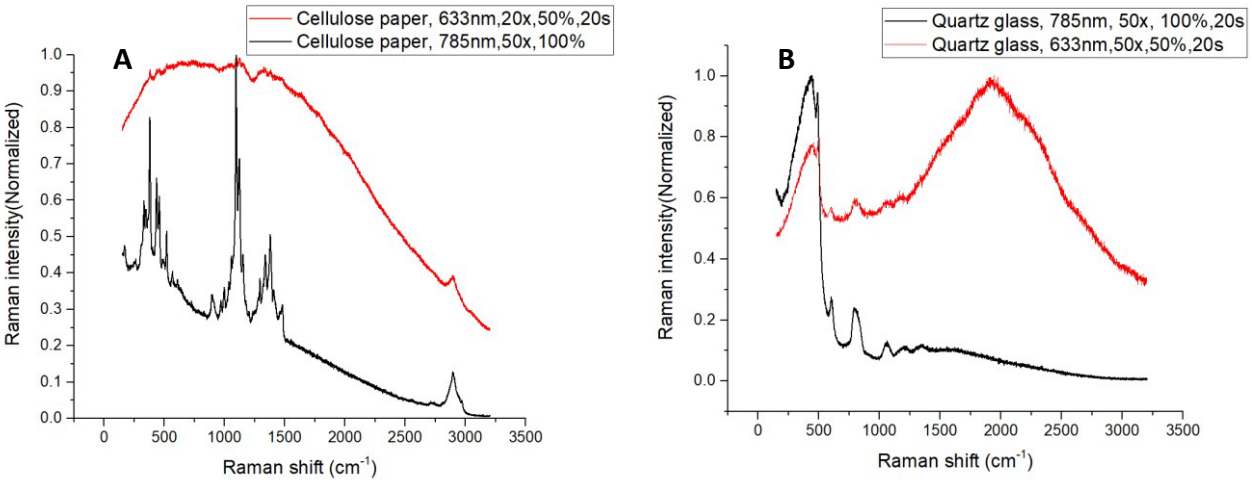

Figure 9. (A) Cellulose paper with 633 nm laser, under 20x microscope objective, 50% laser power, and 20 seconds laser exposure time (red). Cellulose paper with 785 nm laser, under 50x microscope objective, and 100% laser power (black). (B) Quartz glass with 785 nm laser, under 50x microscope objective, 100% laser power, and 20 seconds laser exposure time (black). Quartz glass with 633 nm laser, under 50x microscope objective, 50% laser power, and 20 seconds laser exposure time.

The 633 nm laser has a higher photon energy compared with the 785 nm laser. This higher energy can enhance the Raman scattering efficiency and may result in stronger Raman signals for certain samples. However, it can also increase fluorescence background, which can obscure Raman peaks, especially in biological or fluorescent samples. The 785 nm laser has lower energy, which reduces fluorescence interference, but can produce weaker Raman signals. From Figure 9. it can be observed that the 785 nm laser is better suited for both substrate materials. With the 633 nm laser the quartz sample provides a higher background signal that can obscure Raman peaks. The 785 nm laser minimizes fluorescence, which results in a cleaner spectrum with better signal-to-noise ratios. The 633 nm laser can excite fluorescence from organic materials, such as the cellulose in cellulose paper, due to the 633 nm laser operating in the visible region. With the 785 nm laser the fluorescence excitation is significantly reduced. It leads to a much cleaner Raman spectra with better signal-to-noise ratio. The Raman bands are more prominent and less affected by background

noise using the 785 nm laser for both samples. So, the 785 nm laser was chosen for further measurements as it was better suited for both substrate materials.

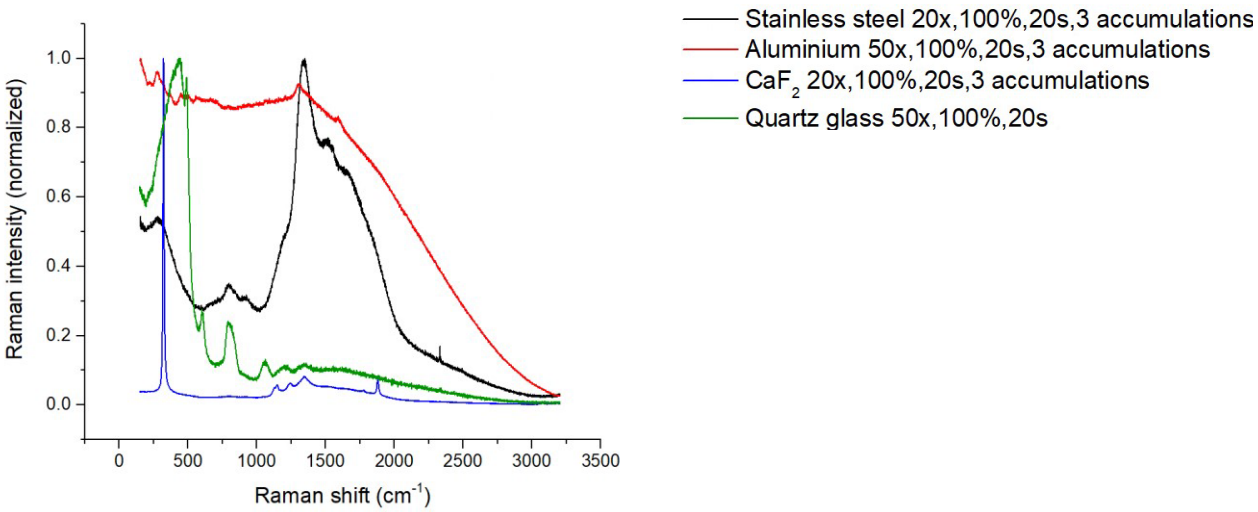

Figure 10. Mirror-polished stainless steel under 20x microscope objective, using 100% laser power, 20 seconds laser exposure time, and 3 accumulations (black). Aluminium under 50x microscope objective, using 100% laser power, 20 seconds laser exposure time, and 3 accumulations (red). Calcium fluoride under 20x microscope objective, using 100% laser power, 20 seconds laser exposure time, and 3 accumulations (blue). Quartz glass under 50x microscope objective, using 100% laser power, and 20 seconds laser exposure time (green). All measured with 785 nm laser.

In Figure 10. the different substrate materials mirror-polished stainless steel, aluminium, calcium fluoride, and quartz glass are compared with each other. The stainless-steel spectrum has a wide peak in the range of 1000-2500 cm^{-1}. Stainless steel should theoretically have no background signal. The spectrum of aluminium also exhibits a high fluorescence background, although it is slightly lower than stainless steel. Calcium fluoride shows a sharp, distinct peak in the 300-500 cm^{-1} range. Otherwise, it has a very low background fluorescence, which makes it ideal for Raman spectroscopy substrate material. Quartz glass shows sharp peaks in the 0-1000 cm^{-1} range. But it also has low background fluorescence, which makes it a quite good choice as a background material. Both aluminium, and stainless steel have broad features with no distinct peaks due to fluorescence.

Theoretically stainless steel should provide no background signal and due to this feature, stainless steel should be a very optimal substrate material. Metals typically do not exhibit Raman scattering due to their high reflectivity and free electron density. But with the 785 nm laser there was an issue of a broad fluorescence spectrum. The issue was deduced to be caused by the glasses of the microscope objectives in the Raman instrumentation. It is an issue with the 785 nm laser. The

manufacturer of the instrumentation was contacted, and they suggested a shorter collection time, but this did not solve the issue. Even with the shorter measuring time, a signal coming from the objective's glass could be observed. Later 532 nm laser was tested out also, but it also had the same problem, even with the shorter collection time.

6.2 Microorganisms lyophilized on cellulose paper

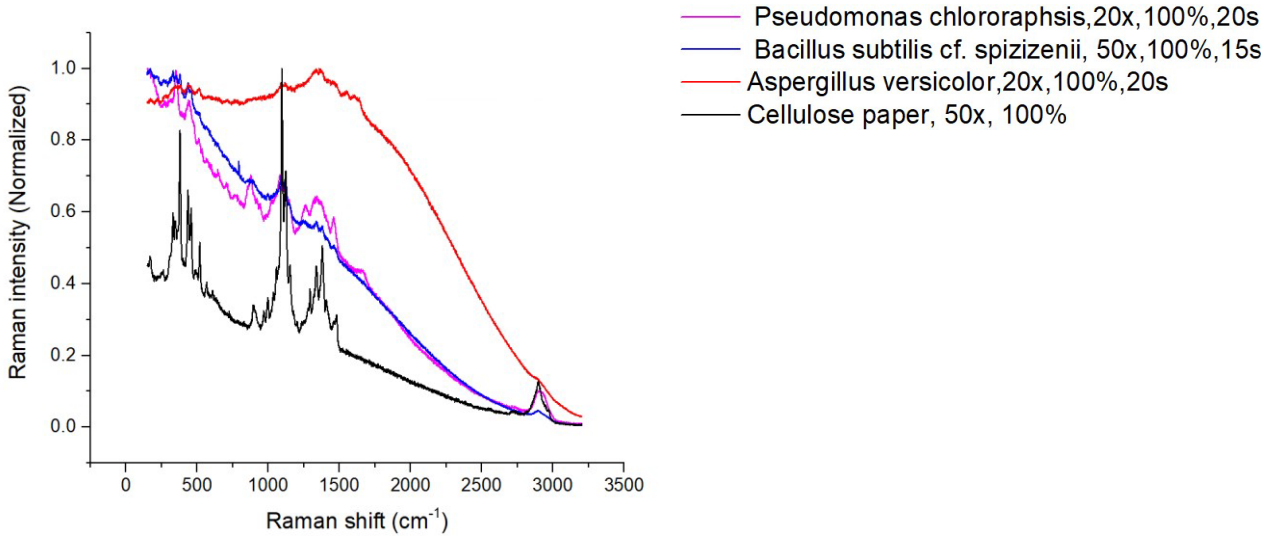

Figure 11. *Pseudomonas chlororaphsis* lyophilized on cellulose paper under 20x microscope objective, using 100% laser power, and 20 seconds laser exposure time (pink). *Bacillus subtilis* lyophilized on cellulose paper under 50x microscope objective, using 100% laser power, and 15 seconds laser exposure time (blue). *Aspergillus Versicolor* lyophilized on cellulose paper under 20x microscope objective, using 100% laser power, and 20 seconds laser exposure time (red). Cellulose paper under 50x microscope objective, using 100% laser power (black).

In Figure 11. it can first be observed that *Aspergillus Versicolor* (red line) shows a very high fluorescence background that dominates the spectrum. Very few Raman peaks can be observed due to the intense fluorescence overshadowing the signal. Both bacterial samples (*Pseudomonas*

Chlororaphsis pink line, and *Bacillus Subtilis* blue line) have moderate fluorescence background, but Raman peaks are still distinguishable. Bot samples display characteristic peaks in the 1000–1600 cm^{-1} region, which correspond to biomolecular vibrations, such as proteins, lipids, and nucleic acids. Peaks below 1000 cm^{-1} correspond to bacterial cell wall components. The black line corresponding with the cellulose paper has a lower Raman intensity compared with the intensities of the biological samples. The cellulose spectrum has well defined peaks that are typical for the material, especially in the 500-1600 cm^{-1} rang.

6.3 Placebo silica microparticles

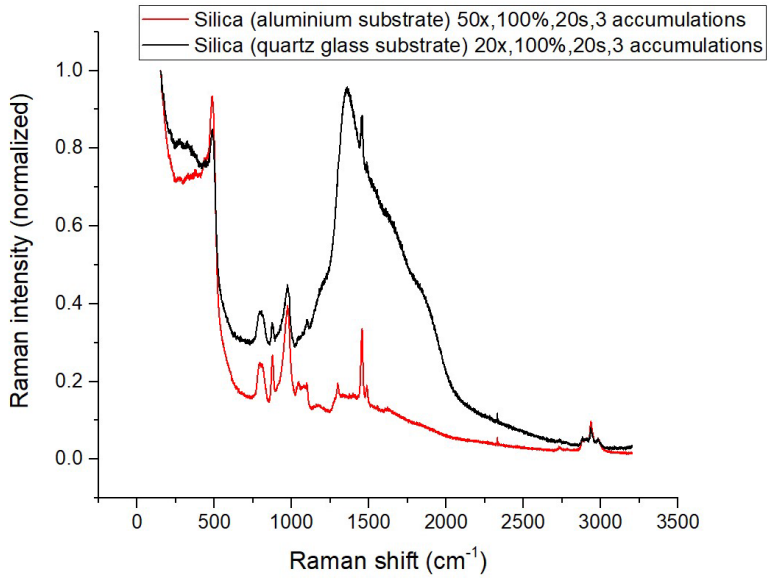

Figure 14. Dry silica on an aluminium substrate under 50x microscope objective, using 100% laser power, 20s laser exposure time, and 3 accumulations (red). Dry silica on a quartz glass substrate under 20x microscope objective, using 100% laser power, 20s laser exposure time, and 3 accumulations (black).

In Figure 14. Raman spectra of the dry placebo silica microparticles on two different substrate materials are compared. With the quartz glass substrate, the fluorescence background is relatively low, and the Raman peaks are well defined. There is a peak near ~440 - 490 cm^{-1} that is typical for

quartz glass. The silica beads on the aluminium substrate exhibits stronger Raman peaks compared to the quartz glass substrate. With the aluminium substrate there is a broad peak in the ~1000- 2000 cm^{-1} region.

6.4 Silica solution

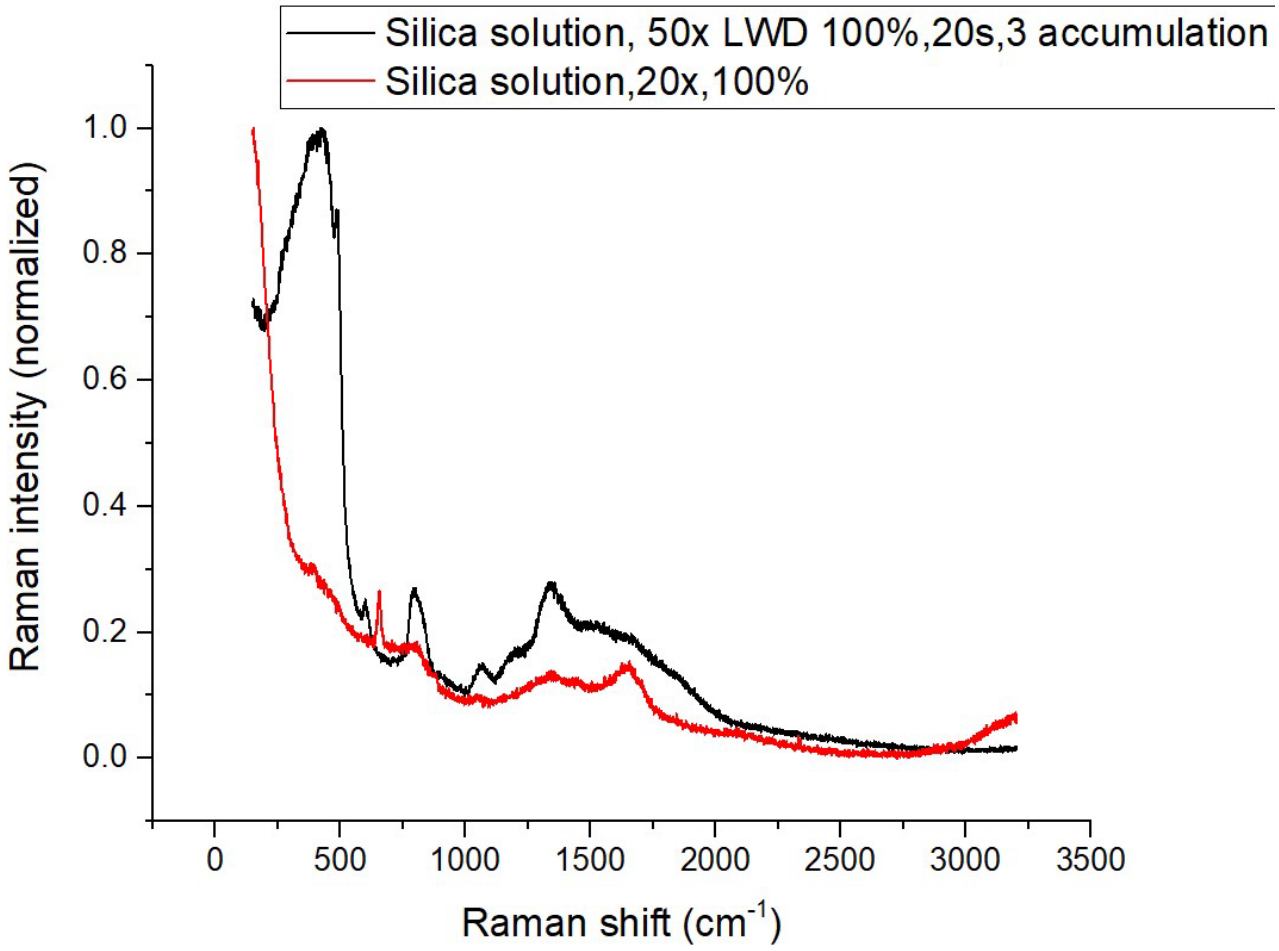

Figure 15. Silica solution measured in a quartz glass cuvette under 50x LWD microscope objective, using 100% laser power, 20 seconds laser exposure time, and 3 accumulations (black). Silica solution measured in a quartz glass cuvette under 20x microscope objective, using 100% laser power (red).

In Figure 15. two spectra of silica solution are compared. The two spectra have different measurement conditions, but both measurements were done in a quartz cuvette. The spectra measured with the 50x LWD microscope objective are more defined in the 400-1200 cm^{-1} region. The accumulations also likely improve the signal-to-noise ratio. But no measurements with accumulations were done with the 20x microscope objective.

The spectrum measured with the 20x microscope objective was noisier and the fluorescence background is higher. With the 20x microscope only results from the surface of the quartz cuvette were obtained. The spectrum provided with the 20x microscope objective in Figure 15. is similar with the spectrum of just quartz glass with minimal interferences from the sample. This was a common occurrence when measuring samples using the quartz cuvette. With the 20x and 50x microscope objectives, only a spectrum correlating with a spectrum of quartz glass could be obtained.

Even though the results were better with the 50x LWD objective, the measuring setup was not simple. The measuring depth needed to be adjusted many times so that any signal other than the signal belonging to quartz glass of the cuvette could be observed.

You could not take advantage of the microscope view to determine when you had reached the sample instead of the quartz glass surface, as everything on the screen looked homogenous whether you were focused on the quartz glass or the sample. The view of the microscope showed only blue when you were focused on quartz glass and the view stayed the same when you reached the sample. So, the measuring depth was determined by trial and error. Before you reached the actual sample you had to measure several spectra of the quartz surface, and you knew you had reached the sample only when you got a result that differed from a spectrum of quartz. This made the reproducibility of the measurements harder as you would need to find the suitable measurement depth for each sample by trial and error every time you wanted to study a new sample inside the quartz cuvette.

6.5 Organic solutions and micro-organisms

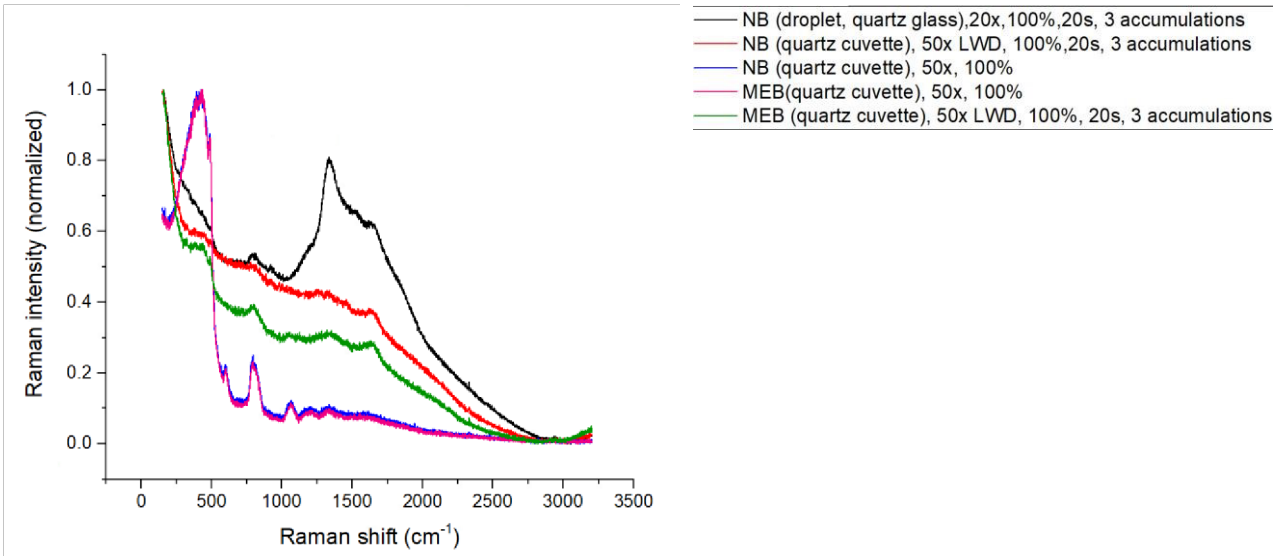

Figure 16. Nutrient broth (NB) measured as a droplet on a quartz glass substrate under 20x microscope objective, using 100% laser power, 20 seconds laser exposure time, and 3 accumulations (black). Nutrient broth measured in a quartz glass cuvette under 50x LWD microscope objective, using 100% laser power, 20 seconds laser exposure time, and 3 accumulations (red). Nutrient broth (NB) measured in a quartz glass cuvette under 50x microscope objective, using 100% laser power (blue). Malt extract broth (MEB) measured in a quartz glass cuvette under 50x microscope objective, using 100% laser power (pink). Malt extract broth (MEB) measured in a quartz glass cuvette under 50x LWD microscope objective, using 100% laser power, 20 seconds laser exposure time, and 3 accumulations (green).

In Figure 16. spectra of nutrient broth and malt extract broth measured with different measuring parameters are compared. The strongest Raman signal is seen on the black spectrum which corresponds to nutrient broth measured on a quartz glass substrate as a droplet. The red spectrum, which is nutrient broth measured in a quartz cuvette using 50x LWD microscope objective has very little defined peaks but shows a quite strong signal. The blue spectrum is nutrient broth studied inside the quartz cuvette using 50x microscope objective. The measurement done with the 50x microscope objective mainly shows a spectrum that corresponds with a spectrum of quartz glass, which was a reoccurring problem with all measurements done in the quartz cuvette. The most intense peaks for nutrient broth are in the 400-1600 cm^{-1}. The green spectrum corresponding to malt extract broth measured in a quartz cuvette with the 50x LWD objective has a lower Raman intensity, compared with the nutrient broth that was measured with the same parameters. The pink spectrum that corresponds to malt extract broth studied inside the quartz cuvette, using 50x microscope objective. It also had the same problem as the blue spectrum. The pink spectrum also mainly corresponds with a spectrum of quartz glass. Malt extract broth has a stronger fluorescence background, but some peaks can be distinguished in the 500-1600 cm^{-1} region. Malt extract broth was not studied as a droplet.

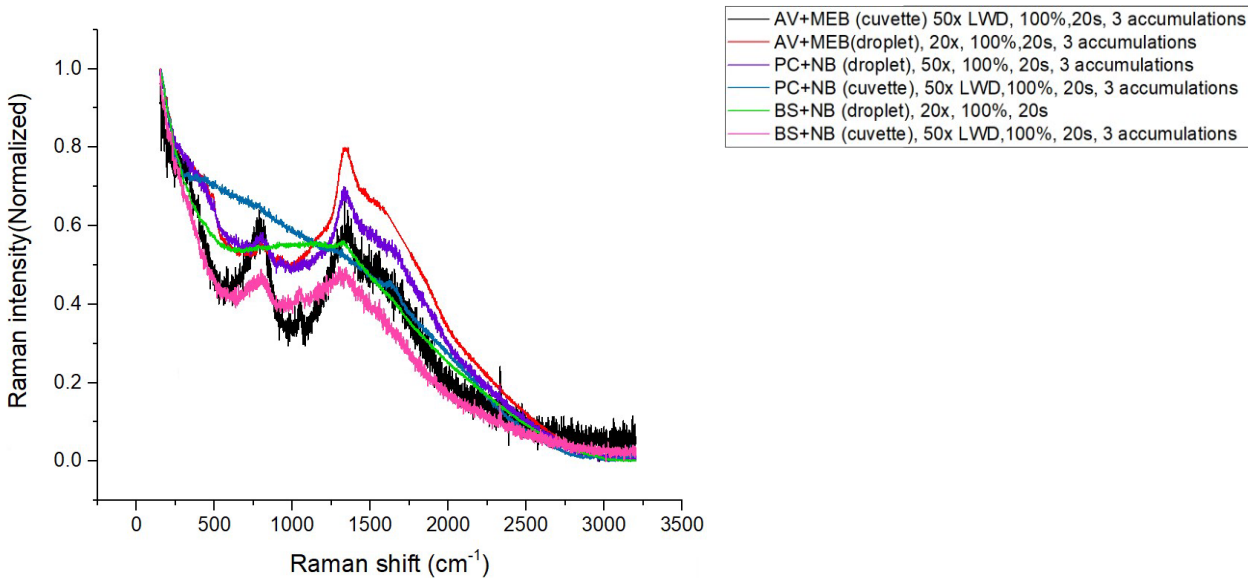

Figure 17. *Aspergillus Versicolor* (AV) + malt extract broth (MEB) measured in a quartz cuvette under 50x LWD microscope objective, using 100% laser power, 20 seconds laser exposure time, and 3 accumulations. *Aspergillus Versicolor* (AV) + malt extract broth (MEB) measured as a droplet on a quartz glass slip under 20x microscope objective, using 100% laser power, 20 seconds laser exposure time, and 3 accumulations. *Pseudomonas chlororaphsis* (PC) + nutrient broth (NB) measured as a droplet on a quartz glass slip under 50x microscope objective, using 100% laser power, 20 seconds laser exposure time, and 3 accumulations. *Pseudomonas chlororaphsis* (PC) + nutrient broth (NB) measured in a quartz glass cuvette under 50x LWD microscope objective, using 100% laser power, 20 seconds laser exposure time, and 3 accumulations. *Bacillus subtilis* (BS) + nutrient broth (NB) measured as a droplet on a quartz glass slip under 20x microscope objective, using 100% laser power, and 20 seconds laser exposure time. *Bacillus subtilis* (BS) + nutrient broth (NB) measured in a quartz glass cuvette under 50x LWD microscope objective, using 100% laser power, 20 seconds laser exposure time, and 3 accumulations.

In Figure 17. spectra of both bacterial samples in nutrient broth and *Aspergillus Versicolor* in malt extract broth are compared. Malt extract- based spectra (blue and pink lines) show higher fluorescence background compared to the nutrient broth- based samples. The nutrient broth- based samples exhibit stronger and clearer Raman peaks, especially in the 1000-1600 cm^{-1} range. The *Aspergillus Versicolor* samples show less distinct peaks compared to the bacterial samples. Overall, the measurements done as a droplet on the quartz glass substrate provide stronger Raman peaks compared with the result gathered from measurements in the quartz cuvette. After these measurements, it was decided that the quartz cuvette would no longer be used for measurements as there were issues with choosing the measuring depth and measurements done in the quartz cuvette provided spectra with a lower Raman intensity, compared with measurements done from a droplet on the quartz glass slip.

6.6 First API in organic solutions

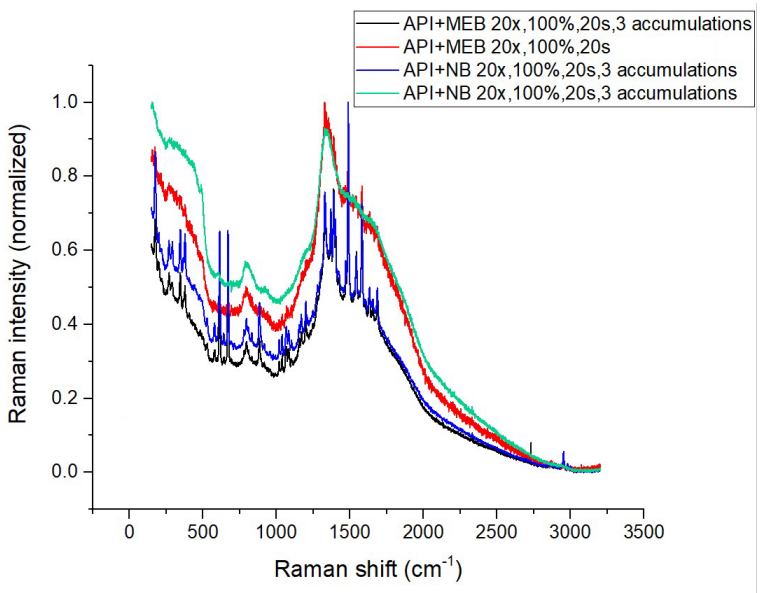

Figure 18. First API + malt extract broth (MEB) under 20x, using 100% laser power, 20 seconds laser exposure time, and 3 accumulations (black). First API + malt extract broth (MEB) under 20x microscope objective, 100% laser power, and 20 seconds laser exposure time (red). First API+ nutrient broth (NB) under 20x microscope objective using 100% laser power, 20 seconds laser exposure time, and 3 accumulations (blue). First API+ nutrient broth (NB) under 20x microscope objective using 100% laser power, 20 seconds laser exposure time, and 3 accumulations (green). All measurements were done as a droplet on a quartz glass slip.

In Figure 18. all spectra share similar overall features with broad bands around ~1300–1600 cm^{-1}. The first API) is a nucleoside analog, so the broad bands can be indicative of C=C and C=N ring vibrations. The fingerprint region (600–1800 cm^{-1}) shows distinct differences depending on the broth. Nutrient broth mixtures have sharper, more intense peaks between ~500–1600 cm^{-1}.

6.7 Placebo microparticles and API microparticles

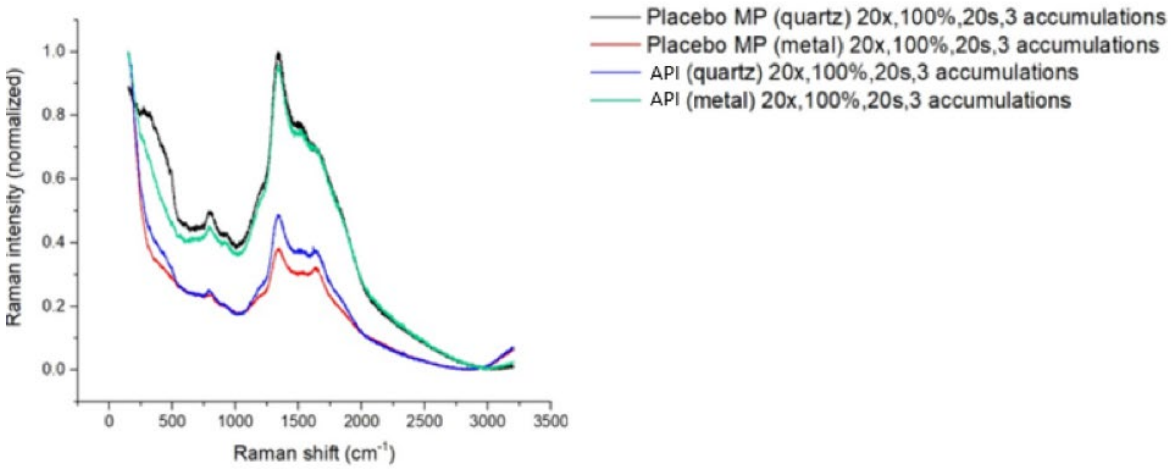

Figure 19. Placebo microparticles (MP) measured on a quartz glass slip under 20x, using 100% laser power, 20 seconds laser exposure time, and 3 accumulations (black). Placebo microparticles (MP) measured on an aluminium substrate under 20x microscope objective, using 100% laser power, 20 seconds laser exposure time, and 3 accumulations (red). API measured on a quartz glass slip under 20x, using 100% laser power, 20 seconds laser exposure time, and 3 accumulations (blue). API measured on an aluminium substrate under 20x microscope objective, using 100% laser power, 20 seconds laser exposure time, and 3 accumulations (green).

In Figure 19. all samples were studied in Milli-Q water. Placebo MP spectra are largely featureless or contain broad low-intensity bands. The API spectra exhibit sharp, structured peaks, especially between ~700 cm^{-1} and 1600 cm^{-1}.

6.8 API/Placebo microparticles + microorganisms + nutrient broth/malt extract broth

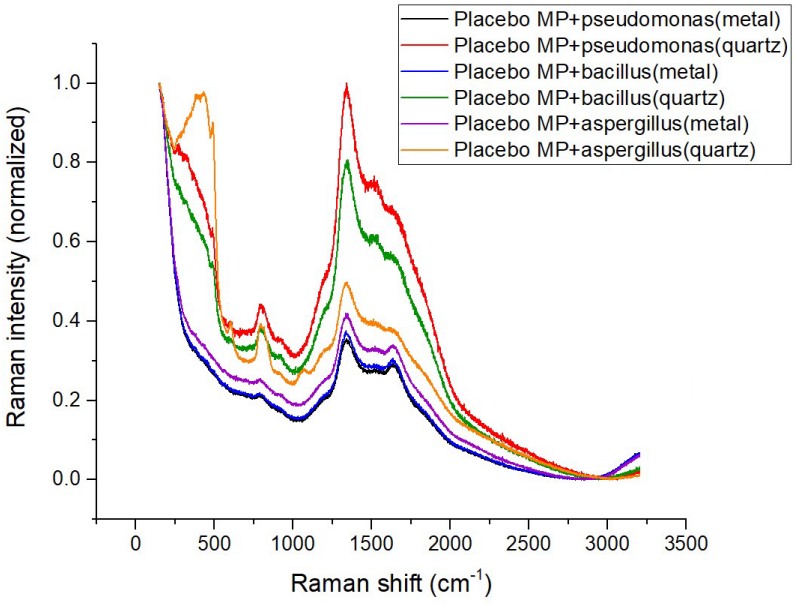

Figure 20. Placebo microparticles (MP) + *Pseudomonas chlororaphsis* measured on an aluminium substrate(black). Placebo microparticles (MP) + *Pseudomonas chlororaphsis* measured on a quartz glass substrate(red). Placebo microparticles (MP) + *Bacillus subtilis* measured on an aluminium substrate(blue). Placebo microparticles (MP) + *Bacillus subtilis* measured on a quartz glass substrate(green). Placebo microparticles (MP) + *Aspergillus Versicolor* measured on an aluminium substrate(violet). Placebo microparticles (MP) + *Aspergillus Versicolor* measured on a quartz glass substrate(yellow). Measuring parameters for all of the samples were 20x microscope objective, 100% laser power, 20 seconds laser exposure time, and 3 accumulations.

All spectra in Figure 20. show broad features from 600–1700 cm^{-1} but differences can be seen depending on microbial strain and substrate. The *pseudomonas chlororaphsis* samples show stronger peaks at ~1350 and ~1550 cm^{-1}. *Bacillus subtilis* samples have peaks in the 800–1300 cm^{-1} region, likely from peptidoglycan wall components. *Aspergillus Versicolor samples* present broad and structured signals, which may stem from chitin, glucans, and fungal pigments. Generally metal substrate enhances the intensity slightly but may broaden the peaks.

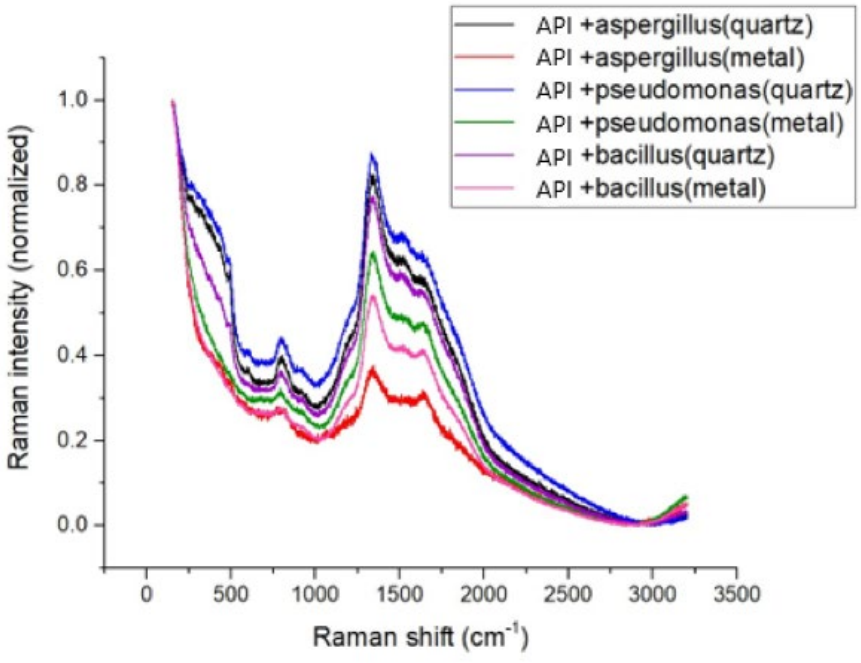

Figure 21. API + *Aspergillus Versicolor* measured on a quartz glass substrate(black). API+ *Aspergillus Versicolor* measured on an aluminium substrate(red). API + *Pseudomonas chlororaphsis* measured on a quartz glass substrate(blue). API+ *Pseudomonas chlororaphsis* measured on an aluminium substrate(green). API + *Bacillus subtilis* measured on a quartz glass substrate(violet). API+ *Bacillus subtilis* measured on an aluminium substrate(pink). Measuring parameters for all the samples were 20x microscope objective, 100% laser power, 20 seconds laser exposure time, and 3 accumulations.

In Figure 21. all API samples exhibit distinct Raman bands that can be attributed to the API, for example in the ~1350–1600 cm^{-1}: region C=C/C=N aromatic ring stretches can be observed. Peaks in this area are stronger than those observed for placebo microparticles in Figure 20. Each microorganism has slightly different spectral modifications, but no considerable differences can be observed.

6.9 API/Placebo microparticles + microorganisms + Milli-Q water

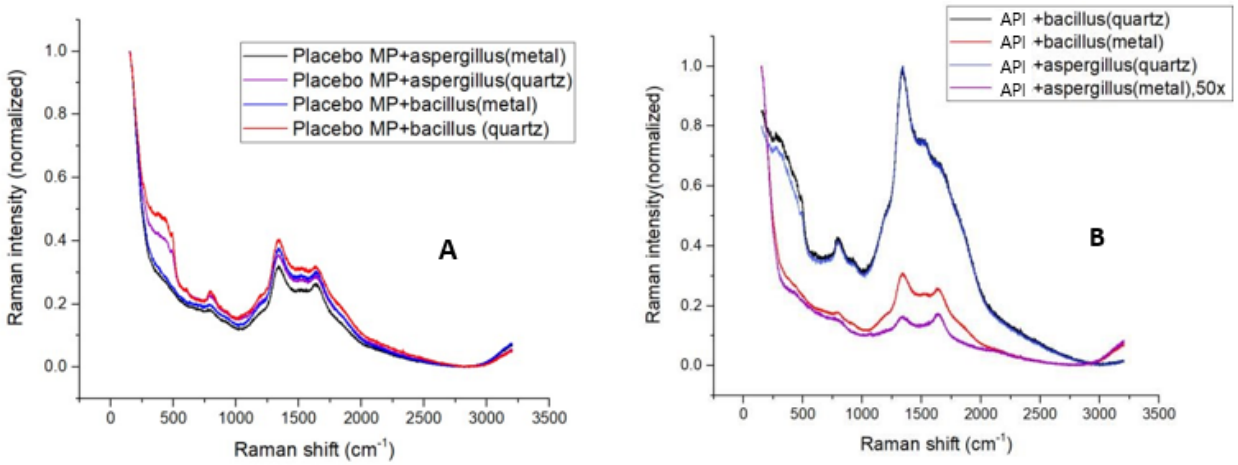

Figure 22. (A) Placebo microparticles (MP) + *Aspergillus Versicolor* + Milli-Q water on aluminium substrate (black) and on a quartz glass slip (violet). Placebo microparticles (MP) + *Bacillus subtilis* + Milli-Q water on aluminium substrate (blue) and on a quartz glass slip (red). (B) API + *Aspergillus Versicolor* + Milli-Q water on aluminium substrate (violet) and on a quartz glass slip (blue). API + *Bacillus subtilis* + Milli-Q water on aluminium substrate (red) and on a quartz glass slip (black). All measurements were done using 20x microscope objective, 100% laser power, 20 seconds laser exposure time, and 3 accumulations.

In Figure 22. (A) there are slight differences in band intensities and positions between *Aspergillus* and *Bacillus.* Bacillus shows slightly stronger bands in the ~1300–1600 cm^{-1} region, likely due to the thicker cell walls. These placebo spectra could serve as a baseline, showing how microbial presence alone (without API) affects Raman output. In Figure 22 (B) the spectra again show peaks that are typical for the API in the ~1350–1600 cm^{-1}. Measurements done on the quartz substrate exhibit more sharp and distinguishable peaks for the API. On the metal substrate peaks remain visible but slightly broadened.

6.10 Serial dilutions of the microorganisms + NH_4HF_2

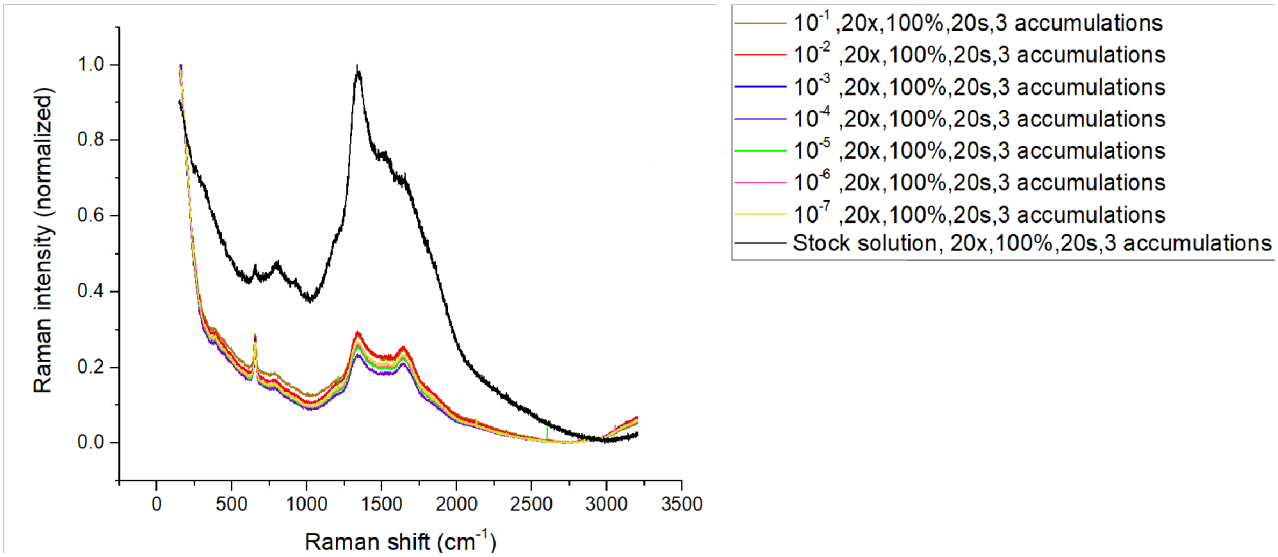

Figure 23. Stock solution and serial dilution 10^{-1}-10^{-7} of *Aspergillus Versicolor*.

The undiluted stock sample shows very strong, sharp Raman bands in Figure 23. There are prominent peaks in the ~750 cm^{-1} and ~1350–1600 cm^{-1} range. The stock solution dominates the scale due to significantly higher signal intensity. As dilution increases, peak intensities progressively decrease as is expected. The shape of the spectrum remains stable. Even at 10^{-6} and 10^{-7}, faint spectral features are still present in the fingerprint region (~750, ~1350 cm^{-1}).

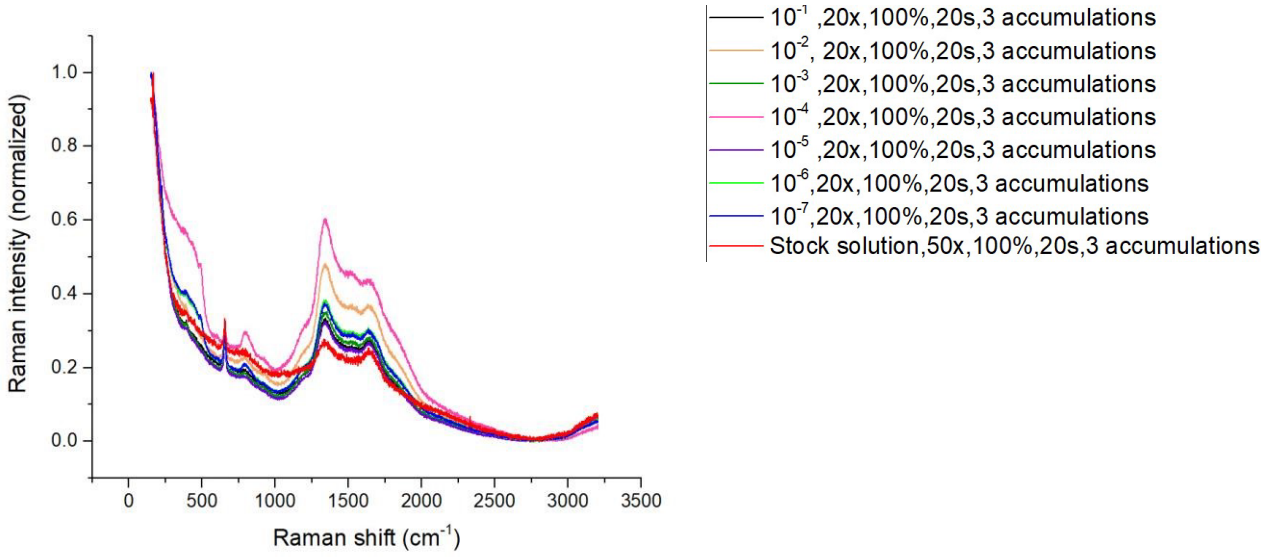

Figure 24. Stock solution and serial dilution 10^{-1}-10^{-7} of *Bacillus subtilis*.

In Figure 24. it can be observed that as expected, the Raman intensity gradually decreases as the dilution increases. It can be most clearly seen in the ~1350–1600 cm^{-1} region, where the signature peaks for *Bacillus subtilis* are located. At 10^{-6} to 10^{-7} serial dilutions (purple and pink), the signal is significantly weakened, although still traceable. The shape of the spectrum in consistent with diluted samples.

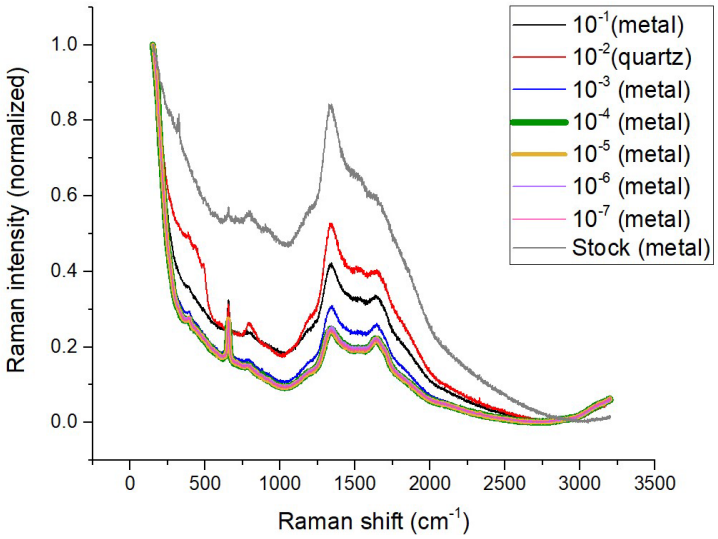

Figure 25. Stock solution and serial dilution 10^{-1}-10^{-7} of *Pseudomonas chlororaphsis*. Measuring parameters for all the samples were 20x microscope objective, 100% laser power, 20 seconds laser exposure time, and 3 accumulations. All measurements were done on an aluminium substrate, except for the 10^{-2} serial dilution that was done on a quartz glass slip.

The stock solution shows a high-intensity, broad signal profile with clear peaks in Figure 25. At around ~1350 cm^{-1} there is a significant peak, likely related to nucleic acids and lipids. Again, as the dilution increases, the signal intensity declines, and the shape of peaks is retained.

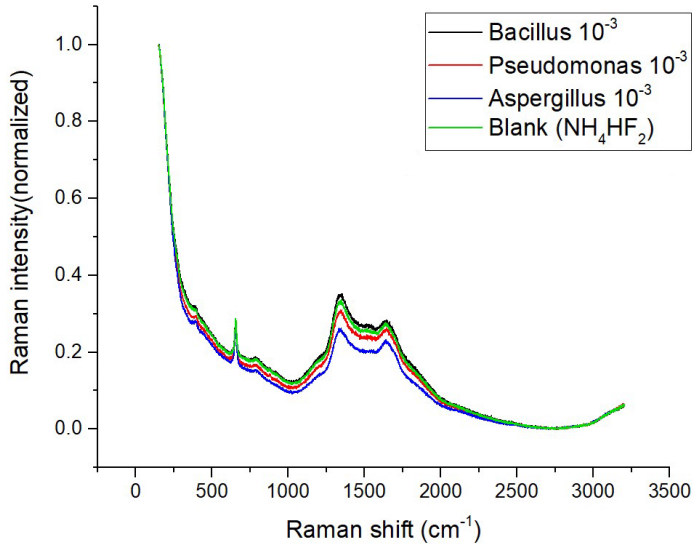

Figure 26. Serial dilution 10^{-3} of all the microorganisms and blank of ammonium bifluoride. All the measurements were done using 20x microscope objective, 100% laser power, 20 seconds laser exposure time and 3 accumulations. All the measurements were also done on an aluminium substrate.

All the samples show similar baseline and overall structure in Figure 26. The microbial samples exhibit slightly elevated peaks relative to the blank, particularly in the fingerprint region (600–1800 cm^{-1}).

6.11 Final tests

As the final step of the project some samples were studied again with different measuring parameters. For example, the 10^{-3} serial dilution of *Bacillus subtilis* was studied again but on a CaF_2 substrate. During the final testing 532 nm laser was also used. Stainless steel was also studied again, as metals typically do not exhibit Raman scattering but in the results Raman scattering for stainless steel could be observed. So, a new stainless steel piece and the measuring parameters they use was sent by the manufacturer of the Raman equipment used during the project.

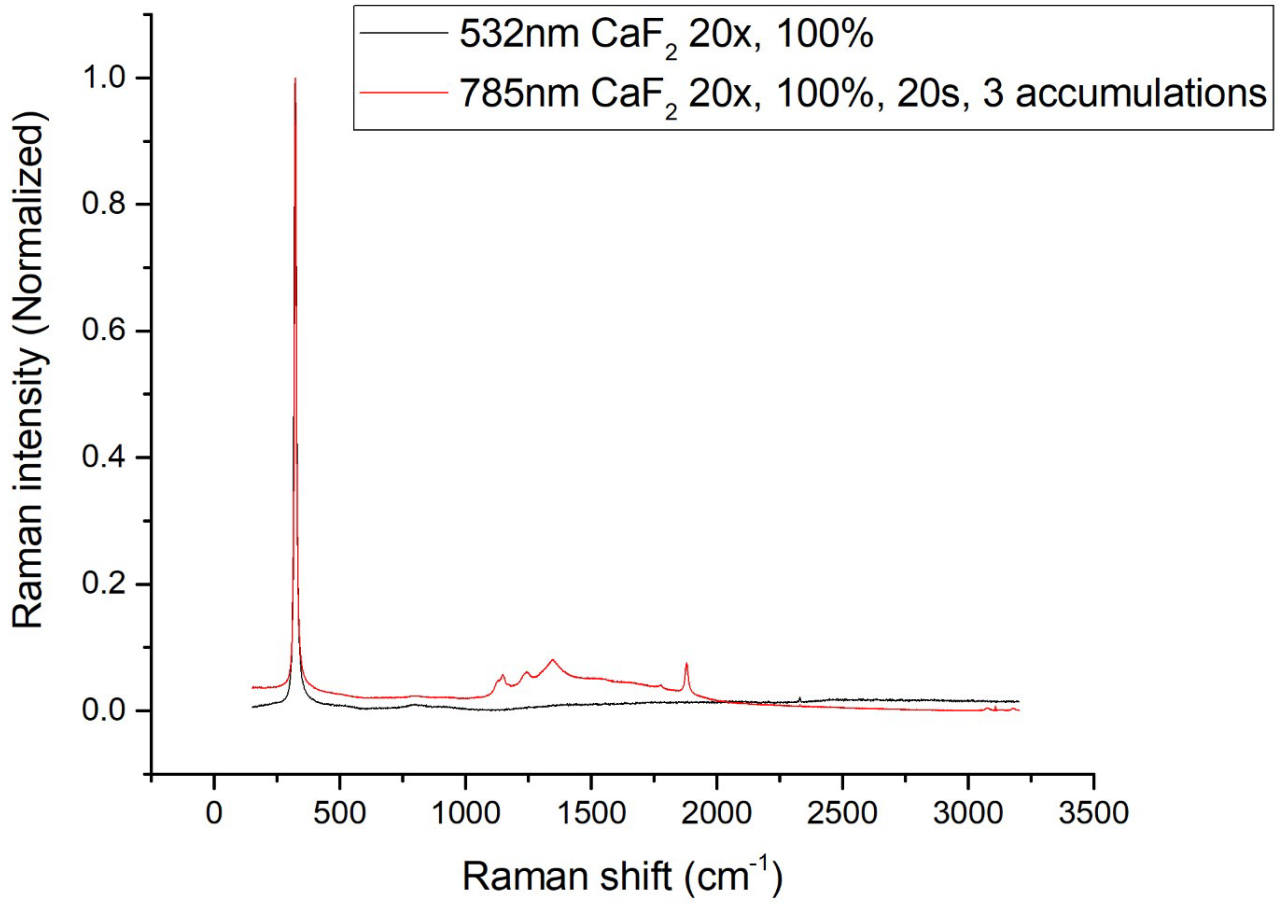

Figure 27. CaF_2 measured with the 532 nm laser, using the 20x microscope objective and 100% laser power (black). CaF_2 measured with the 785 nm laser, using the 20x microscope objective, 100% laser power, 20 seconds laser exposure time, and 3 accumulations (red).

In Figure 27. both spectra of CaF_2 have a sharp and intense peak a ~322 cm^{-1}. This corresponds to the F–Ca–F symmetric stretching mode. The 532 nm laser produces a slightly sharper baseline. The spectrum measured with 785 nm laser displays some weak additional background features in the 1300–1700 cm^{-1} range. Overall, there are no significant differences between the spectra.

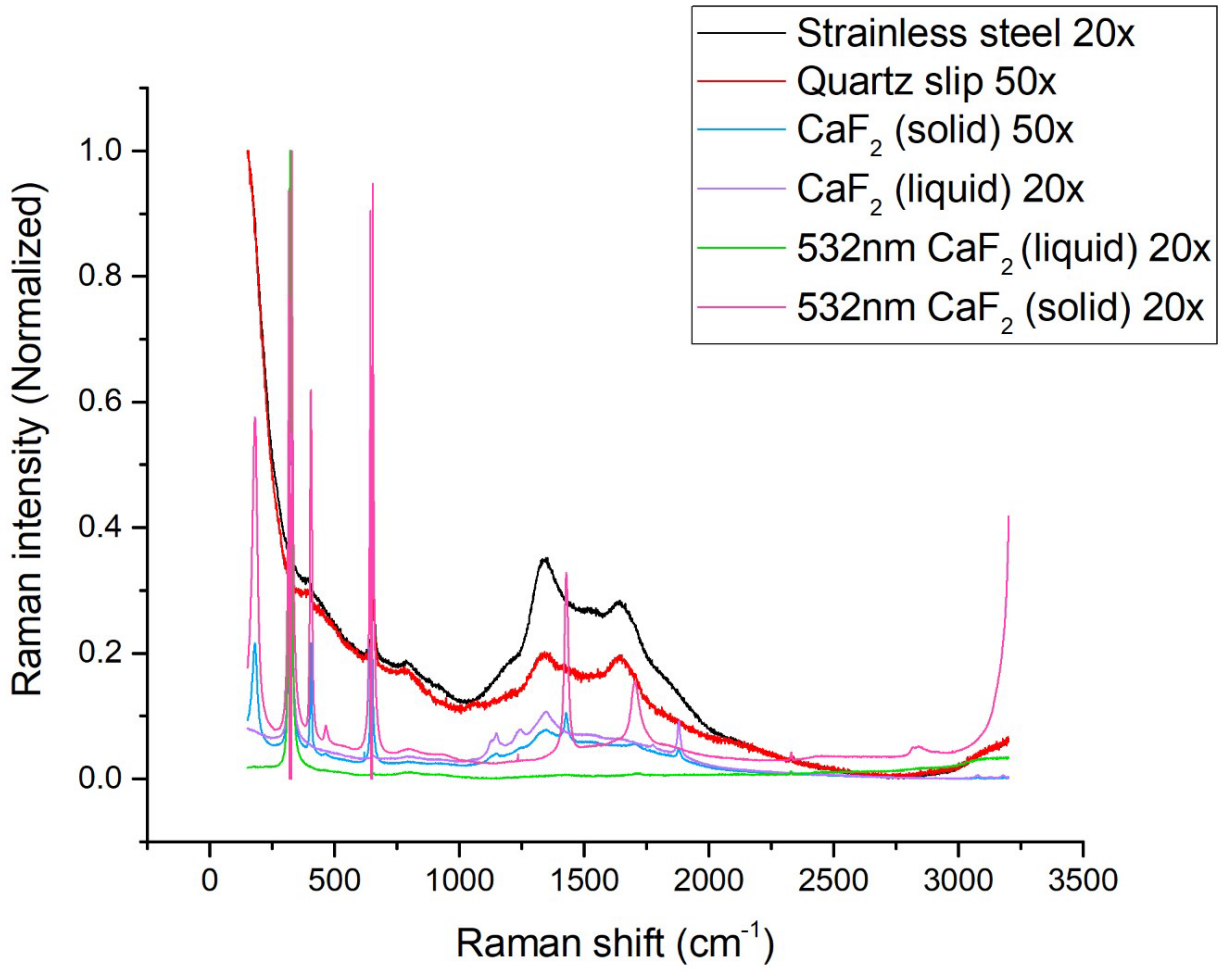

Figure 28. Serial dilution 10^{-3} of *Bacillus subtilis* on different substrate materials. All the measurements were done using 100% laser power, 20 seconds laser exposure time and 3 accumulations. Black, red, blue, and violet spectra were measured with 785 nm laser. The green and pink with 532 nm laser.

In Figure 28. spectra of serial dilution 10^{-3} of *Bacillus subtilis* was studied on three different substrate materials and two different lasers. The sample was prepared as was described in chapter 5.2.10. When measuring the sample on the CaF_2 substrate two separate phases could be observed as can be seen in Figure 29.

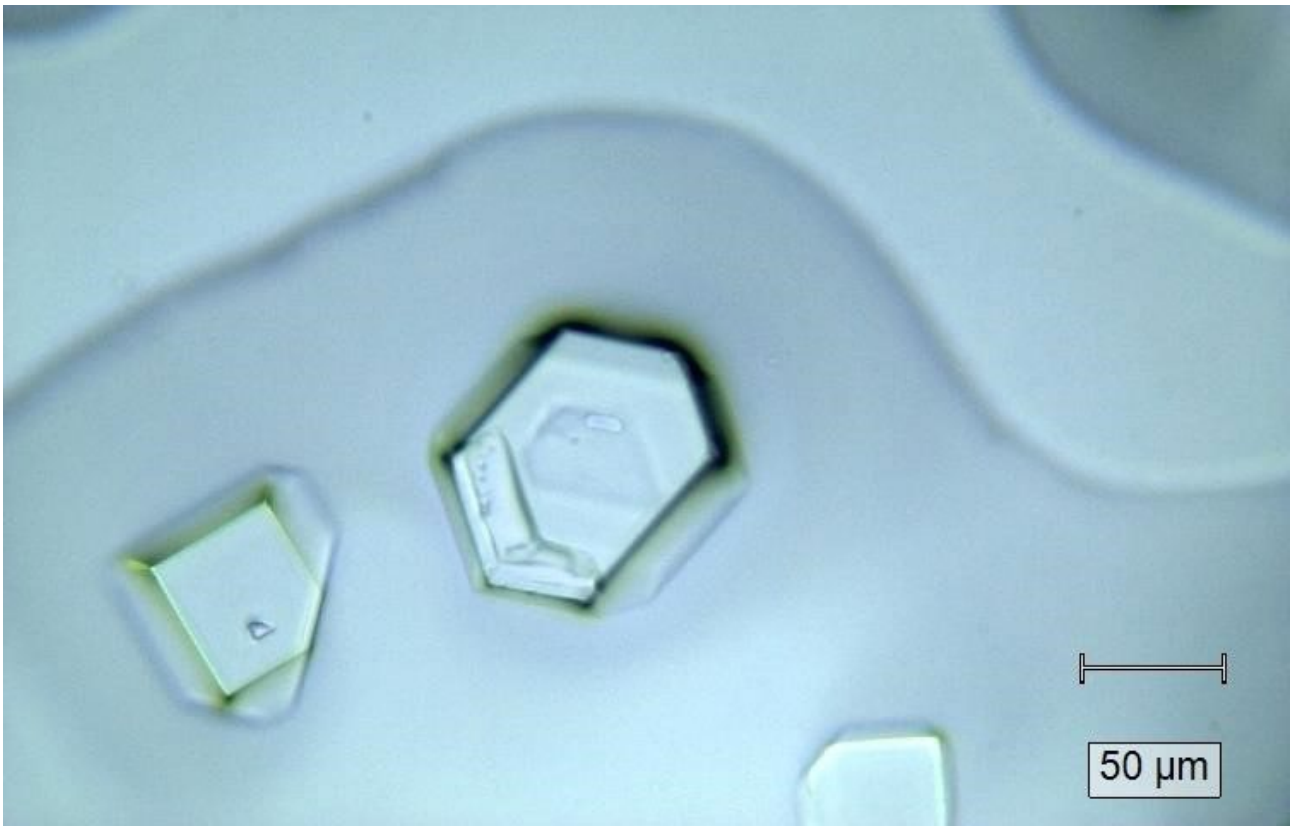

Figure 29. Serial dilution 10^{-3} of *Bacillus subtilis* on CaF_2.

The solid particles are likely silica that was used to neutralize the ammonium bifluoride. Measurements were done both from the solid particle, and from the surrounding liquid.

The measurements from the solid particles, done with both lasers, the 532 nm and 785 nm, show strong well-defined peaks. These peaks are likely to correspond with silica. The peaks are stronger in intensity with the 532 nm laser. The 532 nm laser measurement of the liquid surrounding the solid particle has no significant peaks outside of the peak ~330 cm^{-1} region, where all the spectra that were measured on the CaF_2 have a significant peak, which is caused by the substrate material. The measurement done from the liquid surrounding the solid particle on the CaF_2 substrate with the 785 nm laser has some peaks in the ~1000–2000 cm^{-1} region. Measurements done on the quartz substrate and stainless-steel substrate have peaks in the ~1000–2000 cm^{-1} region.

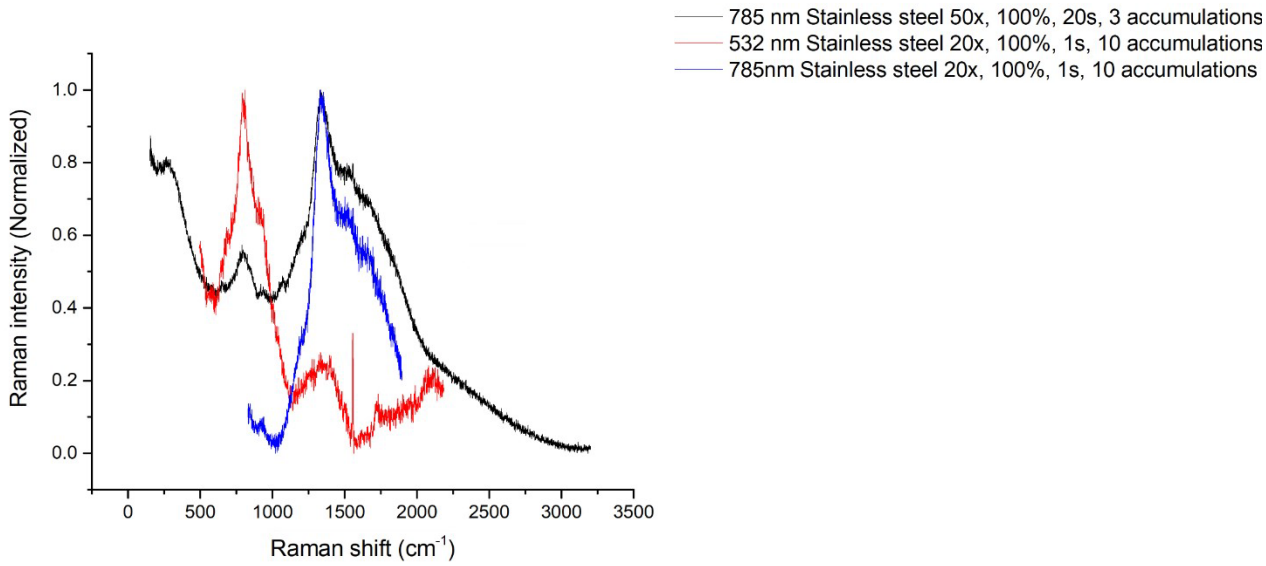

Figure 30. Stainless steel measured with 785 nm laser, using 50x microscope objective, 100% laser power, 20 seconds laser exposure time, and 3 accumulations (black). A static measurement of stainless steel, measured with the 532 nm laser, using 20x microscope objective, 100% laser power, 1 second laser exposure time, and 10 accumulations. The static centre for the measurement was 1400 (red). A static measurement of stainless steel, measured with the 785 nm laser, using 20x microscope objective, 100% laser power, 1 second laser exposure time, and 10 accumulations. The static centre for the measurement was 1600 (blue).

The stainless-steel substrate was studied again using different measuring parameters. Stainless steel should produce no background signal and be the ideal substrate material. But as can be seen in Figure 30. the stainless-steel substrate produces a signal. The measurements were done from a stainless-steel substrate that was provided by the manufacturer of the Raman equipment used in this project. The measuring parameters used in the blue and red spectra were supplied by the manufacturer also.

7 Conclusions

This thesis explored the application of Raman spectroscopy as a microbial detection method for silica-based drug delivery systems, with the aim of providing an alternative to traditional pharmacopeial methods. The experimental work included the analysis of three microorganisms: *Bacillus subtilis cf. spizizenii, Pseudomonas chlororaphsis, and Aspergillus versicolor*. The microorganisms were in various physical states and chemical environments. One active

pharmaceutical ingredient (API) was also studied in the same chemical environments with and without the different microorganisms. Raman measurements were carried out on different substrates, using different measuring parameters, and under different laser wavelengths, mainly with the 785 nm laser.

While microbial Raman spectra were successfully acquired in several conditions, the overall results remained inconclusive. Clear differentiation between microorganisms was not achieved, and signal variation was influenced by substrate material, laser wavelength, and sample state. Solid-phase samples generally produced more distinct features than liquid-phase ones, and calcium fluoride (CaF_2) and quartz performed better as substrates than stainless steel. However, the effect of different measurement parameters, such as laser wavelength and substrate material, could have been explored in more detail earlier in the project, as more systematic variation may have led to clearer insights.

The spectral differences observed were often subtle and difficult to interpret visually. Therefore, advanced data processing techniques such as principal component analysis (PCA) or partial least squares discriminant analysis (PLS-DA), which are commonly used in similar studies, could have been applied to enhance signal interpretation and identify meaningful patterns. In addition, machine learning algorithms could offer powerful tools for classifying spectral data and improving detection sensitivity, especially in low-concentration or noisy samples.

Future work should consider integrating multivariate analysis and machine learning workflows into Raman data processing to improve microbial discrimination. It would also be beneficial to explore Surface-Enhanced Raman Scattering (SERS) substrates, which can significantly amplify weak signals and improve the detection of trace-level analytes. These developments could help establish Raman spectroscopy as a more applicable and practical method for microbial quality control in complex pharmaceutical compounds.

8 References

1. Rostron P, Gaber S, Gaber D. Raman Spectroscopy , Review. 2016;(October).

2. Das RS, Agrawal YK. Raman spectroscopy: Recent advancements, techniques and applications. *Vib Spectrosc*. 2011;57(2):163-176. doi:10.1016/j.vibspec.2011.08.003

3. Orlando A, Franceschini F, Muscas C, et al. A comprehensive review on Raman spectroscopy applications. *Chemosensors*. 2021;9(9):1-28. doi:10.3390/chemosensors9090262

4. Mitsutake H, Poppi RJ, Breitkreitz MC. Raman imaging spectroscopy: History, fundamentals and current scenario of the technique. *J Braz Chem Soc*. 2019;30(11):2243-2258. doi:10.21577/0103-5053.20190116

5. Zhang W, He S, Hong W, Wang P. A review of Raman-based technologies for bacterial identification and antimicrobial susceptibility testing. Published online 2022.

6. Grosso RA, Walther AR, Brunbech E, et al. Detection of low numbers of bacterial cells in a pharmaceutical drug product using Raman spectroscopy and PLS-DA multivariate analysis. *Analyst*. 2022;147(15):3593-3603. doi:10.1039/d2an00683a

7. Wang L, Liu W, Tang JW, et al. Applications of Raman Spectroscopy in Bacterial Infections: Principles, Advantages, and Shortcomings. *Front Microbiol*. 2021;12(July). doi:10.3389/fmicb.2021.683580

8. Geraldes CFGC. Introduction to infrared and raman-based biomedical molecular imaging and comparison with other modalities. *Molecules*. 2020;25(23). doi:10.3390/molecules25235547

9. Downes A, Elfick A. Raman spectroscopy and related techniques in biomedicine. *Sensors*. 2010;10(3):1871-1889. doi:10.3390/s100301871

10. Butler HJ, Ashton L, Bird B, et al. Using Raman spectroscopy to characterize biological materials. *Nat Protoc*. Published online 2016. doi:10.1038/nprot.2016.036

11. Kalantri PP, Somani RR, Makhija DT. Raman spectroscopy : A potential technique in analysis of pharmaceuticals. *Der Chem Sin*. 2010;1(1):1-12.

12. Pence I, Mahadevan-Jansen A. Clinical instrumentation and applications of Raman spectroscopy. *Chem Soc Rev*. 2016;45(7):1958-1979. doi:10.1039/c5cs00581g

13. Bumbrah GS, Sharma RM. Raman spectroscopy – Basic principle, instrumentation and selected applications for the characterization of drugs of abuse. *Egypt J Forensic Sci*. 2016;6(3):209-215. doi:10.1016/j.ejfs.2015.06.001

14. Denson SC, Pommier CJS, Denton MB. The impact of array detectors on Raman spectroscopy. *J Chem Educ*. 2007;84(1):67-74. doi:10.1021/ed084p67

15. Lin YC, Sinfield J V. Characterization of raman spectroscopy system transfer functions in intensity,wavelength, and time. *Instruments*. 2020;4(3). doi:10.3390/instruments4030022

16. Vítek P, Ali EMA, Edwards HGM, Jehlička J, Cox R, Page K. Evaluation of portable Raman spectrometer with 1064 nm excitation for geological and forensic applications. *Spectrochim Acta - Part A Mol Biomol Spectrosc*. 2012;86:320-327. doi:10.1016/j.saa.2011.10.043

17. Gnyba M, Smulko J, Kwiatkowski A, Wierzba P. Portable Raman spectrometer - Design rules and applications. *Bull Polish Acad Sci Tech Sci*. 2011;59(3):325-330. doi:10.2478/v10175-011-0040-z

18. Smith R, Wright KL, Ashton L. Raman spectroscopy: An evolving technique for live cell studies. *Analyst*. 2016;141(12):3590-3600. doi:10.1039/c6an00152a

19. Pahlow S, Meisel S, Cialla-May D, Weber K, Rösch P, Popp J. Isolation and identification of bacteria by means of Raman spectroscopy. *Adv Drug Deliv Rev*. 2015;89:105-120. doi:10.1016/j.addr.2015.04.006

20. Cui D, Kong L, Wang Y, Zhu Y, Zhang C. In situ identification of environmental microorganisms with Raman spectroscopy. *Environ Sci Ecotechnology*. 2022;11:100187. doi:10.1016/j.ese.2022.100187

21. Buckley K, Matousek P. Recent advances in the application of transmission Raman spectroscopy to pharmaceutical analysis. *J Pharm Biomed Anal*. 2011;55(4):645-652. doi:10.1016/j.jpba.2010.10.029

22. Zhang W, He S, Hong W. A Review of Raman-Based Technologies for Bacterial Identification and Antimicrobial Susceptibility Testing. Published online 2022.

23. Strola SA, Baritaux J-C, Schultz E, et al. Single bacteria identification by Raman spectroscopy. *J Biomed Opt*. 2014;19(11):111610. doi:10.1117/1.jbo.19.11.111610

24. Maquelin K, Choo-smith L, Vreeswijk T Van, et al. Raman Spectroscopic Method for Identification of Clinically Relevant Microorganisms Growing on Solid Culture Medium. 2000;72(1):12-19.

25. Stöckel S, Kirchhoff J, Neugebauer U. The application of Raman spectroscopy for the detection and identification of microorganisms. 2016;(October 2015):89-109. doi:10.1002/jrs.4844

26. Rebrosova K, Samek O, Kizovsky M, Bernatova S, Hola V, Ruzicka F. Raman Spectroscopy—A novel method for identification and characterization of microbes on a single-cell level in clinical settings. *Front Cell Infect Microbiol*. 2022;12(April):1-10. doi:10.3389/fcimb.2022.866463

27. Samek O, Bernatová S, Dohnal F. The potential of SERS as an AST methodology in clinical settings. *Nanophotonics*. 2021;10(10):2537-2561. doi:10.1515/nanoph-2021-0095

28. Rösch P, Harz M, Schmitt M, et al. Chemotaxonomic identification of single bacteria by micro-Raman spectroscopy: Application to clean-room-relevant biological contaminations. *Appl Environ Microbiol*. 2005;71(3):1626-1637. doi:10.1128/AEM.71.3.1626-1637.2005

29. Ho CS, Jean N, Hogan CA, et al. Rapid identification of pathogenic bacteria using Raman spectroscopy and deep learning. *Nat Commun*. 2019;10(1). doi:10.1038/s41467-019-12898-9

30. Tadesse LF, Safir F, Ho CS, et al. Toward rapid infectious disease diagnosis with advances in surface-enhanced Raman spectroscopy. *J Chem Phys*. 2020;152(24). doi:10.1063/1.5142767

31. Almarashi JFM, Kapel N, Wilkinson TS, Telle HH. Raman spectroscopy of bacterial species and strains cultivated under reproducible conditions. *Spectrosc (New York)*. 2012;27(5-6):361-365. doi:10.1155/2012/540490

32. Beveridge TJ. Structures of gram-negative cell walls and their derived membrane vesicles. *J Bacteriol*. 1999;181(16):4725-4733. doi:10.1128/jb.181.16.4725-4733.1999

33. Rohde M. The Gram-Positive Bacterial Cell Wall. doi:10.1128/microbiolspec.GPP3-0044-2018.Correspondence

34. Atanasova KR. Interactions between porcine respiratory coronavirus and bacterial cell wall toxins in the lungs of pigs. 2010;(January 2010):140. doi:https://www.researchgate.net/publication/294263540

35. Tang A, Shi Y, Dong Q, et al. Prognostic differences in sepsis caused by gram-negative bacteria and gram-positive bacteria: a systematic review and meta-analysis. *Crit Care*. 2023;27(1):1-12. doi:10.1186/s13054-023-04750-w

36. Tavares TD, Antunes JC, Padrão J, et al. Activity of specialized biomolecules against grampositive and gram-negative bacteria. *Antibiotics*. 2020;9(6):1-16. doi:10.3390/antibiotics9060314

37. Wang L, Liu W, Tang J, et al. Applications of Raman Spectroscopy in Bacterial Infections : Principles , Advantages , and Shortcomings. 2021;12(July). doi:10.3389/fmicb.2021.683580

38. Klein DA, Paschke MW. Filamentous fungi: The indeterminate lifestyle and microbial ecology. *Microb Ecol*. 2004;47(3):224-235. doi:10.1007/s00248-003-1037-4

39. Shigeto S, Takeshita N. Raman Microspectroscopy and Imaging of Filamentous Fungi. *Microbes Environ*. 2022;37(6). doi:10.1264/JSME2.ME22006

40. Garcia-Rubio R, de Oliveira HC, Rivera J, Trevijano-Contador N. The Fungal Cell Wall: Candida, Cryptococcus, and Aspergillus Species. *Front Microbiol*. 2020;10(January):1-13. doi:10.3389/fmicb.2019.02993

41. Géry A, Rioult JP, Heutte N, Séguin V, Bonhomme J, Garon D. First characterization and description of aspergillus series versicolores in French bioaerosols. *J Fungi*. 2021;7(8). doi:10.3390/jof7080676

42. Siqueira JPZ, Sutton DA, García D, et al. Species diversity of Aspergillus section Versicolores in clinical samples and antifungal susceptibility. *Fungal Biol*. 2016;120(11):1458-1467. doi:10.1016/j.funbio.2016.02.006

43. Paudel A, Raijada D, Rantanen J. Raman spectroscopy in pharmaceutical product design. *Adv Drug Deliv Rev*. 2015;89:3-20. doi:10.1016/j.addr.2015.04.003

44. Vankeirsbilck T, Vercauteren A, Baeyens W, et al. Applications of Raman spectroscopy in pharmaceutical analysis. *TrAC - Trends Anal Chem*. 2002;21(12):869-877. doi:10.1016/S0165-9936(02)01208-6

45. Gao M, Liu S, Chen J, Gordon KC, Tian F, McGoverin CM. Potential of Raman spectroscopy in facilitating pharmaceutical formulations development – An AI perspective. *Int J Pharm*. 2021;597(December 2020):120334. doi:10.1016/j.ijpharm.2021.120334

46. Chen J, Wang J, Hess R, Wang G, Studts J, Franzreb M. Application of Raman spectroscopy during pharmaceutical process development for determination of critical quality attributes in Protein A chromatography. *J Chromatogr A*. 2024;1718(February):464721. doi:10.1016/j.chroma.2024.464721

47. Esmonde-White KA, Cuellar M, Uerpmann C, Lenain B, Lewis IR. Raman spectroscopy as a process analytical technology for pharmaceutical manufacturing and bioprocessing. *Anal Bioanal Chem*. 2017;409(3):637-649. doi:10.1007/s00216-016-9824-1

48. Ratajczak M, Kubicka MM, Kamińska D, Sawicka P, Długaszewska J. Microbiological quality of non-sterile pharmaceutical products. *Saudi Pharm J*. 2015;23(3):303-307. doi:10.1016/j.jsps.2014.11.015

49. Sandle T. A new standard for bioburden testing : USP chapter in development A new standard for bioburden testing : USP chapter in development. 2013;(October).

50. Masashi M, Tsuguo S. Guidance on the Manufacture of Sterile Pharmaceutical Products Produced by Terminal Sterilization. Published online 2012:1-74. https://www.pmda.go.jp/files/000160794.pdf

51. Grosso RA, Walther AR, Brunbech E, et al. Detection of low numbers of bacterial cells in a pharmaceutical drug product using Raman spectroscopy and PLS-DA multivariate analysis †. Published online 2022:3593-3603. doi:10.1039/d2an00683a

52. Masucci EM, Hauschild JE, Gisler HM, Lester EM, Balss KM. Raman spectroscopy as an alternative rapid microbial bioburden test method for continuous, automated detection of contamination in biopharmaceutical drug substance manufacturing. *J Appl Microbiol*. 2024;135(8). doi:10.1093/jambio/lxae188

53. Ramos I, Najera M, Schaefer G. Integration of rapid bioburden testing into production quality management systems and process control. *Biotechnol Prog*. 2024;40(3):1-14. doi:10.1002/btpr.3431

54. Maruthamuthu MK, Raffiee AH, De Oliveira DM, Ardekani AM, Verma MS. Raman spectra-based deep learning: A tool to identify microbial contamination. *Microbiologyopen*. 2020;9(11):1-8. doi:10.1002/mbo3.1122

55. Bryans TD, Leckwart C, Dos Santos HB. Bioburden Method Suitability: A Practical Solution to Screening for Inhibition. *Biomed Instrum Technol*. 2023;57(3):81-86. doi:10.2345/08998205-57.3.81